Dispersion of Single-Walled Carbon Nanotubes (SWCNTs) in Aqueous Solution and Reversion of SWCNT Aggregates

by

Byumseok Eric Koh

A dissertation submitted in partial fulfillment
of the requirements for the degree of
Doctor of Philosophy
(Pharmaceutical Sciences)
in the University of Michigan
2013

Doctoral Committee:

Assistant Professor Wei Cheng, Chair
Professor Raoul Kopelman
Professor Kyung-Dall Lee
Professor Steven Schwendeman

To my family and friends

: With my love and respects

Acknowledgements

I would like to express my sincere gratitude to Dr. Wei Cheng for his support and insightful guidance throughout my PhD training years. He taught me the attitude to keep discover science in every single experiment. I deeply respect his perseverance and enthusiasm in his research as a scientist. I also would like to thank my committee members, Dr. Steven Schwendeman, Dr. Kyung-Dall Lee, and Dr. Raoul Kopelman for their helpful suggestions and guidance in my project.

I am also grateful to the Department of Pharmaceutical Sciences and the Rackham Graduate School for supporting me during my PhD study. I appreciate the funding sources, Schering Plough scholarship, Hollis and Martha Showalter fund scholarship and Rackham Predoctoral Fellowship.

I thank all my wonderful friends. They were always there for me to make this long journey for a PhD possible; my classmates, Dr. Yajun Liu, Dr. Yeamin Huh, Oluseyi Adeniyi and Ronak B. Shah , for their friendship and good memories through all the years; my previous lab members, Dr. Ximiao Hou for their valuable advice and support, and my present lab members, Dr. Jinhyun Kim, Dr. Michael DeSantis, Dr. Yuanjie Pang, Hanna Song, Jamie Austin, Kristine Schimert and Ziah Dean for their help and friendship.

I would like to dedicate my work to my parents and grandparent who supported me with love and belief throughout my life. Lastly, I greatly thank my family for being beside me all the time.

Table of Contents

List of Tables

List of Figures

List of Appendices

Abstract

Due to their unique physical properties, single-walled carbon nanotubes (SWCNTs) have become increasingly important in applications as diverse as biosensors and building blocks for nano-electronics. SWCNTs are considered to be effective drug and gene carriers because they have the ability to either directly penetrate or be endocytosed into cells with relatively low or no toxicity. However, there is a limitation: in order to be used as drug or gene carriers, SWCNTs must be dispersed in aqueous solution. In fact, studies have shown that an aggregated form of SWCNTs induces a toxic response *in vivo*, thus limiting their use as delivery tools. This toxic response, consisting of aggregate accumulation in the lung and spleen and consequent inflammation and fibrosis, motivated us to study strategies for achieving effective SWCNT dispersion in aqueous solution. We investigated the mechanisms of SWCNT dispersion and aggregation and how certain SWCNT aggregates can be re-dispersed by addition of chelating or reducing agents. We also developed a method to re-disperse SWCNT aggregates by using enzymes, which has the potential to control the aggregation status of SWCNTs in solution. Our studies and findings can advance the development of SWCNTs for future applications in drug/DNA delivery.

Chapter 1

Introduction

1.1 Background

Single-walled carbon nanotubes (SWCNTs) have great potential to be used as drug or single-stranded DNA (ssDNA) delivery reagents due to its ability to either penetrate or endocytosed inside of the cells with relatively low or no toxicity[1-5]. However, in order to use SWCNT as delivery tool for drug molecules, SWCNTs need to be dispersed in aqueous solution[6-10]. In addition, previous studies have shown that SWCNT aggregates accumulate inside biological system inducing inflammation, fibrosis and toxicity[11-13]. Therefore, it is necessary to study dispersion and aggregation of SWCNTs with its mechanism. Many careful studies on SWCNT dispersion were conducted, however not much studies have been carried out on SWCNTs possible aggregation during *in vitro* and *in vivo* delivery. In addition, method of re-dispersing SWCNT aggregates during delivery is required. This current situation motivated us to study effect dispersion of SWCNTs in aqueous solution as well as investigating SWCNT aggregation mechanism as well as to find method to re-disperse SWCNT aggregates.

1.1.1 Introduction to SWCNTs

Ever since their discovery[14,15], SWCNTs have been considered one of the most versatile materials ranging from biosensors to displays due to their unique physical and electrical properties. Their excellent thermal and electrical conductivity, great tensile strength (~20 times stronger than regular steel) and electrical properties has allowed them to be frequently used in items such as biosensors and displays. SWCNTs are allotropes of carbon, with a cylindrical structure that we can consider as a "rolled-up" form of another carbon allotrope, graphene. SWCNTs consist of sp^2-hybridized bonds and have a very high aspect ratio. Structurally, SWCNTs can be defined as chiral vectors (n, m), designated by two integers, *n* and *m*, where. *n* and *m* denote the number of unit vectors along two directions in the honeycomb crystal lattice of a graphene sheet at a given carbon atom (Figure 1-1).

The diameter (*d*) of an individual SWCNT is determined as

$$d = \frac{0.246}{\pi}\sqrt{(n^2 + nm + m^2)}$$

SWCNTs have been used for various purposes, including use in photovoltaic devices[16,17], nanoelectronics[18,19], molecular sensors[20,21], and, potentially, DNA sequencing[22]. They also have the potential to be therapeutic agents delivering anti-cancer agents and other drugs[23,24].

1.1.2 SWCNT Dispersion in Aqueous Solution

Despite their great potentials, SWCNT have significant limitation in biological application that it cannot be solubilized in aqueous solution due to the van der Waals attraction[25], π-π stacking[26] and hydrophobic interaction[27] with nearby SWCNTs. Therefore several studies have been conducted in order to successfully disperse SWCNTs in aqueous solution. These methods include SWCNT dispersion with dispersants[28] and SWCNT dispersion in strong acids (3:1, sulfuric acid, nitric acid mixture) upon sonication[29] (Figure 1-2). Dispersion of SWCNTs in strong acids involves significant surface functionalization of SWCNTs by acid resulting breakage of carbon-carbon double bonds producing hydrophilic carboxylic or amide functional groups which allows stabilization of SWCNTs in aqueous solution. However, functionalization of SWCNTs induces loss of SWCNTs intrinsic properties such as moderate semiconductor, thus significant attention should be made before using functionalized SWCNTs. Dispersion of SWCNTs with dispersants upon sonication occur when hydrophobic moieties of dispersants stacks on the surface of SWCNTs while hydrophilic moieties of dispersants facing aqueous solution thus enabling stable dispersion of SWCNT/dispersants complexes[26]. Dispersion of SWCNTs by dispersants upon sonication are believed to retain their intrinsic properties, however only few studies have shown SWCNTs degree of surface damages upon sonication in the presence of dispersants in aqueous solution[30]. Therefore, studies on SWCNT surface functionalization with dispersants in aqueous solution is required to confirm their retention of properties.

1.1.3 Possible Aggregation of dispersed SWCNTs in Aqueous Solution

SWCNT dispersion in aqueous solution are well described in previous researches[31-34]. However, few or no studies describes SWCNTs' possible aggregation after dispersion. SWCNTs can be dispersed in aqueous solution when hydrophilic moieties in dispersants or functionalized surface of SWCNTs facing aqueous phase. In many cases, these hydrophilic moieties carry charges (either negative or positive charges depending on dispersants and functional group on SWCNTs) and these charges on SWCNT surface allows stable dispersion of SWCNTs in aqueous solution. Even though aggregation of dispersed SWCNTs in aqueous solution were not intensively studied, we hypothesized that neutralization of charges on SWCNT will mediate aggregation of dispersed SWCNTs. Study by Geckeler *et al.*[35] also showed SWCNT aggregation upon neutralization of SWCNT surface charges. This neutralization of SWCNT surface charges can occur when charges on SWCNT surface and opposite charges present in aqueous solution electrostatically bind. We would assume that these molecules with opposite charges bring SWCNTs with same charges closely resulting in aggregation. This potential aggregation of dispersed SWCNTs mediated by charged molecules can be extremely cautious especially when SWCNTs are used in biological purposes such as drug/gene delivery. This is because aqueous environment in *in vitro* as well as *in vivo* contains various charged molecules. Therefore, careful studies on SWCNT aggregation in aqueous solution as well as its mechanism should be carried out in order to prevent unwanted aggregation of SWCNTs during their application.

1.1.4 Current Status of Researches in SWCNT Aggregation and Dispersion

Many careful studies had been carried out in order to create nano-system which is capable of controlling aggregation and re-dispersion of SWCNTs including switching a solution pH[36-40], light induced[41,42], changing the oxidiation and reduction state of dispersants[43-45], using foldamers[46], via temperature changes[36, 38] and via salt addition[43,47-49]. However, regardless of urgent requirement on studies of potential aggregation of dispersed SWCNTs by surface charge neutralization because of possibilities on aggregation of dispersed SWCNTs during *in vitro* as well as *in vivo* delivery, currently no systematic studies on SWCNT aggregation with surface charge neutralization were reported. Therefore it is necessary to conduct systematic studies on SWCNT aggregation upon neutralization of SWCNT surface charges. Studies on SWCNT dispersion in aqueous solution were intensively studied and several methods on dispersing SWCNTs in aqueous solution were reported[28,29,32-34]. However, there are still lack of knowledge on systematically optimizing dispersion method to have highest amount of dispersed SWCNTs in a given amount of SWCNT soot and dispersants. Since, sonication is essential step to disperse SWCNTs in aqueous solution[50,51], studies on analyzing effect of sonication time and sonication power on SWCNT dispersion is needed. In addition, separation of dispersed SWCNTs from SWCNT aggregates after dispersion is necessary and centrifugation is a conventional step for this purpose[26]. Consequently, systematic study on varying centrifugation condition in order to successfully remove SWCNT aggregates from dispersed SWCNTs is needed in order to achieve successful dispersion of SWCNTs.

1.1.5 Controlling Aggregation Status of SWCNTs and its Application

Controlling aggregation status of SWCNTs can have significant implication especially when they used as drug/gene carrier. SWCNTs in aggregated form and dispersed form have both advantages and disadvantages as a potential delivery tool for drugs or genes. Literatures on pharmacokinetic profiles of SWCNTs are showing that SWCNT aggregates have longer blood circulation half-life time (~ 10 hours based on reported values) compare to individually dispersed SWCNTs[52,55]. This longer blood circulation half-life time of SWCNT aggregates is probably due to the fact that they are not easily taken up by macrophages or accumulated in periphery of blood vessels or organs even though detailed reason is still poorly understood. However, SWCNT aggregates have significant disadvantage over individually dispersed SWCNTs that they are not easily excreted from the body, causing inflammatory or fibrotic responses[55]. In contrast, it has been reported that individually dispersed SWCNTs do not accumulate inside biological system inducing little or no toxicity[56,57]. However, individually dispersed SWCNTs are reported to have shorter blood circulation half-life time compare to SWCNT aggregates (~3 hours) which makes them not a suitable delivery tool in terms of their prolonged efficacy[58]. Therefore, controlling aggregation status of SWCNTs during *in vitro* as well as *in vivo* delivery can potentially have significant impact on SWCNT mediate drug or gene delivery. If we are able to control the aggregation status of SWCNTs, our hypothesis is that we can first dose SWCNT aggregates which can protect ligands from damaging or degrading while ensuring prolonged blood circulation half-life compare to dispersed SWCNTs. Once, they reached the target cells, they can be dispersed

and get cleared from the system without accumulation or toxic response. We think that control of SWCNT aggregation status can benefit the future of usage of SWCNTs as a promising delivery tool. Controlling aggregation status of SWCNTs can be applied not only to drug or gene delivery, but also to biosensors. Previous studies have shown that SWCNT/phenoxy dextran complex can detect plant lectin (Concanavalin A) by aggregation upon exposure[59]. Therefore, it is important to create a system with reversible dispersion of SWCNTs in many fields using SWCNTs.

1.1.5 Controlling Dispersion of SWCNTs and Colloid Aggregation

Stable dispersion of colloids (particles) is also critical in colloid system[60-70]. Colloids are often aggregates which are driven by the tendency of dispersed colloids to reduce surface energy[71]. This aggregation of colloids eventually leads in sedimentation of colloids aggregates. Several methods have been developed in order to stably disperse particles in colloid system, by ensuring electrostatic barrier between each particles or by physically deforming (de-stretching) the particles which can reduce van der Waals attraction force in between particles. As dispersed SWCNTs in aqueous solution can be considered as colloidal system in broad sense, studying dispersion of SWCNTs in aqueous system as well as controlling aggregation status of SWCNTs can broaden our knowledge of particle aggregation in colloidal system. We speculate that dispersed SWCNTs can be aggregated upon addition of charged flocculants which can bridge individual SWCNTs by attractive electrostatic interactions. Addition of salts or charged molecules to dispersed SWCNTs can remove electrostatic barrier between SWCNTs

which prevents aggregation of SWCNTs. Therefore, by studying the aggregation as well as dispersion of SWCNTs, we can expand our understanding of colloid aggregation and dispersion to SWCNTs.

1.2 Rationale and Significance

Systemic studies on SWCNT dispersion is important, because SWCNTs need to be dispersed in aqueous solution if we want to use them in biological system. We also speculate that surface of SWCNTs can be damaged upon sonication, which is routine and conventional method to disperse SWCNTs in aqueous solution. Since, damage of SWCNT surface can result in loss of their intrinsic properties, it is necessary to conduct systematic evaluation on sonication and its influence in SWCNT surface damage. In addition, potential aggregation of SWCNTs during drug or gene delivery must be overcome since previous researches have shown that SWCNT aggregates tend to accumulate inside biological system causing inflammation and fibrosis. Therefore, we conducted systematic experiments on investigating mechanism of SWCNT aggregation and methods to re-disperse SWCNT aggregates in order to reduce toxic response when they are administered *in vitro* as well as *in vivo*. We think that this study can provide in-depth understanding on dispersion and aggregation of SWCNTs in aqueous solution and able to provide methods to successfully control aggregation status of SWCNTs for future application.

1.3 Questions and Hypotheses

As we discussed so far, in-depth study on dispersion and aggregation of SWCNTs is important when they are used as drug or gene delivery tool. In addition, studying effective SWCNT dispersion as well as understanding chemical elements of SWCNT dispersants are important as we want to solubilize SWCNTs in aqueous solution. Lastly, evaluating toxicity of SWCNTs regarding its aggregation and dispersion status as well as investigating mechanism of SWCNT aggregation and finding methods to re-disperse SWCNT aggregates are also urgently needed. Therefore, goal of our studies is to develop and validate our hypothesis on following questions which are closely related to problems and needs described above.

(1) How we can effectively disperse SWCNTs in aqueous solution in order to achieve maximum dispersion of SWCNTs and successfully separating dispersed SWCNTs from SWCNT aggregates?

Optimal sonication power and sonication time can effectively disperse SWCNTs in aqueous solution while designated centrifugation can successfully separate individually dispersed SWCNTs from aggregates. Finding optimal ratio between SWCNTs and dispersants can ensure maximum dispersion of SWCNTs in aqueous solution.

(2) What is the structural requirement of SWCNT dispersants? Can fluorophore and dye molecules containing both hydrophilic and hydrophobic moieties disperse SWCNTs?

Previous studies have shown that requirement for successful SWCNT dispersant is that they should contain hydrophobic moieties which allows adsorption to SWCNT surface and hydrophilic moieties facing aqueous environment. Fluorophores and dye molecules have both hydrophobic aromatic chains as well as hydrophilic moieties and we hypothesized that these molecules can successfully disperse SWCNTs.

(3) Can sonication induces damage on SWCNT surface?

Radicals can be produced during sonication. This radical can damage surface of SWCNTs during dispersion process, therefore we speculated that there can be damages on SWCNT surface upon sonication.

(4) Can aggregated form of SWCNT induce toxicity?

Previous researches have shown that SWCNT aggregates tend to accumulate inside biological system causing toxic response. We should conduct systematic analysis on toxicity of SWCNT aggregates when they administered *in vivo*.

(5) What is the mechanism of SWCNT aggregation? Can we re-disperse SWCNT aggregates?

Neutralization of surface charges of can induce aggregation of SWCNTs. If we can successfully restore SWCNT surface charges, or recover electrostatic barrier by adding additional reagents, we may able to re-disperse SWCNT aggregates.

1.4 Specific Aims

Accordingly, our studies presented herein will discuss about importance of SWCNT aggregation and dispersion, based on these specific aims to identify:

1) Finding optimized condition to effectively disperse SWCNTs in aqueous solution
2) Discovering and confirming structural elements of SWCNT dispersants using fluorophore and dye molecules as model molecules
3) Verifying surface damages of SWCNTs upon sonication
4) Evaluating toxicity of SWCNTs aggregates
5) Studying mechanism of SWCNT aggregation and finding method to re-disperse SWCNT aggregates

1.5 Figures

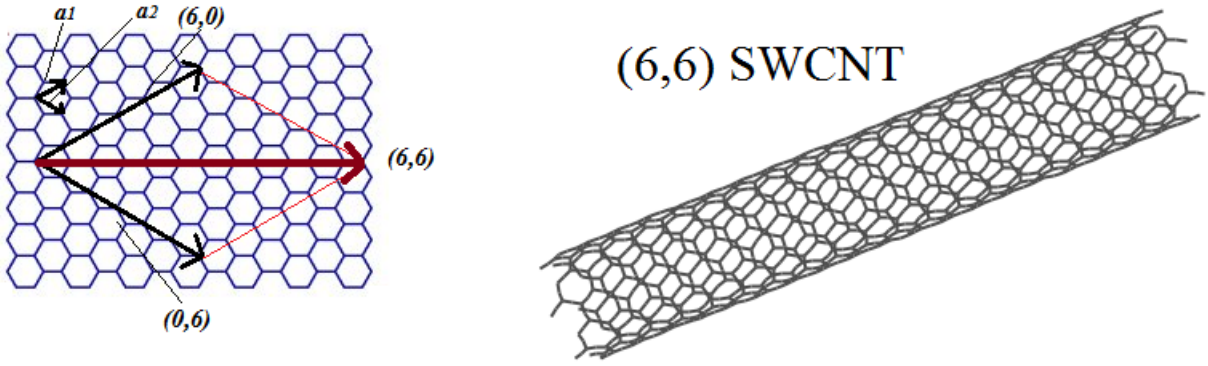

Figure 1.1. Chirality of SWCNTs can be defined by a pair of indices (*n*, *m*) that represent how the graphene sheet is rolled up. Integers *n* and *m* indicate the number of unit vectors across the two directions of the carbon lattice. SWCNTs were drawn using CoNTub 2.0 (http://www.ugr.es/~gmdm/contub.htm).

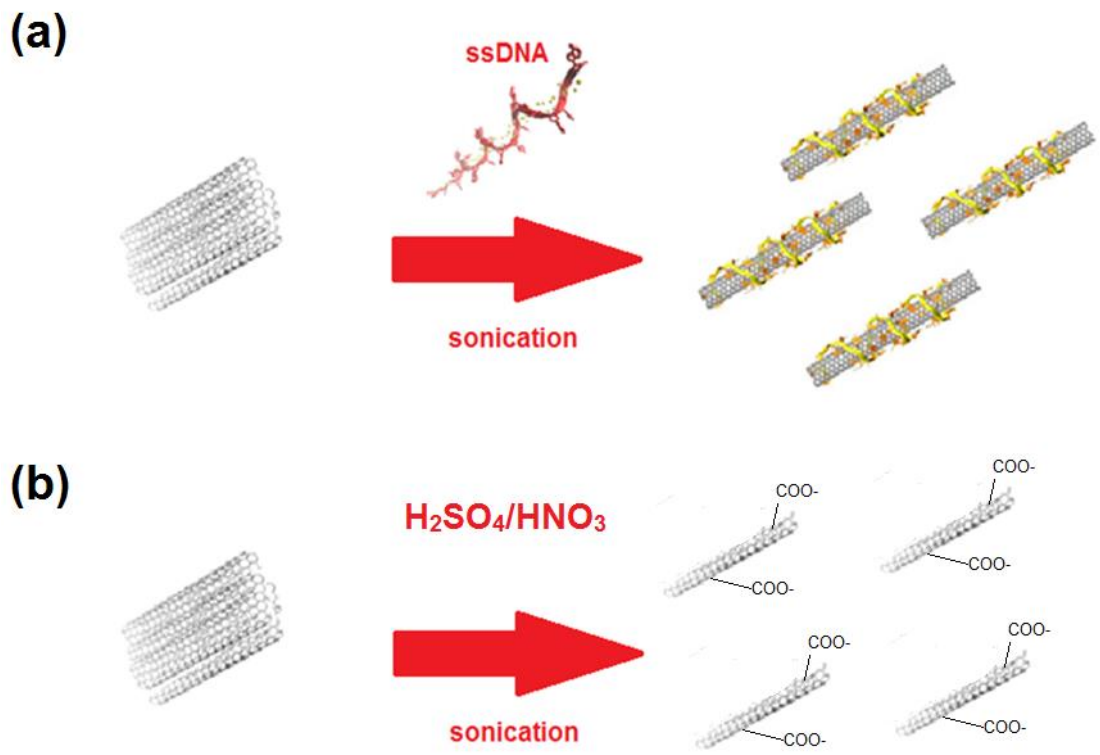

Figure 1-2. SWCNT dispersion with (a) dispersants, ssDNA and in (b) strong acids upon sonication.

1.6 References

(1) Liu, Z.; Winters, M.; Holodniy, M. and Dai, H. *Angew. Int. Chem.*, **2007**, 46, 2023.

(2) Cai, D.; Mataraza, J. M.; Qin, Z-H.; Huang, Z.; Huang, J.; Chiles, T. C.; Carnahan, D.; Kempa, K.; Ren, Z. *Nat. Methods.*, **2005**, 2, 449.

(3) Bhirde, A. A.; Patel, V.; Gavard, J.; Zhang, G.; Sousa, A. A.; Masedunkas, A.; Leapman, R. D.; Weigert, R.; Gutkind, J. S.; Rusling, J. F. *ACS Nano.*, **2009**, 3, 307.

(4) Kam, N. W. S.; Jessop, T. C.; Wender, P. A.; Dai, H. *J. Am. Chem. Soc.*, **2004**, 126, 6850.

(5) Singh, R.; Pantarotto, D.; McCarthy, D.; Chaloin, O.; Hoebeke, J.; Partidos, C. D.; Briand, J-P.; Prato, M.; Bianco, A.; Kostarelos, K. *J. Am. Chem. Soc.*, **2005**, 127, 4388.

(6) Rastogi, R.; Kaushal, R.; Tripathi, S. K.; Sharma, A. L.; Kaur, I.; Bharadwaj, L. *J. Coll. Int. Sci.*, **2008**, 328, 421.

(7) Fagan, J. A.; Landi, B. J.; Mandelbaum, I.; Simpson, J. R.; Bajpai, V.; Bauer, B. J.; Migler, K.; Hight Walker, A. R.; Raffaelle, R.; Hobbie, E. K. *J. Phys. Chem. B.*, **2006**, 110, 23801.

(8) Matarredona, O.; Rhoads, H.; Li, Z.; Harwell, J. H.; Balzano, L.; Resasco, D. E. *J. Phys. Chem. B*, **2003**, 107, 13357.

(9) Zheng, M.; Jagota, A.; Semke, E. D.; Diner, B. A.; Mclean, R. S.; Lustig, S. R.; Richardson, R. E.; Tassi, N. G. *Nat. Mater.*, **2003**, 2, 338.

(10) Bandyopadhyaya, R.; Nativ-Roth, E.; Regev, O.; Yerushalmi-Rozen, R. *Nano Lett.*, **2002**, 2, 25.

(11) Mutulu, G. M.; Budinger, G. R. S.; Green, A. A.; Urich, D.; Soberanes, S.; Chiarella, S. E.; Alheid, G. F.; McCrimmon, D. R.; Szleifer, I.; Hersam, M. C. *Nano Lett.*, **2010**, 10, 1664.

(12) Murphy, F. A.; Poland, C. A.; Duffin, R.; Al-Jamal, K. T.; Ali-Boucetta, H.; Nunes, A.; Byrne, F.; Prina-Mello, A.; Volkov, Y.; Li, S.; Mather, S. J.; Bianco, A.; Prato, M.; Macnee, W.; Wallace, W. A.; Kostarelos, K.; Donaldson, K. *Am. J. Pathol.*, **2011**, 178, 2587.

(13) Robinson, J. T.; Hong, G.; Liang, Y.; Zhang, B.; Yaghi, O. K.; Dai, H. *J. Am. Chem. Soc.*, **2012**, 134, 10664.

(14) Iijima, S.; Ichihashi, T. *Nature*, **1993**, 363, 603.

(15) Bethune, D. S.; Kiang, C. H.; Devries, M. S.; Gorman, G.; Savoy, R.; Vazquez, J.; Beyers, R. *Nature*, **1993**, 363, 605.

(16) Dang , X.; Yi, H.; Ham, M. H.; Qi, J.;Yun, D. S.; Ladewski, R.; Strano, M. S.; Hammond, P. T.; Belcher, A. M. *Nat. Nanotechnol*., **2011**, 6, 374.

(17) Kongkanand, A.; Martinez, Dominguez, R.; Kamat, P. V. *Nano Lett.*, **2007**, 7, 676.

(18) Kong, J.; Franklin, N. R.; Zhou, C. W.; Chapline, M. G.; Peng, S.; Cho, K. J.; Dai, H. *Science*, **2000**, 287, 622.

(19) Chen, R. J.; Bangsaruntip, S.; Drouvalakis, K. A.; Kam, N. W. S.; Shim, M.; Yi, L. Kim, W.; Utz, P. J.; Dai, H. *Proc. Natl. Acad. Sci. U.S.A.*, **2003**, 100, 4984.

(20) Qi, P.; Vermesh, O.; Grecu, M.; Javey, A.; Wang, Q.; Dai, H.; Peng, S.; Cho, K. J. *Nano Lett*., **2003**, 3, 347.
(21) Kong, J.; Franklin, N. R.; Zhou, C.; Chapline, M. G.; Peng, S.; Cho, K.; Dai, H. *Science*, **2000**, 287, 622.
(22) Jung, S.; Cha, M.; Park, J.; Jeong, N.; Kim, G.; Park, C.; Ihm, J.; Lee, J. *J. Am. Chem. Soc*., **2010**, 132, 10964.
(23) Bhirde, A. A.; Patel, V.; Gavard, J.; Zhang, G.; Sousa, A. A.; Masedunskas, A.; Leapman, R. D.; Weigert, R.; Gutkind, J. S.; Rusling, J. F. *ACS Nano*, **2009**, 24, 306.
(24) Bianco, A.; Kostarelos, K.; Prato, M. *Curr. Opin. Chem. Biol*., **2005**, 9, 674.
(25) Schröder, E.; Hyldgaard, P. *Mater. Sci. Engineer. C*., **2003**, 23, 721.
(26) Zheng, M.; Jagota, A.; Semke, E. D.; Diner, B. A.; Mclean, R. S.; Lustig, S. R.; Richardson, R. E.; Tassi, N. G. *Nat. Mater*. **2003**, 2, 338.
(27) Chen, R. J.; Zhang, Y.; Wang, D.; Dai, H. *J. Am. Chem. Soc*., **2001**, 123, 3838.
(28) Rastogi, R.; Kaushal, R.; Tripathi, S. K.; Sharma, A. L.; Kaur, I.; Bharawaj, L. M. *J. Coll. Int. Sci.*, **2008**, 328, 421.
(29) Itkis, M. E.; Perea, D. E.; Niyogi, S.; Richard, S. M.; Hammon, M. A.; Hu, H.; Zhao, B.; Haddon R. C. *Nano Lett*., **2003**, 3, 309.
(30) Ziegler, K. J.; Gu, Z.; Peng, H.; Flor, E. L.; Hauge, R. H.; Smalley, R. E. *J. Am. Chem. Soc*., **2005**, 127, 1541.
(31) Blanch, A. J.; Lenehan, C. E.; Quinton, J. S. *J. Phys. Chem. B*, **2010**, 114, 9805.
(32) Sinani, V. A.; Gheith, M. K.; Yaroslavov, A. A.; Rakhnyanskaya, A. A.; Sun, K.; Mamedov, A. A.; Wicksted, J. P.; Kotov, N. A. *J. Am. Chem. Soc.*, **2005**, 127, 3463.
(33) Zorbas, V.; Smith, A. L.; Xie, H.; Ortiz-Acevedo, A.; Dalton, A. B.; Dieckmann, G. R.; Draper, R. K.; Baughman, R. H.; Musselman, I. H. *J. Am. Chem. Soc*., **2005**, 127, 12323.
(34) Edri, E.; Regev, O. *Langmuir*, **2009**, 25, 10459.
(35) Nepal, D.; Geckeler, K. E. *Small*, **2007**, 3, 1259.
(36) Wang, D.; Chen, L. *Nano Lett.*, **2007**, 7, 1480.
(37) Zhang, J.; Wang, A. *J. Colloid Interface Sci.*, **2009**, 334, 212.
(38) Grunlan, J. C.; Liu, L.; Kim, Y. S. *Nano Lett.*, **2006**, 6, 911.
(39) Wang, Y.; Xu, H.; Zhang, X. *Adv. Mater.*, **2009**, 21, 2849.
(40) Rodgers, T.; Shoji, S.; Sekkat, Z.; Kawata, S. *Phys. Rev. Lett.*, **2008**, 101, 127402.
(41) Chen, S.; Jiang, Y.; Wang, Z.; Zhang, X.; Dai, L.; Smet, M. *Langmuir*, **2008**, 24, 9233.
(42) Matsuzawa, Y.; Kato, H.; Ohyama, H.; Nishide, D.; Kataura, H.; Yoshida, M. *Adv. Mater.*, **2011**, 23, 3922.
(43) Lemasson, F.; Tittmann, J.; Hennrich, F.; Stürzl, N.; Malik, S.; Kappes, M. M.; Mayer, M. *Chem. Commun*., **2011**, 47, 7428.
(44) Nobusawa, K.; Ikeda, A.; Kikuchi, J.; Kawano, S.; Fujita, N.; Shinkai, S. *Angew. Chem. Int. Ed.*, **2008**, 47, 4577.
(45) Liang, S.; Chen, G.; Peddle, J.; Zhao, Y. *Chem. Commun.*, **2012**, 48, 3100.
(46) Ding, Y.; Chen, S.; Xu, H.; Wang, Z.; Zhang, X.; Ngo, T. H.; Smet, M. *Langmuir*, **2010**, 26, 16667.
(47) Zhang, Z.; Che, Y.; Smaldone, R. A.; Xu, M.; Bunes, B. R.; Moore, J. S.; Zang, L.

J. Am. Chem. Soc., **2010**, 132, 14113.
(48) Niyogi, S.; Boukhalfa, S.; Chikkannanavar, B.; McDonald T. J.; Heben, M. J.; Doorn, S. K *J. Am. Chem. Soc.*, **2007**, 129, 1898.
(49) Niyogi, S.; Densmore, C. G.; Doorn, S. K. *J. Am. Chem. Soc.*, **2009**, 131, 1144.
(50) Park, C.; Ounaies, Z.; Watson, K. A.; Crooks, R. E.; Smith Jr, J.; Lowther, S. E.; Connell, J. W.; Siochi, E. J.; Harrison, J. S.; St Clair, T. L. *Chem. Phys. Lett*., **2002**, 364, 303.
(51) Huang, W.; Lin, Y.; Taylor, S.; Gaillard, J.; Rao, A. M.; Sun, Y-P. *Nano Lett*., **2002**, 2, 231.
(52) Mutulu, G. M.; Budinger, G. R. S.; Green, A. A.; Urich, D.; Soberanes, S.; Chiarella, S. E.; Alheid, G. F.; McCrimmon, D. R.; Szleifer, I.; Hersam, M. C. *Nano Lett.*, **2010**, 10, 1664.
(53) Wei, Q.; Zhan, L.; Juanjuan, B.; Jing, W.; Jianjun, W.; Taoli, S.; Yi'an, G.; Wangsuo, W. *Nanoscale Res. Lett.*, **2012**, 23, 473.
(54) Robinson, J. T.; Hong, G.; Liang, Y.; Zhang, B.; Yaghi, O. K.; Dai, H. *J. Am. Chem. Soc.*, **2012**, 134, 10664.
(55) Murphy, F. A.; Poland, C. A.; Duffin, R.; Al-Jamal, K. T.; Ali-Boucetta, H.; Nunes, A.; Byrne, F.; Prina-Mello, A.; Volkov, Y.; Li, S.; Mather, S. J.; Bianco, A.; Prato, M.; Macnee, W.; Wallace, W. A.; Kostarelos, K.; Donaldson, K. *Am. J. Pathol.*, **2011**, 178, 2587.
(56) Liu, Z.; Davis, C.; Cai, W.; He, L.; Chen, X.; Dai, H. *Proc. Natl. Acad. Sci. U.S.A.*, **2008**, 105, 1410.
(57) Bhirde, A. A.; Patel, S.; Sousa, A. A.; Patel, V.; Molinolo, A. A.; Ji, Y.; Leapman, R. D.; Gutkind, J. S.; Rusling, J. F. *Nanomedicine*, **2010**, 10, 1535.
(58) Singh, R.; Pantarotto, D.; Lacerda, L.; Pastorin, G.; Klumpp, C.; Prato, M.; Bianco, A.; Kostarelos, K. *Proc. Natl. Acad. Sci. U.S.A.*, **2006**, 103, 3357.
(59) Barone, P. W.; Strano, M. S. *Angew. Chem*., **2006**, 118, 8318.
(60) Matijevic, E. *Langmuir*, **1994**, 10, 8.
(61) Comba, S.; Sethi, R. *Water Res*., **2009**, 43, 3717.
(62) Stepto, R. F. T. *Pure Appl. Chem*., **2009**, 81, 351.
(63) Yu, R.; Hartmann, J.; Tauer, K. Macromol. *Rapid Commun*., **2013**, In press.
(64) Estruga, M.; Chen, L.; Choi, H.; Li, X.; Jin, S. *ACS Appl. Mater. Int*., **2013**, In press.
(65) Klinger, D.; Landfester, K. *Macromol. Rapid Commun*., **2011**, 32, 1979.
(66) Zhang, X.; Yin, L.; Tang, M.; Pu, Y. J. *Nanosci. Nanotechnol*., **2010**, 10, 5213.
(67) Li, X. N.; Guo, H. X.; Heinamaki, J. *J. Coll. Int. Sci*., **2010**, 345, 46.
(68) Franks, R.; Morefield, S.; Wen, J.; Liao, D.; Alvarado, J.; Strano, M.; Marsh, C. *J. Nanosci. Nanotechnol*., **2008**, 8, 4404.
(69) Xu, J. P.; Stevenson, G.; Lu, C. Q.; Lu, S. Q. *J. Phys. Chem. B*, **2006**, 110, 16923.
(70) Bouhamed, H.; Boufi, S.; Magnin, A. J. *Coll. Int. Sci*., **2007**, 312, 279.
(71) Sab ń, J.; Prieto, G.; Ruso, J. M.; Messina, P.; Sarimiento, F., *Phys. Rev. E Stat. Nonlin. Soft Matter. Phys.*, **2007**, 76, 011408.

Chapter 2

Optimization of carbon nanotube dispersion in aqueous solution

The contents in this Chapter have been published in The Journal of Physical Chemistry B with title of "Comparative Dispersion Studies of Single-Walled Carbon Nanotubes in Aqueous Solution" (Koh, B., Park J., Ximiao, H., Cheng, W. *J. Phys. Chem. B.* 2011; 115(11): 2627-2633). My contribution to this paper was design and conduct overall experiments analysis of experimental data and the writing of the manuscript. My collaborators took AFM images and analyzed AFM images.

2.1 Background

It is necessary SWCNTs to be dispersed in aqueous solution in order to use as therapeutic purposes. SWCNTs can be dispersed in aqueous solution in the presence of dispersants or by functionalizing its surface with hydrophilic functional group with aid of sonication. SWCNT dispersion is depending upon sonication time, sonication power, ratio between SWCNTs and dispersants as well as centrifugation steps. Although many

studies have shown successful dispersion of SWCNTs, there are only a few systemic studies regarding optimization of SWCNT dispersion in aqueous solution. This study is focusing on optimizing dispersion condition of SWCNTs in order to ensure maximum dispersion as well as removing impurities and insoluble metallic substances.

2.2 Rationale and Significance

SWCNT dispersion is important as they cannot be spontaneously dispersed in aqueous solution. Currently, only few studies have been carried out for systematic and standardizing SWCNT dispersion protocol. This optimization of SWCNT dispersion study can benefit those who wants to use SWCNTS as a drug/gene carrier and therapeutic reagents.

2.3 Abstract

SWCNTs produced by various methods are commercially available, but systematic characterization of their dispersion behavior in aqueous solution is rare. Here we compare the properties of various SWCNTs after their dispersion in aqueous solution assisted by DNA oligo. UV-visible-NIR absorbance measurement and atomic force microscopy (AFM) imaging showed marked differences among SWCNTs produced from arc-discharge (AD) method, high-pressure carbon monoxide deposition (HiPCO), and chemical vapor deposition (CVD). To our surprise, the SWCNTs produced from AD method showed the highest nanotube purity and the cleanest AFM image, better than

HiPCO SWCNTs that has been used extensively for biological applications. We also report our systematic studies on optimizing dispersing conditions in order to maximize SWCNTs solubility and remove insoluble materials. We recommend a low power and short time of sonication to disperse SWCNTs in order to preserve their average lengths. These results altogether serve as a future guide for the usage of commercial SWCNTs in water-based applications.

2.4 Introduction

Since their discovery in 1993[1,2], SWCNTs have become wonderful materials for diverse applications ranging from building blocks for nanoelectronics[3,4] to potential carriers for drug[5-8] and gene delivery[9,10] owing to their unique physical and chemical properties. Intensive research has been conducted on SWCNTs-mediated DNA delivery to cells[7,9-11]. Although the potential toxicity of SWCNTs on biological system is still under debate[12-14], they are effective carriers of DNA owing to their ability to penetrate cell membrane[7,10]. The solubility of SWCNTs in aqueous solution is very important for their applications as gene carriers. Even though dispersion of SWCNTs in aqueous solution has been widely reported with the aid of dispersive agents including single-stranded DNA oligo (ssDNA) [15], surfactants[16], polymers[17], peptides[18] and proteins[19], currently no systemic studies have been reported on SWCNTs dispersion with ssDNA. It is, therefore, a difficult decision as to which specific SWCNTs to work with, especially for beginners. SWCNTs are known to contain impurities that are often the result of synthesis process[20]. For SWCNTs produced by various methods, how different are they

in terms of impurities? Whether these impurities may carry over to SWCNTs solution during the dissolution process is not yet known. Since these aspects of SWCNTs are very important for their potential biological applications, we therefore set up to carry out a systematic study on the dissolution of SWCNTs in aqueous solution.

Among different types of SWCNTs produced by various methods, SWCNTs made from AD method, HiPCO, and CVD are commercially available. In particular, HiPCO SWCNTs has been extensively used for biological applications. We have measured the distinctive UV-visible-NIR absorbance spectra for these materials under identical conditions after they are dispersed into aqueous solution. By analyzing AFM images of SWCNT/ssDNA complexes, distinct features among these SWCNTs were also observed. To our surprise, the SWCNTs produced from AD method showed the highest nanotube purity and the cleanest AFM image, better than HiPCO SWCNTs. In an effort to optimize the dispersion of SWCNTs, maximize SWCNTs solubility and remove insoluble materials, we report our systematic studies on the effect of sonication time, input power and centrifuge time on the efficiency of SWCNTs dispersion. The results we report herein will hopefully serve as a future guide for the use of commercial SWCNTs in water-based applications.

2.5 Materials and Methods

SWCNTs dispersion and absorbance measurement. AD SWCNTs was purchased from Helix Materials (Richardson, TX) and exists as plain sheet upon arrival. We ground the sheet with pipette tip and used it for dispersion studies. CVD SWCNTs was a gift

from SES research (Houston, TX). It exists as a powder upon arrival. HiPCO SWCNTs was purchased from Unidym (Sunnyvale, CA) and exists as granules. Equal amount of each SWCNTs and DNA oligo $(dT)_{30}$ were sonicated in pH 7.4 phosphate buffer (10mM NaH_2PO_4/Na_2HPO_4, PB) in a Tabletop sonic bath cleaner (Fisher Scientific, FS20H) for 1.5 hours unless otherwise noted. Samples were then centrifuged for 99 minutes at 17,000 g (Thermo Scientific, Legend Pro 17) unless otherwise noted. Supernatant were carefully collected. Dispersed SWCNTs in PB were diluted with 10 mM PB before taking UV-visible-NIR absorbance in UV spectrophotometer (Shimadzu UV-1800, Varian Cary 5000). All spectra were taken using buffer PB as blank. All Buffers throughout this study were made with reagent grade chemicals using distilled water that was further deionized using a Milli-Q System (Millipore Corp., Bedford, MA), ddH_2O.

AFM images of SWCNTs. To deposit dispersed SWCNTs onto mica surface for AFM imaging, newly cleaved mica surface was treated with 0.01% poly-L-lysine solution (Sigma, St. Louis, MO) and incubated for 15 minutes at room temperature, then rinsed with ddH_2O and dried with N_2. Diluted SWCNTs samples were then deposited and incubated for 5 minutes at room temperature and rinsed with ddH_2O and air-dried with N_2. SWCNTs samples for Figure 2-2 (b) and 2-2 (c) were also dialyzed with 100 nm pore size polycarbonate membrane filter (Millipore Corp., Bedford, MA) before imaging. AFM images were taken using a Nanoscope IV multimode AFM (Veeco, Carmarillo, CA) in tapping mode with Si tip (tip size < 10 nm, Nanoworld, Switzerland) unless otherwise noted. Length of SWCNTs was quantitated using Nanoscope III ver 5.31R1.

Inhomogeneity of SWCNTs. Various amounts of SWCNTs were placed in 100 μL 10 mM PB in the presence of 0.1 mg of $(dT)_{30}$ and sonicated for 6 hours in sonic cleaner. Samples were centrifuged as described above and UV-visible-NIR absorbance spectra were measured.

Measurement of extinction coefficient of SWCNTs. Same amount (150 μg each) of SWCNTs and $(dT)_{30}$ were dispersed in same volume (150 μl each) of aqueous solution. After dispersion with sonication, samples were centrifuged as described. Supernatant were carefully removed, and residuals at the bottom of the test tube were delicately dried in the fume hood for one day at room temperature. Weights of residuals were carefully measured using a microbalance (Sartorius ME36S, Gottingen, Germany) with a readability of 1 μg and repeatability weighing ranges of ± 2 μg. The difference between initial weight and the weight of the residues measures the amount of SWCNTs dispersed in aqueous solution. The UV-visible-NIR absorbance of the supernatant was measured and the extinction coefficient of corresponding SWCNTs was calculated.

Acid treatment of SWCNTs. 200 μg of each SWCNTs was added into 1 mL 3:1 concentrated H_2SO_4/HNO_3 solution. The mixture was sonicated for 24 hours in a sonic bath cleaner. After sonication, the mixture was centrifuged for 99 minutes at 17,000 g and the supernatant were collected. The supernatant were dialyzed against 100 nm polycarbonate membrane filter in the presence of ddH_2O for a total of 1 hr and deposited on to the mica surface for AFM analysis.

2.6 Results and discussion

UV-visible-NIR absorbance measurement of SWCNTs. A common method to disperse SWCNTs into aqueous solution is to sonicate the mixture in the presence of a ssDNA. In particular, $(dT)_{30}$ has been identified as the optimal sequence for this process[15]. We therefore dispersed three different SWCNTs in buffer PB in the presence of $(dT)_{30}$, with the mass ratio between SWCNTs and $(dT)_{30}$ set at 1:1. After sonication, the samples were centrifuged at high speed to remove insoluble materials, and the supernatant was taken for UV-visible-NIR absorbance measurement. As shown in figure 2-1, each SWCNTs showed unique absorbance spectrum compare to other samples. Each peak in the absorbance spectrum results from electronic transition of SWCNTs from ground state to excited states, and it has been suggested that the peak position varies with the diameter and chiral angle of each SWCNTs species[21]. Therefore, characteristic peaks which can be seen in both AD and HiPCO SWCNTs absorbance spectrum suggest that these materials contain SWCNTs that have relatively narrow distributions of tube diameter and chiral angle, which is especially true for HiPCO SWCNTs. In contrast, CVD SWCNTs showed no distinct peaks in their UV-visible-NIR spectrum, which suggests that SWCNTs prepared by CVD method have a very broad distribution of diameters and chiral angles. The absorbance spectrum of SWCNTs has been used to provide quantitative information on the relative purity of SWCNTs preparations[22]. Based on this published method and using the S_{22} transition in between 7750 and 11750 cm^{-1} as shown in figure 2-1 (b), we estimate that AD SWCNTs has the highest relative purity

(RP) with the RP of 225.64%, followed by HiPCO SWCNTs with the RP of 186.96% and CVD SWCNTs with the RP of 156.70%. These RP values for SWCNTs are in the range of reported values in the literature: for example, as-prepared SWCNTs: 50~110%[23,24], and purified SWCNTs: 118~170%[24,25]. The analytically pure SWCNTs is estimated to have an RP value of ~230%[26].

AFM images of dispersed SWCNTs. To examine the quality and structural features of the SWCNTs samples dispersed in buffer PB in the presence of oligo, we used tapping mode AFM to image these SWCNTs samples. Samples were deposited on the mica that was treated with poly-(L)-lysine, which binds DNA tightly so that oligo-dispersed SWCNTs can attach to the surface. Figure 2-2 shows these AFM images. Statistics over the height of the tubular structures observed in all these images confirms that they were individual dispersed SWCNTs, with an average height of 0.80 ± 0.35 nm for AD SWCNTs shown in figure 2-2 (a), 0.75 ± 0.07 nm for CVD SWCNTs shown in figure 2-2 (b) and 0.70 ± 0.20 nm for HiPCO SWCNTs shown in figure 2-2 (c), respectively. Consistently and reproducibly, AD SWCNTs showed relatively clean AFM images as compared to either CVD SWCNTs or HiPCO SWCNTs. The white particles seen on AFM images of SWCNTs are impurities that are either carbonaceous material or metal catalysts used during SWCNTs synthesis. The number of these particles on individual AFM images is 19, 203 and 167 for AD, CVD and HiPCO SWCNTs respectively. These images suggest that either AD SWCNTs contains fewer impurities than the other two, or the impurities present in AD SWCNTs may be effectively removed after centrifugation, while these impurities are still present in large quantities for both

CVD and HiPCO SWCNTs, and cannot be removed by additional dialysis right before imaging. AFM images of SWCNTs dispersed in the presence of DNA oligos have been carefully studied by Campbell *et al*.[27]. They revealed distinct periodic pitches around SWCNTs in AFM images that result from wrapping of DNA oligos on the sidewall of SWCNTs. We were also able to observe these periodic pitches around SWCNTs for all the different types of SWCNTs samples, although quantitative features of these pitches vary across different samples (data not shown).

Inhomogeneity determination of SWCNTs samples. It is well known that as-prepared SWCNTs powder is typically very inhomogeneous, i.e., varying in its composition on a micrometer scale[20]. To determine if this is the case for the three different SWCNTs we are using, we measured the concentration of SWCNTs in the supernatant after dispersing an increasing amount of SWCNTs in the presence of DNA oligo under identical conditions. The expectation is that we will obtain a linear relationship between the final concentration of SWCNTs dissolved in the buffer and the starting weight of the SWCNTs material if the sample is homogeneous. However, this is clearly not the case for each SWCNTs sample we have examined on figure 2-3. For each SWCNTs sample, we precisely measured the dry power weight of the sample before the sonication process, and measured the IR absorbance at 808 nm after centrifugation. We choose IR absorbance at 808 nm for concentration estimation in order to directly compare our data with those reported by Kam *et al*.[7] who showed the relationship between absorbance at 808 nm versus SWCNT concentration. In addition, a careful analysis of our UV-visible-IR absorbance spectra for each SWCNTs showed that any wavelength within

the visible-IR range from 400 nm to 1,100 nm displayed linear relationship between absorbance and SWCNTs concentration. The red lines in figure 2-3 represent the best linear fit of all the measured data points. From this result, it is very clear that all these samples, regardless of method of preparation, are all inhomogeneous at microscopic scale, despite the fact that they are all well-mixed powders before we disperse them into aqueous solution. We also measured the concentration of SWCNTs in the supernatant after dispersing exactly the same amount of starting materials each time. The concentration of resulting SWCNTs solution varies broadly based on IR absorbance measurement (data not shown), consistent with the notion that these SWCNTs samples are not homogeneous. To determine the extent of sample inhomogeneity, we have tried to accurately estimate the weight of SWCNTs dispersed in the buffer by measuring the weight of the residual undissolved SWCNTs after centrifugation process. The fraction of dispersed SWCNTs in each sample can therefore be determined, which varies broadly from 0.2% to 12%. From this measurement, we also estimate the extinction coefficients of our SWCNTs samples to be around 8.27 $(mg/mL)^{-1}cm^{-1}$, 22.0 $(mg/mL)^{-1}cm^{-1}$, and 17.4 $(mg/mL)^{-1}cm^{-1}$) for AD, CVD and HiPCO SWCNTs respectively, at 808 nm. The inhomogeneity of SWCNTs samples may be partly explained by the complexity of SWCNTs manufacturing processes and difficulties in removing all the impurities and metal catalysts after the manufacturing process.

Uniform solution of SWCNTs after dispersion. The inhomogeneity of SWCNTs powders makes one wonder whether the mixture is homogeneous after SWCNTs is dispersed into aqueous solutions. In order to address this question, we performed a serial

dilution of the dispersed SWCNTs sample and measured the IR absorbance at 808 nm. The expectation is that the data should follow Beer-Lambert law if the resulting solution of SWCNTs is homogeneous. Indeed, as shown in figure 2-4, the IR absorbance of the diluted SWCNTs sample follows very nicely with the expected sample dilutions in a linear relationship, with R^2 values greater than 0.999. This is true for all the three SWCNTs samples produced using different methods, i.e., AD, CVD and HiPCO. This result suggests that after dispersion by sonication process, each SWCNTs sample is distributed uniformly throughout the aqueous solution, even though each individual SWCNTs may have different diameters and chiral angles. In conclusion, although raw samples of SWCNTs are very inhomogeneous, after they are dispersed into aqueous solutions, the mixture is a homogeneous solution whose absorbance is described by the Beer-Lambert law.

Optimization of sonication time for SWCNTs dispersion. Although DNA oligo-assisted dispersion of SWCNTs has been adopted by many different research groups, a systematic study on sonication conditions that may affect this process has not been reported. We therefore decided to carry out a systematic study on the effect of sonication time, sonicator input power and centrifugal time on the dispersion of SWCNTs in the presence of DNA oligo, with our aim to optimize this process. To investigate the effect of sonication time on the dispersion of SWCNTs in aqueous solution, we started with a fixed amount of SWCNTs powder and sonicated the sample in the presence of $(dT)_{30}$ in buffer PB. At designated time points, we centrifuged the sample to clear the supernatant, and took a small aliquot from the cleared supernatant for IR absorbance measurement in

order to quantitate the amount of SWCNTs dispersed into the buffer. We then vortexed the entire mixture to re-suspend the SWCNTs pellet into the solution, and continued the sonication process. Figure 2-5 shows the result from such measurements for the three different SWCNTs. The time point shown on the x-axis is the time in between successive centrifugation, while the time in parenthesis is the total amount of time lapsed from the beginning. Interestingly, although majorities of the cases show that a longer sonication time leads to a higher concentration of SWCNTs in solution, there are also cases in which no general trend exists. This phenomenon may again be related to the sample inhomogeneity; for certain samples, 1 hour sonication is sufficient as shown in figure 2-5 (b) black line while for other samples, more than 10 hours is needed to disperse all the available SWCNTs as shown in figure 2-5 (b) dark green line.

Optimization of sonication power for SWCNTs dispersion. Dispersion of SWCNTs into aqueous solution is a process of breaking bundled CNT into individual SWCNTs. It is therefore likely that the input sonication power may quantitatively affect this process. To examine the effect of sonication power on SWCNTs dispersion, we started with a fixed amount of SWCNTs powder and sonicated the sample in the presence of $(dT)_{30}$ in buffer PB using an Ultrasonic processor S-4000 (Misonix, Farmingdale, NY) at a power setting of 90, which is equivalent to an output power of 77 W in contrast to the 3 W output power from the regular ultrasonic bath cleaner. At designated time points, we centrifuged the sample to clear the supernatant, and took a small aliquot from the cleared supernatant for IR absorbance measurement in order to quantitate the amount of SWCNTs dispersed into the buffer. We then vortexed the entire mixture to re-suspend

the SWCNTs pellet into the solution, and continued the sonication process. Figure 2-6 red lines show the result from such measurements for the three different SWCNTs, in which the boxplots are averaged results from figure 2-5 at 3 W power for comparison. We noted that although the amount of SWCNTs dispersed into aqueous solution increases with sonication time for certain cases, within error there are no significant differences in SWCNTs concentration obtained from different sonication powers at any given time point. In addition, we conducted experiments where samples were subjected to an increasing power of sonication at designated time points as shown in figure 2-6 black lines. However, the high power sonication did not increase the dispersion of SWCNTs in comparison to the results from low power bath cleaner (box plots). This trend is true for all the three SWCNTs samples tested. One possibility to account for these results is that high power of sonication may shear the DNA to shorter pieces and decrease their ability to disperse SWCNTs. To check for this possibility, we examined the DNA oligo $(dT)_{30}$ before and after sonication at different power setting by running a polyacrylamide gel. The condition of sonication for these oligos was made identical to that in the presence of SWCNTs. Interestingly, the quantity and length of the DNA oligo were the same before and after sonication process (data not shown), suggesting that even at the highest sonication power used, $(dT)_{30}$ was not fragmented and its integrity was fully preserved. Therefore, this result suggests that the low sonication power is already sufficient to disperse bundled SWCNTs into individual pieces in the presence of DNA oligo.

Effects of sonication time and power on SWCNTs length. Study by Zheng *et al*.[15] suggested that sonication may lead to reduction in SWCNTs length. Therefore, we investigated the effects of sonication time and power on SWCNTs length by taking AFM images after sonication under different conditions. AD, CVD and HiPCO SWCNTs all showed significant length reduction after long sonication time as shown in figure 2-7. In addition, high power sonication further reduces the average length of carbon nanotubes. These results suggest that all these SWCNTs may have defects along their side-walls. Upon sonication, the sites of defects are prone to breakage.

Effect of centrifuge time on SWCNTs dispersion. Centrifuge after sonication is necessary in order to remove undissolved SWCNTs and impurities. All the centrifugation steps throughout this study were done at maximum setting, 17,000 g using a tabletop microcentrifuge. We found that 90 min centrifuge time is necessary for all the samples to reach a stable concentration in the supernatant, as shown in figure 2-8 by measuring the absorbance of supernatant at 808nm after various time of centrifugation. AFM images of these samples after >90 minutes of centrifuge at 17,000 g showed no bundled SWCNTs. This result suggests that under our buffer conditions, at least 90 minutes of centrifugation is required in order to remove insoluble materials from SWCNTs samples.

Dispersion of acid-treated SWCNTs in aqueous solution. Acid reflux is a widely-used method to cut and disperse bundled CNT[28]. Treatment of SWCNTs by strong oxidative acid also introduces carboxyl functional groups on the side walls and at

the ends, which may facilitate the dissolution of SWCNTs in aqueous solution. To test this hypothesis, we used the acid mixture (3:1 concentrated H_2SO_4/HNO_3 solution) to treat raw SWCNTs samples for 24 hours to produce oxidized SWCNTs. We then dispersed these acid-treated SWCNTs in buffer PB. Interestingly, acid-treated SWCNTs was successfully dispersed in buffer PB even without $(dT)_{30}$, suggesting that oxidation of SWCNTs indeed create sufficient amount of hydrophilic groups that facilitate the dissolution of SWCNTs in water. However, AFM images of these acid-treated SWCNTs showed marked morphological changes compared to raw SWCNTs dispersed by DNA oligo. Many small particles were stuck around the carbon nanotube side-walls that were not seen in oligo-dispersed SWCNTs as shown in figure 2-9 (a)–(c). In addition, visible-IR absorbance spectra for these acid-treated SWCNTs also changed significantly compared to those dispersed in the presence of DNA oligo as shown in figure 2-9 (d)-(f). Significant loss of peak structures in absorbance spectra was observed for all SWCNTs samples, suggesting an extensive disruption of electronic structures[29].

2.7 Conclusion

We have conducted a systematic study on the dissolution of commercially available SWCNTs in aqueous solution. These SWCNTs were prepared using different methods, AD, CVD, and HiPCO, respectively. Although acid-treatment of these raw materials resulted in the dissolution of these SWCNTs in aqueous solution without the need of DNA oligo or surfactants, the SWCNTs electronic structures are modified significantly. For DNA oligo-assisted dispersion, AD SWCNTs consistently showed the least amount

of impurities as seen from both AFM images and UV-Vis-IR absorbance spectral measurements. Although SWCNTs raw materials are very inhomogeneous, upon dispersion into aqueous solution, they form uniform solutions that are very stable for days. In addition, we investigated sonication time and power on SWCNTs dispersion. Longer time or higher power sonication is not efficient means to increase dispersion of SWCNTs in solution; on the other hand, either condition can promote the breakage of SWCNTs to shorter pieces. Therefore, we recommend a low power and short sonication time for dispersion of SWCNTs in order to preserve their average lengths.

2.8 Acknowledgements

We thank Dr. Adam Matzger, Dr. Bart Bartlett and Dr. Zhan Chen in Department of Chemistry, University of Michigan for sharing the use of their instruments. We thank Hanna Kyungmin Song for her assistance in SWCNTs dispersion experiments. WC thanks start-up funding support from the University of Michigan. WC was also supported in part by Ara Paul Professorship fund at the University of Michigan.

2.9 Figures

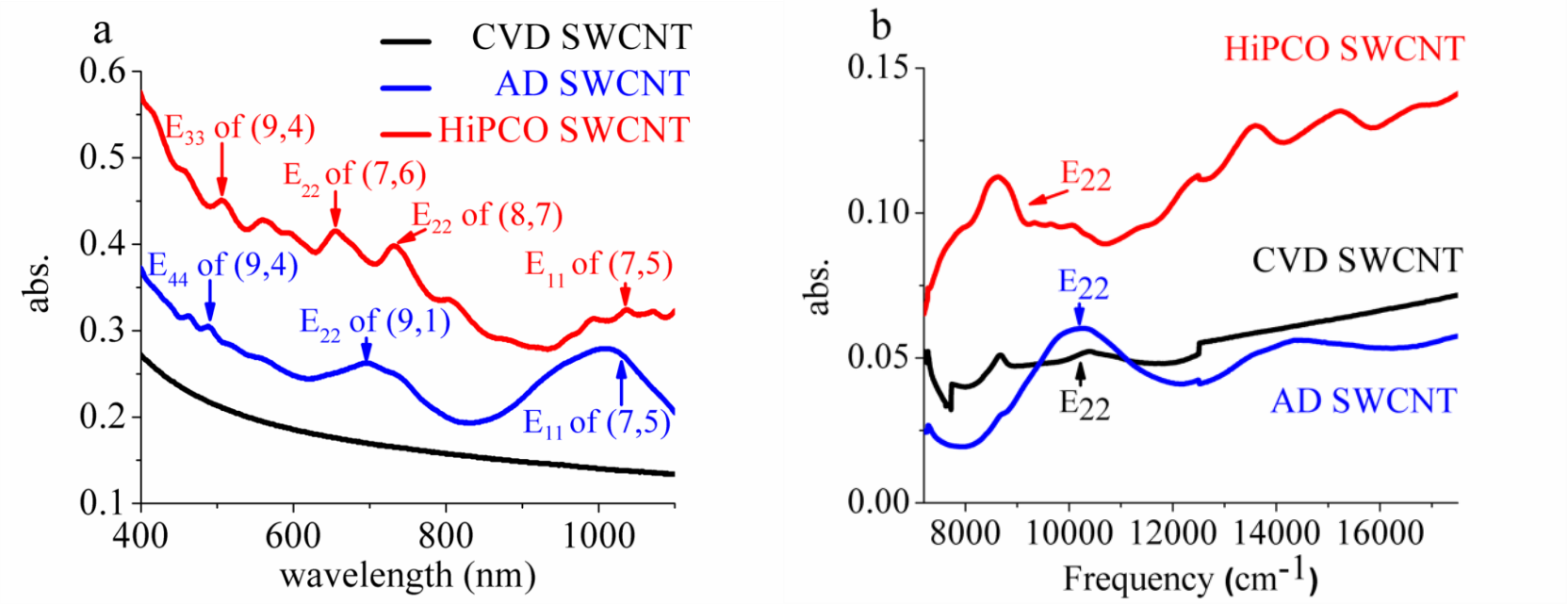

Figure 2-1. (a) UV-visible-NIR spectra of $(dT)_{30}$-dispersed AD, CVD and HiPCO SWCNTs in buffer PB. Each peak corresponds to E_{11}, E_{22}, E_{33} and E_{44} transition of specific SWCNTs {denoted by (n,m)} are shown (b) The spectra region that corresponds to E_{22} transition is shown, based on which the relative purities of SWCNTs are calculated. The spectral discontinuity in (b) is due to change of the lamp during wavelength scanning.

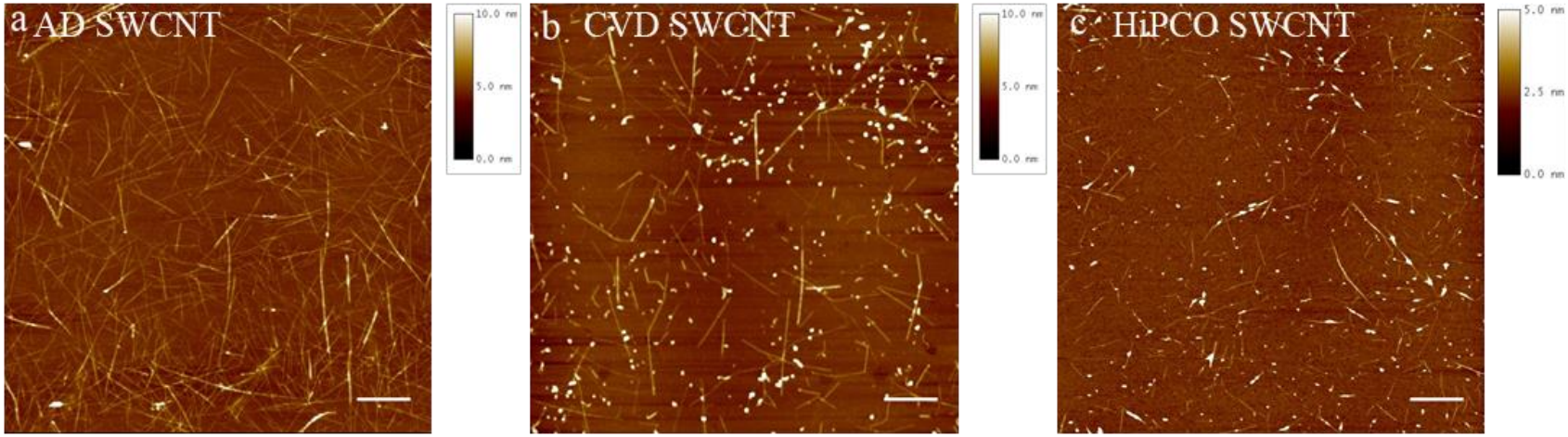

Figure 2-2. AFM images of SWCNTs dispersed in the presence of oligo $(dT)_{30}$ for (a) AD, (b) CVD and (c) HiPCO SWCNTs respectively (scale bar: 500 nm).

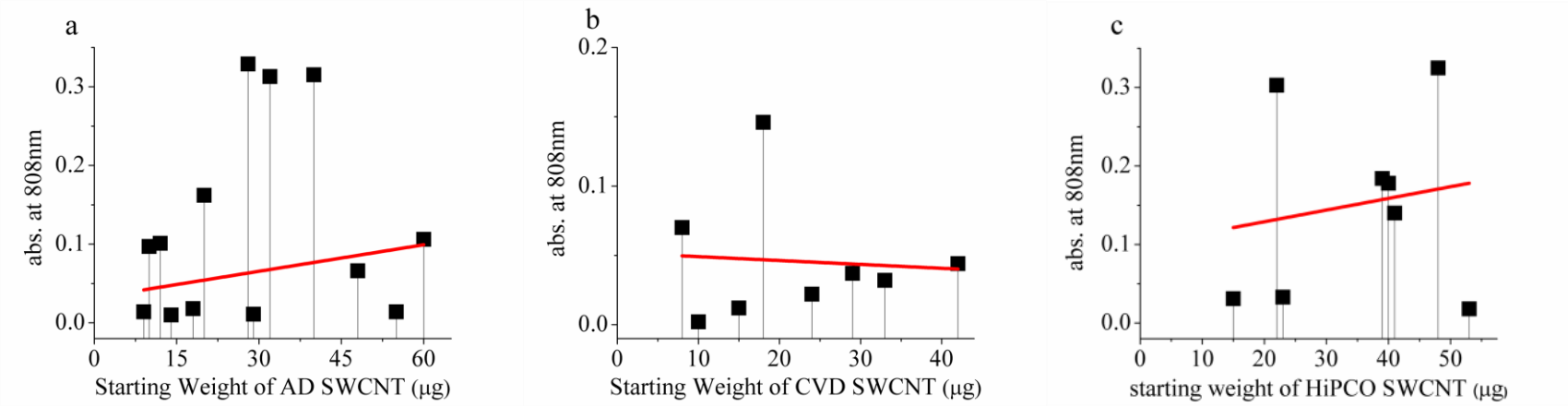

Figure 2-3. Inhomogeneity of SWCNTs samples. Absorbance of SWCNTs dispersed in buffer PB as a function of the starting weight of the SWCNTs powder for (a) AD (b) CVD and (c) HiPCO SWCNTs respectively. The red lines are attempted linear regression analysis with the adjusted R-square value of -0.1163, -0.1605, -0.1340 respectively.

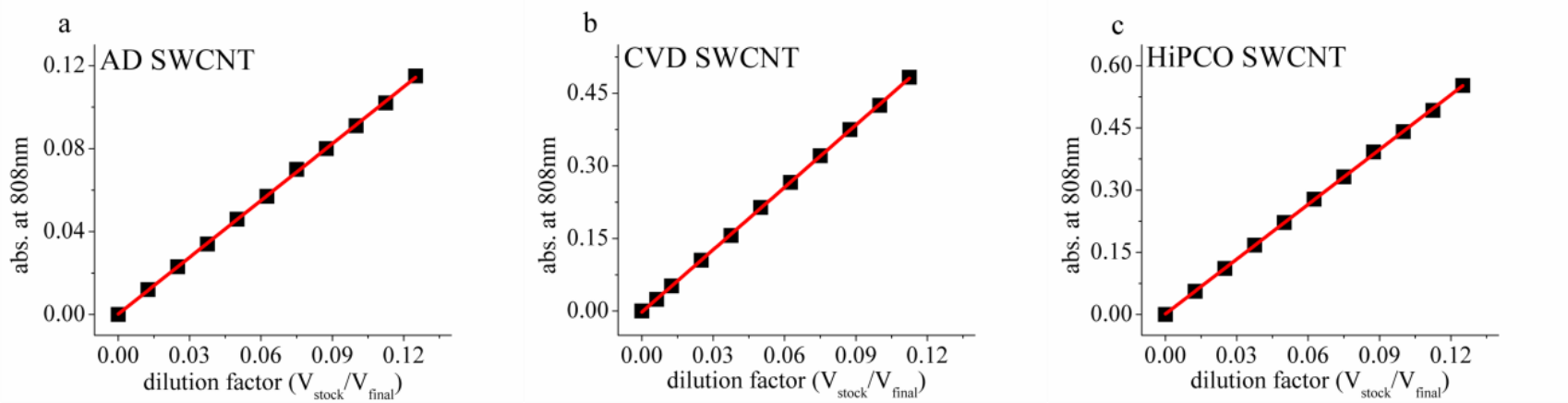

Figure 2-4. Uniformly dispersed SWCNTs in aqueous solution. The absorbance of SWCNTs aqueous solution at 808 nm as a function of the dilution factor is shown for (a) AD (b) CVD and (c) HiPCO SWCNTs, respectively.

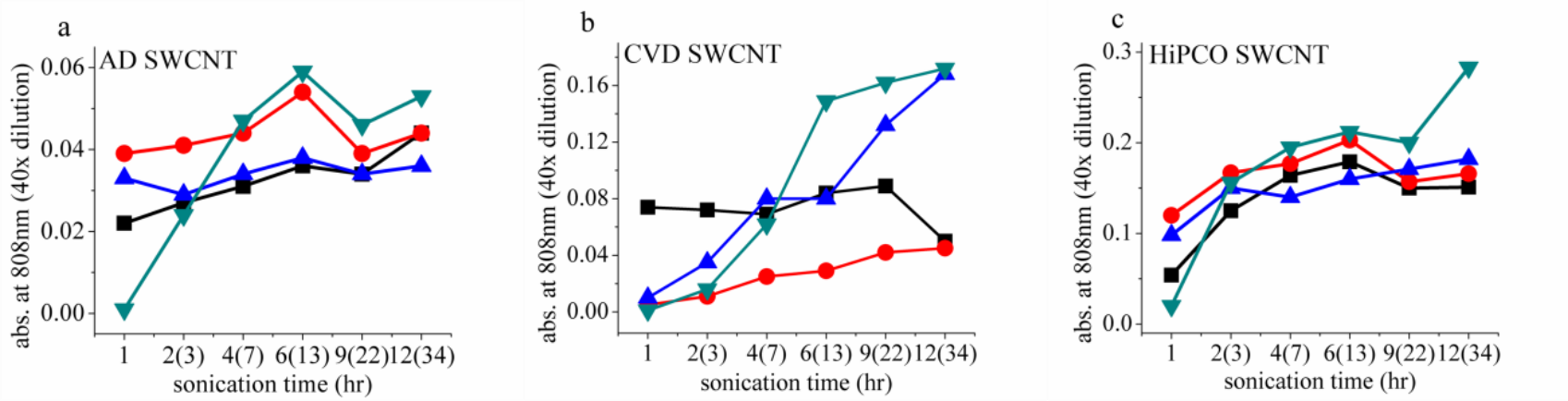

Figure 2-5. Effect of sonication time on SWCNTs dispersion. Absorbance of dispersed SWCNTs (four independent samples for each panel, all under identical conditions) at 808 nm as a function of sonication time shown for (a) AD (b) CVD and (c) HiPCO SWCNTs respectively.

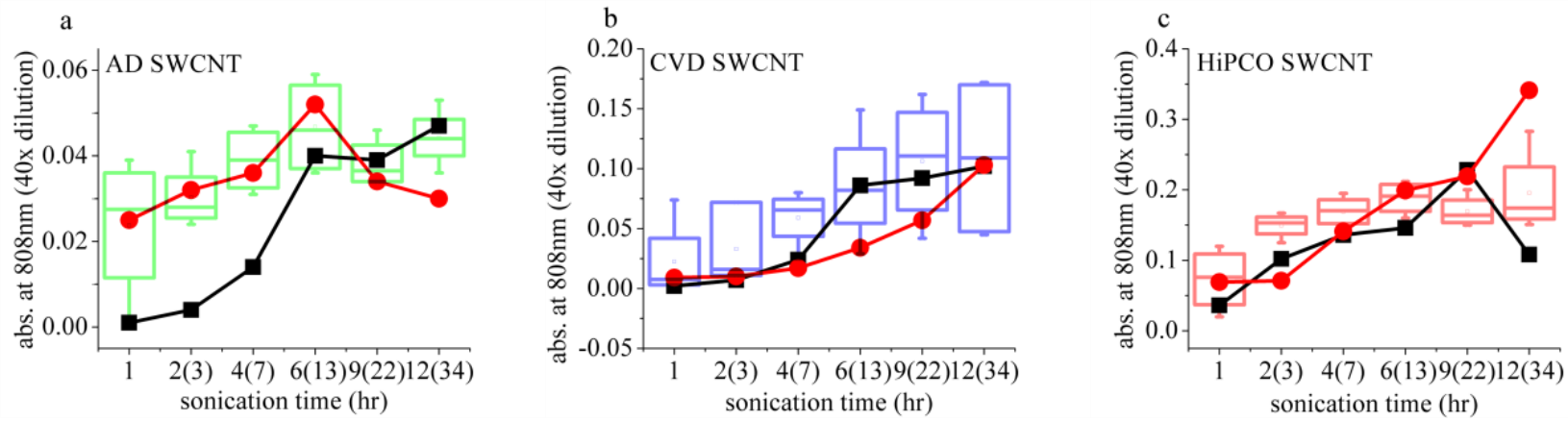

Figure 2-6. Effect of sonication power on SWCNTs dispersion. (a), (b) and (c) are for AD, CVD and HiPCO SWCNTs respectively. For all the panels, red lines show the result from S-4000 at a power level of 77 W (power setting at 90). Green, blue and brown boxplots represent results from low power bath cleaner from figure 5. Black lines show the result from increasing power levels, where 3W was applied during the first three hours using bath cleaner, 15 W was applied for the next 4 hours using S-4000, 40 W was applied for the next 6 hours, 55 W was applied for the next 9 hours, and 77 W was applied for the final 12 hours. The time in parenthesis is the total amount time elapsed since the beginning of the sonication process.

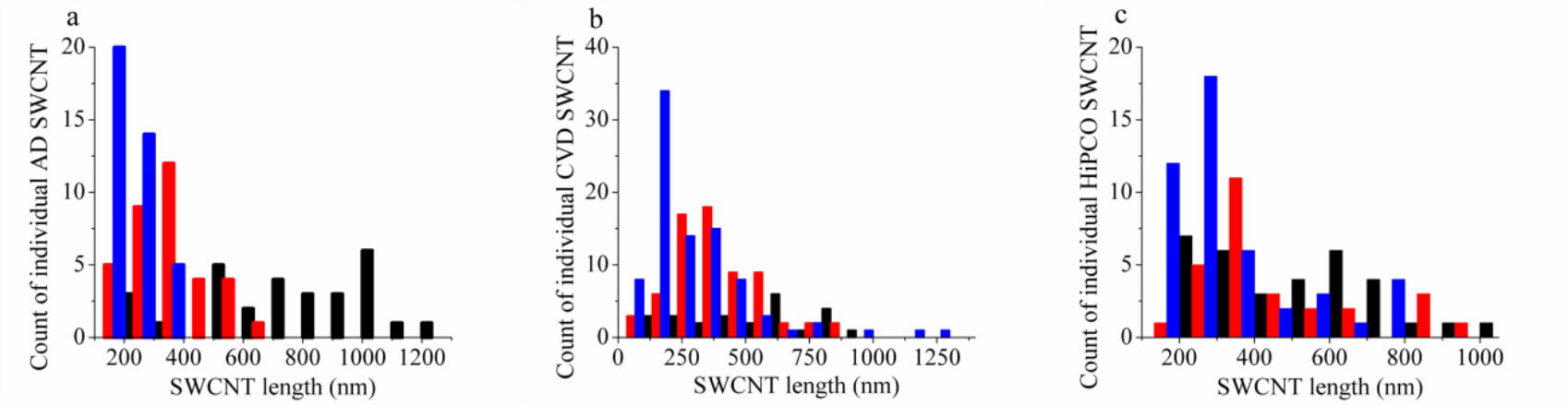

Figure 2-7. Dependence of SWCNTs length distribution on sonication time and power. Black bars represent SWCNTs length after 6 hours sonication in low power sonic cleaner; red bars represent SWCNTs length after 34 hours sonication in sonic cleaner; blue bar represent SWCNTs length after 34 hours sonication in S-4000 sonicator at a power setting of 90 (~ 77 W). (a) AD SWCNTs, the average lengths are 747, 329, and 189 nm for black, red and blue bars respectively; (b) CVD SWCNTs, the average lengths are 561, 366, and 185 nm for black, red and blue bars respectively; (c) HiPCO SWCNTs, the average lengths are 510, 353, and 227 nm for black, red and blue bars respectively.

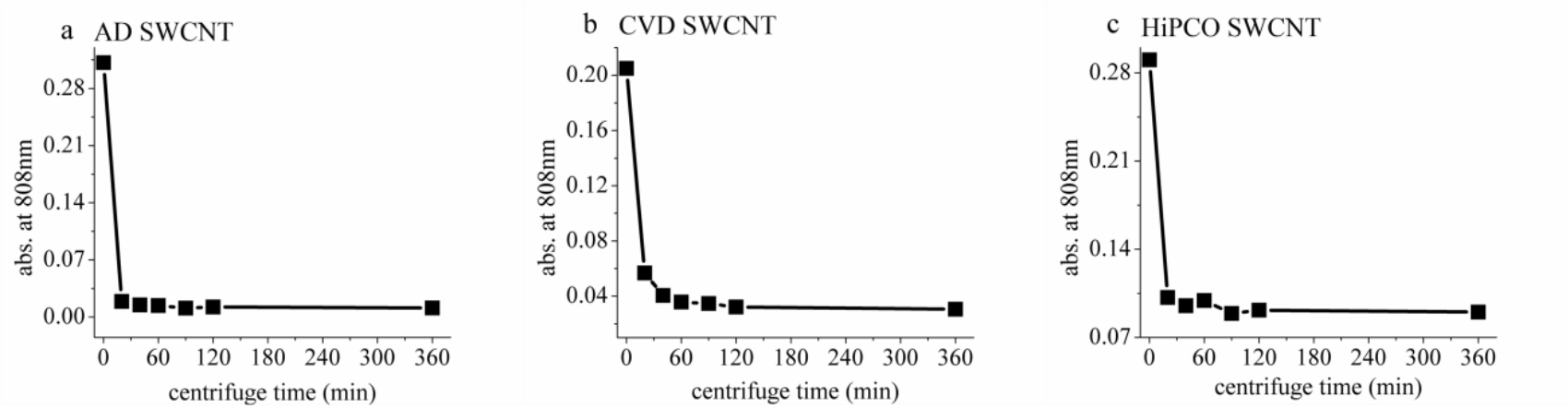

Figure 2-8. Absorbance of supernatant as a function of the centrifugation time for (a) AD (b) CVD and (c) HiPCO SWCNTs, respectively. 150 µg AD, CVD and HiPCO SWCNTs with 150 µg $(dT)_{30}$ in 150 µL buffer PB were dispersed in sonic cleaner for 6 hours. After dispersion, 2 µL of supernatant was collected after designated centrifuge time and absorbance was measured.

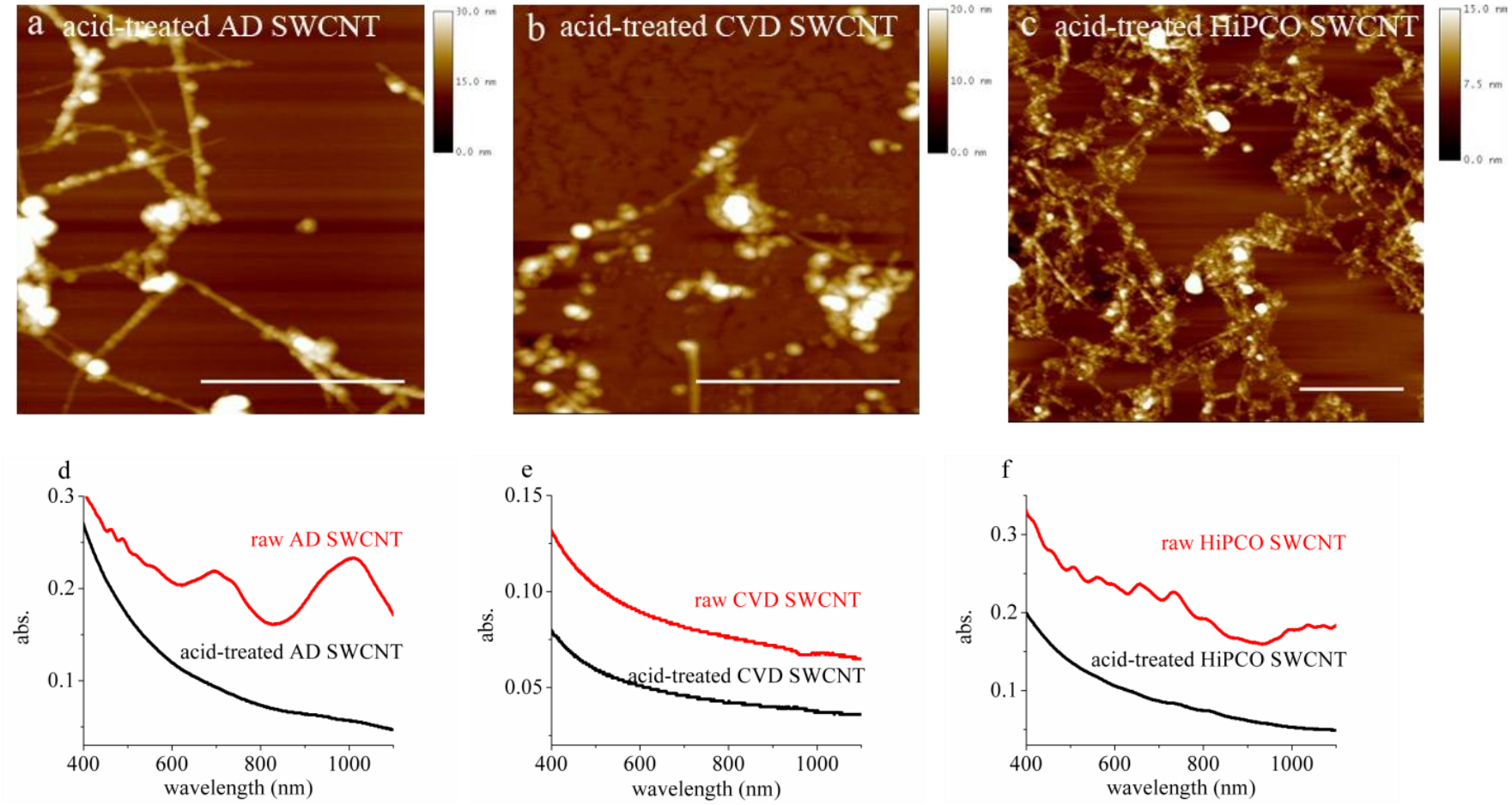

Figure 2-9. Top: AFM images of oxidized SWCNTs dispersed in buffer PB without DNA oligo for (a) AD, (b) CVD and (c) HiPCO SWCNTs respectively (scale bar: 500 nm). Bottom: visible-NIR spectra (red) of acid-treated SWCNTs dispersed in buffer PB, where (d), (e) and (f) represent AD, CVD and HiPCO SWCNTs respectively. The visible-IR absorbance spectra of corresponding raw SWCNTs dispersed with $(dT)_{30}$ are shown in black for comparison.

2.10 References

(1) Iijima, S.; Ichihashi, T. *Nature*, **1993**, 363, 603.
(2) Bethune, D. S.; Kiang, C. H.; Devries, M. S.; Gorman, G.; Savoy, R.; Vazquez, J.; Beyers, R. *Nature*, **1993**, 363, 605.
(3) Mintmire, J. W.; Dunlap, B. I.; White, C. T. *Phys. Rev. Lett.*, **1992**, 68, 631.
(4) Dekker, C. *Phys. Today*, **1999**, 52, 22.
(5) Chen, J.; Chen, S.; Zhao, X.; Kuznetsova, L. V.; Wong, S. S.; Ojima, I. *J. Am Chem Soc.*, **2008**, 130, 16778.
(6) Dhar, S.; Liu, Z.; Thomale, J.; Dai, H.; Lippard, S. J. *J. Am. Chem. Soc.*, **2008**, 130, 11467.
(7) Kam, N. W.; O'Connell, M.; Wisdom, J. A.; Dai, H. *Proc. Natl. Acad. Sci. U, S,A.*, **2005**, 102, 11600.
(8) Prato, M.; Kostarelos, K.; Bianco, A. *Acc. Chem. Res.*, **2008**, 41, 60.
(9) Cai, D.; Mataraza, J. M.; Qin, Z. H.; Huang, Z.; Huang, J.; Chiles, T. C.; Carnahan, D.; Kempa, K.; Ren, Z. *Nat. Methods*, **2005**, 2, 449.
(10) Singh, R.; Pantarotto, D.; McCarthy, D.; Chaloin, O.; Hoebeke, J.; Partidos, C. D.; Briand, J. P.; Prato, M.; Bianco, A.; Kostarelos, K. *J. Am. Chem. Soc.*, **2005**, 127, 4388.
(11) Wu, Y.; Phillips, J. A.; Liu, H.; Yang, R.; Tan, W. *ACS Nano*, **2008**, 2, 2023.
(12) Poland, C. A.; Duffin, R.; Kinloch, I.; Maynard, A.; Wallace, W. A.; Seaton, A.; Stone, V.; Brown, S.; Macnee, W.; Donaldson, K. *Nat. Nanotechnol.*, **2008**, 3, 423.
(13) Yang, H.; Liu, C.; Yang, D.; Zhang, H.; Xi, Z. *J. Appl. Toxicol.*, **2009**, 29, 69.
(14) Liu, Z.; Davis, C.; Cai, W.; He, L.; Chen, X.; Dai, H. *Proc. Natl. Acad. Sci. U.S.A.*, **2008**, 105, 1410.
(15) Zheng, M.; Jagota, A.; Semke, E. D.; Diner, B. A.; McLean, R. S.; Lustig, S. R.; Richardson, R. E.; Tassi, N. G. *Nat. Mater.*, **2003**, 2, 338.
(16) Blanch, A. J.; Lenehan, C. E.; Quinton, J. S. *J. Phys. Chem. B*, **2010**, 114, 9805.
(17) Sinani, V. A.; Gheith, M. K.; Yaroslavov, A. A.; Rakhnyanskaya, A. A.; Sun, K.; Mamedov, A. A.; Wicksted, J. P.; Kotov, N. A. *J. Am. Chem. Soc.*, **2005**, 127, 3463.
(18) Zorbas, V.; Smith, A. L.; Xie, H.; Ortiz-Acevedo, A.; Dalton, A. B.; Dieckmann, G. R.; Draper, R. K.; Baughman, R. H.; Musselman, I. H. *J. Am. Chem. Soc.*, **2005**, 127, 12323.
(19) Edri, E.; Regev, O. *Langmuir*, **2009**, 25, 10459.
(20) Freiman, S.; Hooker, S.; Migler, K.; Arepalli, S. NIST Special Publication, **2008**, 960.
(21) Bachilo, S. M.; Strano, M. S.; Kittrell, C.; Hauge, R. H.; Smalley, R. E.; Weisman, R. B. *Science*, **2002**, 298, 2361.
(22) Itkis, M. E.; Perea, D. E.; Niyogi, S.; Rickard, S. M.; Hamon, M. A.; Zhao, B.; Haddon, R. C. *Nano Lett.*, **2003**, 3, 309.
(23) Hu, H.; Yu, A.; Kim, E.; Zhao, B.; Itkis, M. E.; Bekyarova, E.; Haddon, R. C. *J. Phys. Chem. B*, **2005**, 109, 11520.
(24) Yu, A.; Bekyarova, E.; Itkis, M. E.; Fakhrutdinov, D.; Webster, R.; Haddon, R. C. *J. Am. Chem. Soc.*, **2006**, 128, 9902.

(25) Paul, S.; Kim, D. W. *Carbon*, **2009**, 47, 2436.
(26) Itkis, M. E.; Perea, D. E.; Jung, R.; Niyogi, S.; Haddon, R. C. *J. Am. Chem. Soc.*, **2005**, 127, 3439.
(27) Campbell, J. F.; Tessmer, I.; Thorp, H. H.; Erie, D. A. *J. Am. Chem. Soc.*, **2008**, 130, 10648.
(28) Liu, J.; Rinzler, A. G.; Dai, H.; Hafner, J. H.; Bradley, R. K.; Boul, P. J.; Lu, A.; Iverson, T.; Shelimov, K.; Huffman, C. B.; Rodriguez-Macias, F.; Shon, Y. S.; Lee, T. R.; Colbert, D. T.; Smalley, R. E. *Science*, **1998**, 280, 1253.
(29) Bahr, J. L.; Yang, J.; Kosynkin, D. V.; Bronikowski, M. J.; Smalley, R. E.; Tour, J. M. *J. Am. Chem. Soc.*, **2001**, 123, 6536.

Chapter 3

Structural and Chemical Requirement for Carbon Nanotube Dispersants

The contents in this Chapter have been published in Langmuir with title of "Fluorophore and dye assisted dispersion of carbon nanotubes in aqueous solution" (Koh, B., Kim G., Yoon, H. K., Park, J. B., Kopelman, R., Cheng, W. *Langmuir* 2012; 28(32): 11676-11686). My contribution to this paper was design and conduct overall experiments, analysis of experimental data and the writing of the manuscript. My collaborators did cell transfection experiments and transfection data analysis as well as took AFM images of carbon nanotubes dispersed by different fluorophores and dye molecules.

3.1 Background

As we discussed in previous section, SWCNTs can be dispersed in aqueous solution in the presence of dispersants. Studies have been suggested that structural requirements for nanotube dispersants are having both hydrophobic and hydrophilic moieties so that hydrophobic portion of dispersant can adsorb onto surface of SWCNTs

while hydrophilic moiety facing aqueous environment. However, detailed structural elements which are responsible for SWCNT dispersion is still not well understood. Here, using fluorophores and dye molecules, we tried to disperse SWCNTs and find chemical and structural elements of successful SWCNT dispersants.

3.2 Rationale and Significance

Fluorophores and dye molecules both have hydrophobic and hydrophilic moieties which share similar structural requirement of SWCNT dispersants. By using variety of different fluorophores and dye molecules, we tried to investigate and confirm structural and chemical requirement for successful SWCNT dispersants.

3.3 Abstract

DNA short oligo, surfactant, peptides and polymer assisted dispersion of SWCNTs in aqueous solution have been intensively studied. It has been suggested that van der Waals interaction, π-π stacking and hydrophobic interaction are major factors that account for the SWCNTs dispersion. Fluorophore and dye molecules such as rhodamine B and fluorescein have both hydrophilic and hydrophobic moieties. These molecules also contain π-conjugated systems that can potentially interact with SWCNTs to induce its dispersion. Through a systematic study, here we show that SWCNTs can be dispersed in aqueous solution in the presence of various fluorophore or dye molecules. However, the ability of a fluorophore or dye molecule to disperse SWCNTs is not correlated with

the stability of the fluorophore/dye- SWCNT complex, suggesting that the on-rate of fluorophore/dye binding to SWCNTs may dominate the efficiency of this process. We also examined the uptake of fluorophore molecules by mammalian cells when these molecules formed complexes with SWCNTs. The results can have potential applications in the delivery of poor cell-penetrating fluorophore molecules.

3.4 Introduction

Since its discovery[1,2], SWCNTs have found increasing applications in diverse disciplines ranging from nano-electronics[3,4] and photovoltaic devices[5,6] to drug, gene and small molecule delivery[7-10]. However, a major hurdle to these applications is the poor solubility of SWCNTs in aqueous solution. Many careful studies have been conducted to disperse SWCNTs in aqueous solutions using various assisting agents, which include DNA short oligo[11,12], surfactants[13-17], synthetic polymers[18,19], proteins[20], peptides[21,22], natural organic matter[23] and characterization of SWCNTs after dispersion[24]. It has been proposed that the conjugated π system in DNA, proteins or surfactants can form π-stacking with SWCNT surface and thus prevent SWCNTs from aggregation[11,25,26]. In addition, van der Waals interactions and hydrophobic interactions between these molecules and SWCNTs have been considered as the driving force for SWCNT dispersion in aqueous solution[27,28]. Several studies have been conducted on SWCNTs and fluorophore molecules. These include fluorophore (Rhodamine B) and dye (Methylene Blue) mediated precipitation of water solubilized carbon nanotube[29], fluorescence quenching of Rhodamine B near carbon nanotube[30], fluorophore

conjugation to oxidized SWCNTs[31], pegylated dye (PEG-Malachite Green) mediated dispersion of SWCNTs[32], adsorption of dye (Methylene Blue and Orange II) onto functionalized Multi-Walled carbon nanotubes[33], and perylene derivatives assisted dispersion of SWCNTs[34-36]. Here we present systematical studies on SWCNT dispersion in aqueous solution assisted by various common fluorophore or dye molecules. These fluorophores include Rhodamine B isothiocyanate (RB), Fluorescein isothiocyanate (FITC), Fluorescein sodium salt (FSS) and Fluorescein (FLUO). The dye molecules include Trypan blue (TB), Phenol red sodium salt (PR), orange II sodium salt (OII), Malachite green (MG) and Thionin acetate salt (TAS). These molecules have both hydrophilic and hydrophobic moieties and π conjugated systems in their structures, same as all the other reagents that can disperse SWCNTs in aqueous solution (Figure 3-1). We found that almost all these fluorophore or dye molecules can disperse SWCNTs, albeit with different efficiencies. To examine the possible causes for these different efficiencies, we measured the dissociation kinetics for each fluorophore or dye molecules from SWCNTs. To identify possible applications for these findings, we examined SWCNT mediated transport of fluorophores into mammalian cells.

3.5 Materials and Methods

UV-visible-NIR absorbance measurement of SWCNT/fluorophore and SWCNT/dye. AD SWCNTs were produced by Helix Materials Solution, TX. UV-visible-NIR absorbance spectra of dispersed SWCNT samples were taken in Shimadzu UV-1800 (Osaka, Japan) spectrophotometer and extended NIR absorbance spectra

(Figure 3-2 and 3-3 in particular) were recorded with Cary 5000 UV-Vis-NIR spectrophotometer (Agilent Technologies, CA). All spectrophotometers were turned on at least 30 minutes before the measurement to stabilize the baseline. All spectra were taken using ddH_2O or PB as blank. For AD SWCNTs, absorbance at 1023 nm were chosen for further analysis since AD SWCNTs showed peak absorbance at this wavelength {which corresponds to S_{22} transition of AD SWCNTs}. RB, FITC, FSS, FLUO, TB, PR and OII without SWCNTs in aqueous solution showed no apparent absorption at 1023 nm wavelength. 5 fold diluted SWCNT/fluorophore and SWCNT/dye samples were used for UV-vis-NIR absorbance measurement. Using estimated extinction coefficient of AD SWCNTs of 8.27 $(mg/mL)^{-1}cm^{-1}$ at 808 nm[37], we calculated an extinction coefficient of 11.43 $(mg/mL)^{-1}cm^{-1}$ at 1023 nm, based on which we can determine the concentration of SWCNTs in the dispersed samples.

AFM images of SWCNT/fluorophore and SWCNT/dye. SWCNT/fluorophore and SWCNT/dye on mica were measured in air by tapping-mode AFM (Nanoscope IV, Bruker, USA) with a silicon AFM probe (resonance frequency 320 kHz, spring constant 40 N/m, Nanoworld, Switzerland). 4 μl of each fluorophore-SWCNT solutions were dropped on mica surface and incubated for 15 minutes at room temperature, then rinsed with ddH_2O and dried by N_2 gas. The average height and diameter values were statistics over many different locations in at least five different AFM images that we collected from each dispersed SWCNT samples.

Fluorophore and dye concentration-dependent dispersion of SWCNTs. ~500 μg of AD SWCNTs (Helix Materials Solution, TX) were sonicated for 1 hr in Ultrasonic processor (Misonix, Farmingdale, NY, S-4000) at amplitude level 1 (which corresponds to ~15 W) in the presence of various concentrations of fluorophore (25, 50, 250, 400, 500, 1000, 1850 and 20000 μM). The sonication was programmed with pulse on for 15 seconds and pulse off for 5 seconds in order to prevent overheating. In addition, ice was constantly added in order to maintain temperature (<15 ℃). RB, FSS and FLUO were dissolved in double-deionized water (ddH_2O) while FITC (EMD chemicals, NJ) was dissolved in 10 mM pH 7.4 Phosphate buffer (PB). Similarly, ~500 μg of SWCNTs were sonicated in the presence of various concentrations of dye (25, 100, 250, 1000, 2000 and 8000 μM). TB, MG, PR, TAS and OII were all dissolved in ddH_2O. Dispersed SWCNT samples were then centrifuged for 30 minutes at 12,000 g and supernatant was collected for further characterization. All reagents and chemicals listed in this section except FITC were purchased from Sigma-Aldrich (St. Louis, MO).

Raman spectroscopy of SWCNT/fluorophore and SWCNT/dye 20 μL of each SWCNT samples dispersed in D_2O (Sigma-Aldrich) were deposited onto Aluminum foil on a glass slide and analyzed using two different wavelengths of laser (633 and 785 nm, inVia Raman Microscope, Renishaw, IL). Different laser powers were tested to optimize signal to background, and the optimized measurement conditions are as follows; for 633 nm laser, 30 seconds exposure time, 2 times accumulation and 10 % laser power setting were used; for 785 nm laser, 60 seconds exposure time, 1 time accumulation and 100%

laser power setting were used. All the spectra were normalized to G band which has a peak around 1592 cm^{-1}.

SWCNT/fluorophore and SWCNT/dye dialysis experiment. 30 μl of each SWCNT/fluorophore and SWCNT/dye were applied on an Isopore polycarbonate membrane (Millipore, MA, 50 nm pore size membrane were used for the dialysis of SWCNT/RB, SWCNT/FSS, SWCNT/FITC and 100 nm pore size membrane were used for the dialysis of SWCNT/FLUO, SWCNT/TB, SWCNT/PR and SWCNT/OII due to the discontinued production of 50 nm pore size membrane from the supplier). The samples were dialyzed against 30 mL ddH_2O for designated length of time. Samples were then collected and volume changes were recorded. The collected samples were centrifuged for 30 minutes at 17,000 g and supernatant was collected. Changes in concentrations of SWCNT/fluorophore, free fluorophore or free dye were carefully examined by monitoring changes in UV-visible absorbance. The fraction of SWCNTs that remained in aqueous solution was quantitated with the new concentration and volume measured.

SWCNT/fluorophore and SWCNT/dye isochronal temperature assay. This assay estimates thermal stability of SWCNT/fluorophore or SWCNT/dye complex. For isochronal temperature assays, we incubated SWCNT samples at varied temperatures, and determine SWCNT aggregation after fixed length of time. Initial dispersed samples of SWCNT/fluorophore or SWCNT/dye were aliquoted in 40 μl volume in PCR tubes and incubated for 10 minutes at designated temperature (20 ~ 130 ℃). After incubation,

samples were quickly brought to room temperature by plunging into ice and centrifuged at 17,000 g for 30 minutes in order to remove nanotube bundles formed. Supernatant were carefully collected and absorption at 1,023 nm was determined. Fraction of SWCNT/fluorophore or SWCNT/dye that remained in the solution after incubation at designated temperature was relative to "zero time" reference sample.

Dissociation kinetics of SWCNT/Fluorophore and SWCNT/dye by Eyring analysis. Dissociation kinetics of SWCNT samples were measured by incubation of each sample at a fixed temperature for various length of time. Initial dispersed samples of SWCNT/Fluorophore or SWCNT/dye were aliquoted into 40 μl volume in PCR tubes. Each aliquot was heated at designated temperatures, 62, 70, 80, 90, 99 ℃ in thermal cycler (S1000, Bio-Rad, CA). After heating for designated length of time, samples were cooled on ice and then centrifuged at 17,000 g for 30 minutes. Supernatant was probed with UV-visible-NIR absorbance spectrophotometer. We determined fraction that remained after incubation relative to "zero time" reference sample. We used nonlinear least squares analysis to analyze the process curves. For those that can be described by first-order exponential decay function $\{y = A_1*\exp(-x/t_1) + y_0\}$, we extracted the rate constant t_1 and conducted Eyring analysis.

Cell transfection Experiment. 500 μl of 9L gliosarcoma cells were seeded and incubated for 24 hours before transfection with SWCNT/fluorophore in 8-well Lab-Tek glass chamber slide (Nunc, NY). 1 μl of sample (SWCNT/RB in ddH_2O, SWCNT/FITC in 10 mM PB, SWCNT/FSS in ddH_2O and SWCNT/FLUO in ddH_2O, respectively) was

added and incubated with the cells for another 18 hours. Cells were then washed three times with Gibco RPMI (Invitrogen, CA) and examined under the confocal microscope (Olympus IX70, Japan). 60X oil immersion objective lens (Olympus, Japan) were used for imaging. 488 nm laser was used to excite the samples for all experiment except RB, which 561 nm laser was used. 1,000 ms exposure time was adopted for all experiment except for RB samples, in which 400 ms exposure time was used. No autofluorescence was detected at either of the two exposure times (Supplementary figure 3-1). Simultaneously, 1 μl of free fluorophore solution (RB in ddH_2O, FITC in 10 mM PB, FSS in ddH_2O and FLUO in ddH_2O, respectively) was added and incubated with control cells as described above for simultaneous comparison. Surface charge of each SWCNT/fluorophore was measured with Malvern Zetasizer Nano ZS90 (Malvern, UK).

Flow cytometry experiment 500 μl of 9L cells were seeded and incubated for 24 hours on 12-well cell culture plate (Corning, NY) before transfection with each 1 μl of SWCNT/Fluorophore, free fluorophore and blank buffer. After transfection, cells were incubated for another 18 hours and then washed three times with RPMI. Cells were trypsinized and collected into 5 mL polystyrene round-bottom tubes (BD Science, MA) and kept an ice before analysis on FACSDiVa Cell Sorter (BD science, MA). For cells transfected with FITC, SWCNT/FITC, FSS, SWCNT/FSS, FLUO, and SWCNT/FLUO, 488 nm laser excitation was used. For cells transfected with RB or SWCNT/RB, 561 nm laser excitation was used. Cell autofluorescence in the absence of any transfection was also measured as one of the control experiments (Supplementary figure 3-2).

3.6 Results and discussion

Characterization of SWCNT/fluorophore. Recent studies suggested water-soluble perylene derivatives[34-36] can disperse SWCNTs in aqueous solution. To investigate whether conventional fluorophore molecules can disperse SWCNTs, we sonicated raw SWCNTs in the presence of fluorophore molecules (FITC, FSS, FLUO and RB). The samples were centrifuged and supernatant was collected for further characterization. Figure 3-2. (a) shows the appearance of each fluorophore solution before and after SWCNT dispersion. Visible-NIR absorbance spectra of SWCNT/fluorophore were also measured {Figure 3-2. (b)}. Based on previous studies by Haddon and others,[38-40] the peak in between 600~800 nm corresponds to the first metallic transition (M_{11}), while the peak in between 850~1200 nm corresponds to the second semiconducting transition (S_{22}). Overall, the visible-NIR absorbance spectra of SWCNT/fluorophore were similar in patterns to that of dispersed with DNA oligo, $(dT)_{30}$, suggesting that SWCNTs retain their major electronic structures after dispersion with flurophore molecules. However, there were slight shifts in certain peak locations (S_{22} for example), suggesting that these fluorophores stack on SWCNT surface differently from DNA oligo, which in turn changes the energetic level of electronic transitions. Consistent with previous observations[37], the peaks in absorbance spectra are broad, which is due to relatively large diameter of AD SWCNTs and thus the presence of many chiral vectors with similar optical transitions. To examine the structural morphology of these fluorophore-dispersed SWCNTs, we conducted tapping-mode AFM imaging. These images are shown in figure 3-2, with panels (c), (d), (e) and (f) for SWCNTs dispersed

with RB, FITC, FSS and FLUO, respectively. The detailed statistics on the length and height of these SWCNTs are shown in Table 3-1. Briefly, these statistics do not show significant differences (<26% variation) from those SWCNTs dispersed with DNA oligo $(dT)_{30}$ under identical conditions. In addition, height distribution of each SWCNT/fluorophore sample in AFM images ranges from 1.47 to 1.99 nm (Table 3-1), which agrees very well with the single tube diameter of 1.5 ~ 2 nm measured for AD SWCNTs using transmission electron[41]. This suggests that majority of SWCNTs in these samples are singly dispersed. Of note, the samples of each SWCNT/flurophore for imaging were prepared with the same concentration of SWCNTs for all. However, the number of SWCNTs seen on the mica surface varied from sample to sample {Figure 3-2. (c)~ (f)}. This is probably because each SWCNT/fluorophore has different ability to adsorb on the surface of mica.

Characterization of SWCNT/dye. Similar to fluorophore dispersion of SWCNTs, we observed color changes of the dye solution upon dispersion of SWCNTs {Figure 3-3. (a)}. Except TB (originally dark navy color in aqueous solution), both PR and OII solutions became visually darker after dispersion of SWCNTs. NIR absorbance of SWCNTs remained largely unchanged in 850-1400 nm range, although absorption peak locations may be changed slightly after dispersion by dye molecules {Figure 3-3. (b)}. This suggests that dye molecules do not significantly perturb electronic structures of SWCNTs, although these dye molecules may stack differently on SWCNT surface compared to DNA oligo $(dT)_{30}$. AFM images of these dye-dispersed SWCNTs show

lengths and heights that are comparable to each other (<20% variation, Table 3-1), similar to those dispersed by fluorophore or DNA oligos.

Fluorophore and dye concentration-dependent dispersion of SWCNTs.

Typical fluorophore and dye molecules have both aromatic rings and hydrophilic moieties that are necessary for dispersing SWCNTs in aqueous solution. However, depending on the nature of the aromatic ring structures and the chemical groups in the hydrophilic moieties, different molecules may have different threshold concentration that is needed to disperse SWCNTs effectively. To investigate this possibility, we studied the dispersion of SWCNTs as a function of fluorophore or dye concentration. We choose AD SWCNTs for our studies as we discovered previously that AD SWCNTs showed highest SWCNTs purity over either CVD or HiPco SWCNTs after dispersion in our experimental system[37]. We sonicated SWCNTs in aqueous solutions with different concentrations of fluorophores, cleared the resulting solution by sedimentation, and measured the concentration of SWCNTs dispersed in the supernatant by absorbance at 1023 nm. Because these dispersed SWCNT samples have relatively uniform diameter distributions as revealed by AFM measurement, we can thus use absorbance value directly to approximate tube densities. We observed that more SWCNTs were dispersed into the aqueous solution with increasing concentrations of fluorophore. This trend is true for all the fluorophores we tested {Figure 3-4. (a)}. This phenomenon can be explained by a simple model where binding of fluorophore molecules to SWCNT surface is necessary to destabilize SWCNT bundles and stabilize individual dispersed SWCNTs. However, this concentration dependence is quantitatively different for different

fluorophores as follows: first, the amount of SWCNTs that can be dispersed by FITC, RB or FSS is ~6 fold higher than that by FLUO; maximum concentrations of dispersed SWCNTs were 0.290 mg/mL, 0.292 mg/mL and 0.277 mg/mL for FITC, RB and FSS, respectively. These concentrations are comparable to the reported concentration of SWCNTs that was dispersed by bovine serum albumin (BSA) in aqueous solution, which was ~0.3 mg/mL[20]. In contrast, this value was only 0.0455 mg/mL for FLUO. The overall efficiency of dispersion, as measured by the fraction of SWCNTs dispersed into the aqueous phase, was plotted in Supplementary figure 3-3 for each compound. Among the molecules we tested in this study, FITC, FSS, RB and TB show ~30 % dispersion efficiency, which is comparable to that of short ssDNA, however 10~20% lower than those of typical surfactants[16]. Second, among FITC, RB and FSS, FITC can achieve the same amount of SWCNT dispersion with the lowest FITC concentration (~0.5 mM). In contrast, it will require 40 fold higher concentrations of FSS to achieve the same amount of SWCNT dispersion. These results suggest that each fluorophore is different in their ability to disperse SWCNTs, and these differences may be related to the differences in aromatic ring structures and the hydrophilic moiety. We also examined the ability of five different dye molecules to disperse SWCNTs in aqueous solution. These results are summarized in figure 3-4. (b). We noticed that not all the dye molecules tested can disperse SWCNTs in aqueous solution. Interestingly, differences in functional groups on the aromatic ring structures can have significant influence on the result of dispersion, represented by PR and MG: PR can disperse SWCNTs while MG were not able to disperse SWCNTs under all concentrations we have tested, although both share similar aromatic ring structures {Figure 3-4. (b) inset}. This suggests that the functional groups

on aromatic rings can have a profound impact on the ability of a dye molecule to disperse SWCNTs. For dye molecules that can disperse SWCNTs, we observed more SWCNT dispersion as we increase the dye concentration, which is qualitatively similar to the flurophore-assisted dispersion of SWCNTs {Figure 3-4. (a)}. However, different dye molecules also have distinct abilities to disperse SWCNTs; the maximum concentrations of dispersed SWCNTs are 0.254 mg/mL, 0.075 mg/mL, and 0.040 mg/mL for TB, PR and OII, respectively. These differences may directly relate to their differences in chemical structures, including both aromatic ring structures and the hydrophilic moieties. Lastly, certain fluorophore or dye molecules require a minimal concentration to disperse SWCNTs efficiently, as can be seen for FITC, FSS, RB and TB. We estimated that these minimal concentrations of dispersant are within two fold of the concentrations required to fully cover the SWCNT surface (Supplementary Table 3-1). Thus, the sigmoidal dependence of SWCNT dispersion on dispersant concentration suggests that the SWCNT surface needs to be covered sufficiently in order to destabilize bundle interactions and keep individual tubes apart. Similar phenomenon was also observed previously by Backes *et al*.[34].

Raman spectroscopy of SWCNT/fluorophore and SWCNT/dye. To determine if dispersant molecules have selectivity over certain chiralities of SWCNTs, we conducted Raman spectra[42,43] measurements for the dispersed SWCNT samples, and compared them with that of dry samples (Figure 3-5). The radial breathing mode (RBM) of SWCNT has been used to diagnose SWCNTs. The specific Raman shift, typically located between 120 and 350 cm^{-1}, is inversely proportional to the diameter of individual

SWCNTs[42,43]. In our spectra, majorities of the Raman shifts were located at a wavenumber below 250 cm^{-1}, and contain a broad peak between 125 and 250 cm^{-1}. This is consistent with the fact that these tubes are relatively large in diameter, and contain a wide variety of diameters and chiralities[44,45]. This broad feature of Raman shifts is true for both dispersed SWCNT samples and dry material, suggesting little or no selectivity of these molecules in dispersing SWCNTs. Moreover, we compared the intensity ratio between D and G band Raman shifts, which serves as an indication of SWCNT quality. The results are shown in supplementary Table 3-2. These ratios range between 1.1 ~ 4.6 %, suggesting that these SWCNT samples are of high quality, without much defects or amorphous carbon[42]. Of note, the Raman spectra of SWCNTs dispersed with FLUO and PR were not analyzed due to the presence of strong background in the spectra.

SWCNT/fluorophore, SWCNT/dye dissociation rate measurement. The above experiments demonstrate that SWCNTs can be dispersed by various types of fluorophores and dyes, although with different efficiencies. To examine if the difference in efficiency of dispersion may relate to the potential difference in the stability of the complex, we measured the relative stability of these complexes using three different methods. The first is kinetic dialysis experiment, in which the dispersed SWCNT samples were dialyzed against water and the fraction of remaining SWCNT complex in solution was measured at different time points. The pore size of the dialysis membrane was chosen to retain SWCNTs but fluorophore/dye molecules could freely diffuse through. The result from this experiment gives a direct assessment on the rate of SWCNT aggregation due to loss of fluorophore/dye molecules through dialysis. These

results are shown in figure 3-6. (a)-(b). The SWCNTs dispersed by RB was lost rapidly within 1 hr of dialysis, suggesting that RB dissociates readily from SWCNT surface, which results in the aggregation and loss of SWCNTs. In contrast, SWCNT/PR was lost by ~20 % after dialysis for 3 hours. All other SWCNT samples remain largely in aqueous solution, suggesting that the fluorophore/dye molecules dissociate negligibly from complexes during the dialysis process. The second experiment is isochronal temperature assay that was described by Albertorio *et al*.[46]. The SWCNT/fluorophore or dye samples were incubated at various temperatures for 10 min, and then immediately brought to room temperature, centrifuged to remove SWCNT aggregates and the supernatant was measured to determine SWCNTs that remained in solution. This experiment directly probes the temperature-dependent dissociation of fluorophore or dye molecules from SWCNTs, which leads to SWCNT aggregation and precipitation out of solution. Similar to the dialysis experiment, SWCNT/RB showed the fastest rate of loss upon incubation at elevated temperatures, followed by FSS, FITC and FLUO. The $T_{1/2}$ values for each SWCNT/fluorophore are listed in Table 3-1 (the temperature at which 50 % of the complex remains in solution). For SWCNTs dispersed by dye molecules, SWCNT/PR showed the fastest rate of loss while SWCNT/OII and SWCNT/TB showed less than 10% loss even after incubation at 100 ℃ for 10 min. These results are quantitatively consistent with those from dialysis experiments, suggesting that RB and PR dissociate from SWCNTs at a faster rate than other fluorophore or dye molecules we have tested. The third experiment is kinetic temperature experiments. The dispersed SWCNT samples were incubated at a designated temperature for various length of time, and then immediately brought to room temperature and centrifuged to remove SWCNT

aggregates. The supernatant was measured to determine SWCNTs that remained in solution. This experiment probes the dissociation kinetic of fluorophore or dye molecules from SWCNTs, which leads to aggregation of SWCNTs. This experiment was then repeated at various temperatures, from which we could conduct Eyring analysis and obtain the activation enthalpy for the reaction. The results from this experiment are shown in Supplementary figure 3-4. Interestingly, these progress curves showed diverse kinetic behaviors. Single-exponential kinetics was reported by Albertorio et al.[46] for SWCNTs dispersed with short DNA oligos. However clearly, single-exponential kinetics was only a subset of all progress curves we had observed, suggesting a very complex mechanism for dissociation of fluorophores/dyes from SWCNT surface and subsequent SWCNT aggregation. For those process curves that could be described by single-exponential kinetics, we were able to conduct Eyring analysis and extract the activation enthalpy for the reaction. These results are shown in figure 3-6 (e), (f) and summarized in Table 3-1 for activation enthalpy and rates of SWCNT aggregation at 99 ℃. Of note, SWCNT/RB does show a very small activation enthalpy, 2.81 kcal/mol, much lower than that of either SWCNT/FSS or SWCNT/FLUO. This result is consistent quantitatively with the other two experiments, which revealed a relatively lower stability for SWCNT/RB complex. This amount of activation enthalpy is comparable to thermal fluctuations (2.48 kcal/mol at 25 ℃) so that dissociation of RB easily occurs during room temperature dialysis {Figure 3-6. (a)}, which was not observed for either FSS or FLUO. For dye molecules, SWCNT/PR does show a lower activation enthalpy than SWCNT/OII, consistent with kinetic dialysis and isochronal temperature experiments. Altogether, these results suggest that the three experiments indeed monitor some common kinetic

events involved in fluorophore/dye dissociation and subsequent SWCNT aggregation; the fluorophore and dye molecules we have tested show very different interactions with SWCNTs. Moreover, the kinetic temperature experiments can reveal differences that are hidden in dialysis experiments. For example, FSS and FLUO showed no difference in kinetic dialysis experiments, which are possibly due to the activation enthalpies that are higher than thermal fluctuations. However, the kinetic temperature experiments revealed a ~5 fold higher activation enthalpy for FLUO than FSS, suggesting that FLUO binds more tightly to SWCNTs than FSS. Lastly, despite these differences in their interactions with SWCNTs, none of these results are correlated with the efficiency to disperse SWCNTs in aqueous solution. For example, RB can disperse a larger amount of SWCNTs at much lower fluorophore concentration than FSS {Figure 3-4. (a)}; PR can disperse a larger amount of SWCNTs at the same concentration as OII {Figure 3-4. (b)}, both of which are in contrast to the kinetic stability experiments in figure 3-6. These differences suggest that the on-rate of fluorophore/dye molecules to SWCNT surface instead of the off-rate may determine the efficiency at which these molecules disperse SWCNTs. Even though fluorophore or dye molecules can dissociate readily from SWCNT surface (RB for example), they can disperse SWCNTs efficiently provided that a large excess fluorophore/dye molecules are present in solution.

Cell transfection experiment of SWCNT/fluorophore. To identify potential applications for fluorophore-assisted SWCNT dispersion in aqueous solution, we tested transfection of mammalian cells using SWCNTs dispersed with fluorophore molecules. The results of the transfection were examined with confocal microscope and quantitated

with flow cytometry. Interestingly, SWCNT/FITC showed 84 % increase in transfection efficiency compared to same amount of FITC free in solution (Figure 3-7). In contrast, SWCNT/FSS and SWCNT/FLUO showed changes in transfection efficiency less than 15 % compared to free fluorophores in solution (Flow cytometry quantification data in Supplementary figure 3-5). Moreover, we observed completely different phenomena for RB; SWCNT/RB showed only 22 % transfection efficiency relative to same amount of RB free in solution (Supplementary figure 3-5). These results suggest that the efficiency of transfection may well depend on individual fluorophore molecule but not determined by SWCNTs. The preferred cellular uptake of SWCNT/FITC compared to SWCNT/FSS complexes suggests that the presence of the isothiocyanate group in FITC may be the molecular underpinning that drives this cellular uptake, since this is the only difference between these molecules under neutral pH conditions. For the low transfection efficiency mediated by SWCNT/RB, one possible explanation among others is that SWCNTs was observed to precipitate out of the solution after we added SWCNT/RB into the culture media and incubated at 37 ℃, which was possibly due to the fast rate of RB dissociation from SWCNT surface (Figure 3-6). We have tried to correlate surface charge of each SWCNT/fluorophore with the efficiency of transfection; these surface charge values were measured with particle analyzer and listed in Supplementary Table 3-3. No apparent correlation between surface charge and transfection efficiency was found.

3.7 Conclusion

Here we reported SWCNT dispersion assisted by different types of fluorophore and dye molecules. Although these molecules have different interactions with SWCNTs as revealed by kinetic measurements, the efficiency of dispersion may be determined more by the on-rate of these molecules to the SWCNT surface instead of the off-rate. This type of conclusions can be gained from kinetic studies of SWCNT dispersion, and are useful in understanding the mechanisms of this complex process. We also note that similar aromatic ring structures but with different functional groups will have very different consequences on SWCNTs dispersion. FITC, FSS and RB share a similar aromatic backbone, but display very different efficiencies in dispersing SWCNTs. Based on the dispersant concentration required to reach saturation for SWCNT dispersion (Figure 3-4), the order of dispersing efficiency follows FITC>RB>FSS. Under current solution conditions, FITC and FSS both are ionizable and carry negative charges (see supplementary Table 3-3 for zeta potential measurement), yet more than 10 fold difference in their efficiency of dispersion, suggesting that the presence of the isothiocyanate group facilitates SWCNT dispersion in aqueous solution. FITC and RB differ ~ 2 fold in dispersion efficiency. However, SWCNTs dispersed by RB were far less stable than that of FITC, as shown by the fast off-rate of RB (Figure 3-6, Table 3-1). This suggests that the presence of $-N(CH_3)_2$ and $=N(CH_3)_2^+$ groups in the aromatic backbones significantly decreases the affinity of the dispersant molecule on SWCNT surface. Whether this fast off-rate is due to less perfect stacking on SWCNT surface remains an open question to be addressed in future studies. Similarly, PR and MG differ in their hydrophilic moieties despite very similar aromatic backbones; PR can disperse SWCNTs but MG cannot in all the concentrations tested. This phenomenon further

supports that the presence of $-N(CH_3)_2$ and $=N(CH_3)_2^+$ groups may destabilize the interaction between a dispersant molecule and SWCNTs and results in poor dispersion. Finally, fluorophore-assisted dispersion of SWCNTs may be useful for delivering molecules that show difficulty in penetrating plasma membrane. However, this needs to be considered case by case.

3.8 Acknowledgements

We thank Dr. Adam Matzger in Department of Chemistry, and Dr. Martin A. Philbert in Department of Environmental Health Sciences, University of Michigan for sharing the use of the instruments. We thank Cheng lab members, especially Dr. Jin Hyun Kim for help on instruments, Dr. Ximiao Hou for critical reading of the manuscript. WC thanks start-up funding support from the University of Michigan at Ann Arbor and the Ara Paul Professorship fund at the University of Michigan. This work is also supported in part by NIH grant R33CA125297 (RK). WC is a Basil O'Connor Starter Scholar of the March of Dimes Foundation, and a recipient of 2011 NIH Director's New Innovator Award (1DP2OD008693-01).

3.9 Table

SWCNT/Fluorophore SWCNT/dye	Average length (nm)*	Average height (nm)*	Aggregation temperature, $T_{1/2}$ (℃)	Activation enthalpy, ΔH (kcal mol^{-1})	Rate of aggregation at 99 ℃, k_{agr} (min^{-1})
SWCNT/$(dT)_{30}$	891 ± 361	1.22 ± 0.30	>130	N. A.	N. A.
SWCNT/FITC	933 ± 346	1.83 ± 0.23	129.40	N.A.	N.A.
SWCNT/FSS	959 ± 390	1.47 ± 0.39	127.21	13.86	0.0708
SWCNT/FLUO	1103 ± 363	1.93 ± 0.25	>130	61.93	0.0963
SWCNT/RB	975 ± 265	1.99 ± 0.31	77.78	2.81	0.0878
SWCNT/TB	1003 ± 336	1.87 ± 0.43	>130	N.A.	0.0228
SWCNT/PR	1024 ± 312	1.63 ± 0.37	84.89	10.23	N.A.
SWCNT/OII	1014 ± 268	1.50 ± 0.20	>130	17.18	0.1254

Table 3-1. Characterization of SWCNT/Fluorophore, SWCNT/dye with various parameters determined from current study. Average length and height were measured for dispersed SWCNTs after 1 hr of sonication. The same parameters measured for $(dT)_{30}$ dispersed SWCNTs are also listed for comparison. Of note, we did not observe any aggregation of SWCNT/$(dT)_{30}$ throughout the temperature range we tested (max. 130 ℃).

3.10 Figures

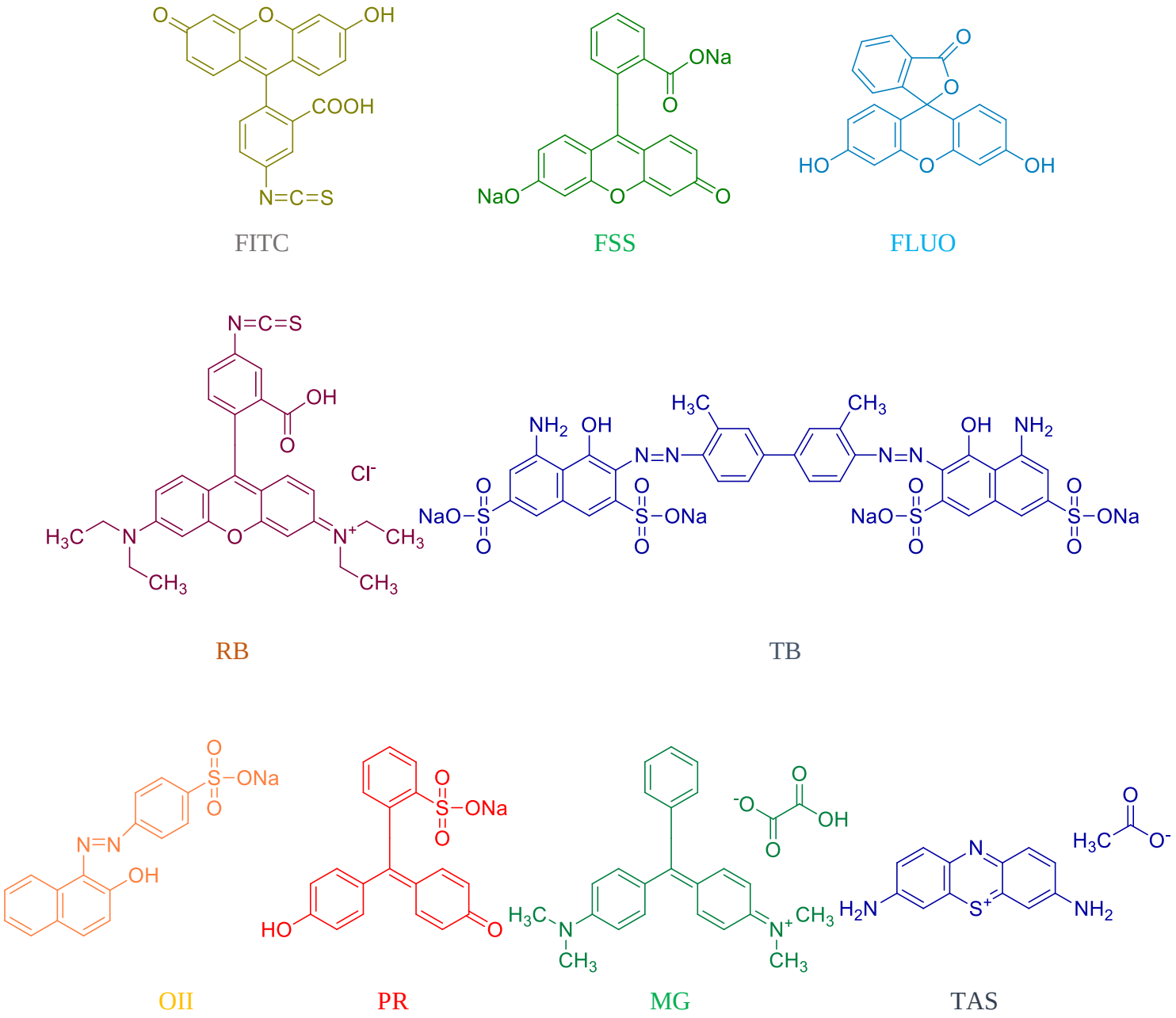

Figure 3-1. List of fluorophores/dyes we used to disperse SWCNTs. (From top to bottom left to right: FITC (Fluorescein isothiocyanate), FSS (Fluorescein sodium salt), FLUO (Fluorescein), RB (Rhodamine B isothiocyanate), TB (Trypan blue), OII (Orange II sodium salt), PR (Phenol red sodium salt), MG (Malachite green) and TAS (Thionin acetate salt).

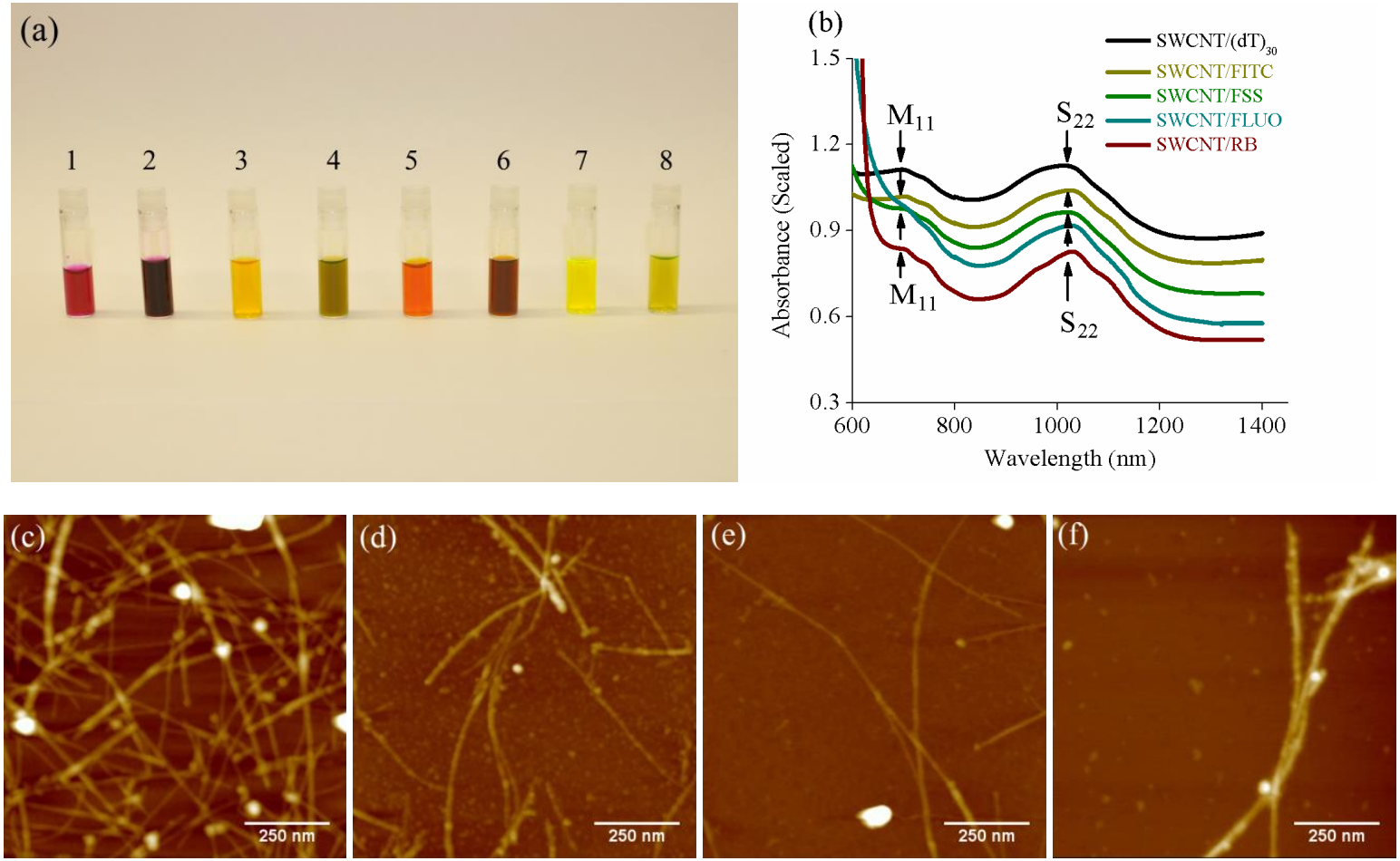

Figure 3-2. (a) Color comparison of fluorophore solutions before and after SWCNT dispersion. 1: RB, 2: SWCNT/RB, 3: FITC, 4: SWCNT/FITC, 5: FSS, 6: SWCNT/FSS, 7: FLUO, 8: SWCNT /FLUO (from left to right) (b) UV-visible-NIR absorbance spectra of SWCNT/fluorophore (c) ~ (f) AFM images of SWCNT/RB SWCNT/FITC, SWCNT/FSS and SWCNT/FLUO. Scale bar for figure 1.(c) ~ (f) and figure 2. (c) ~ (e) is presented in the bottom right of figure 2.

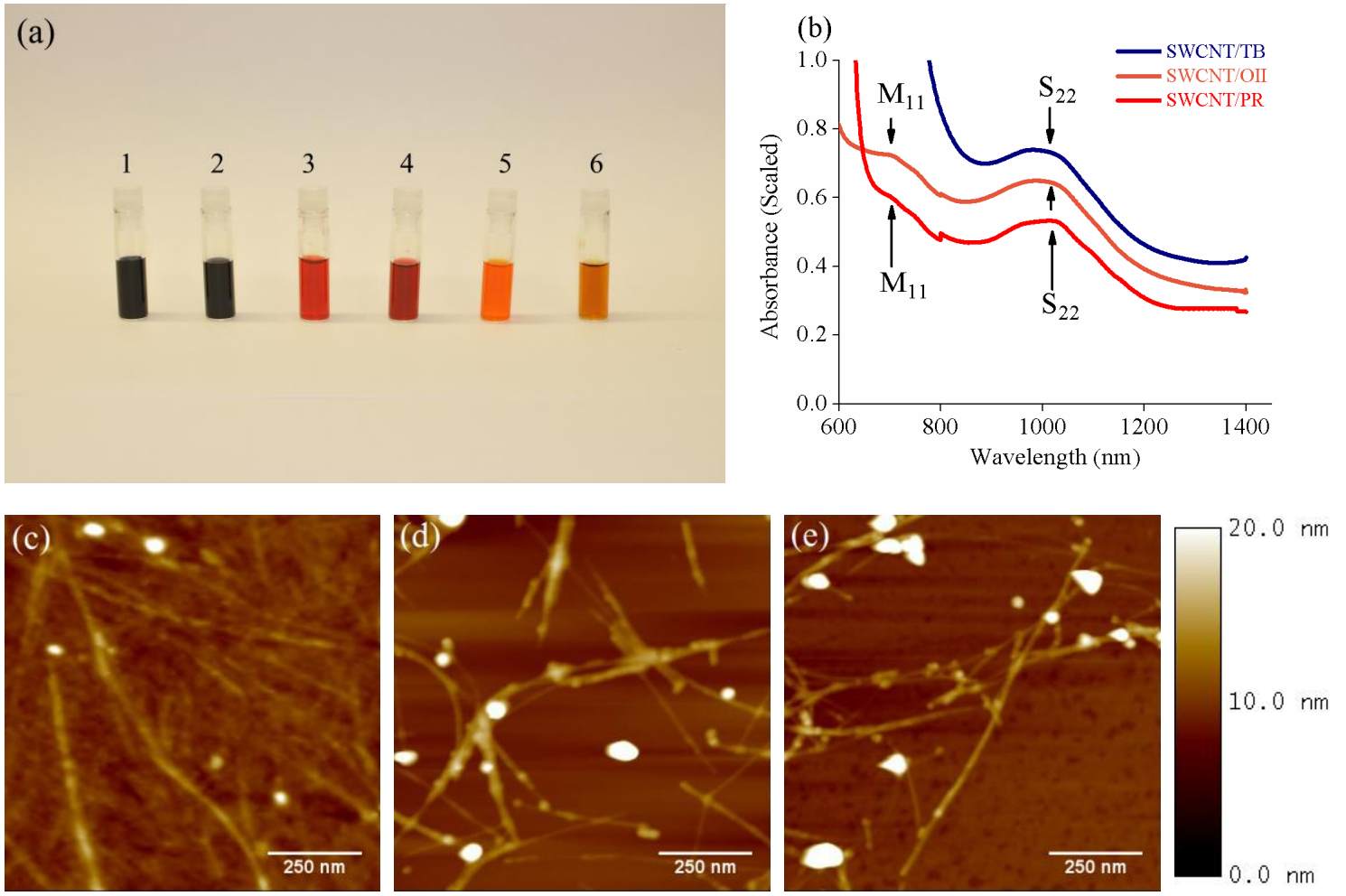

Figure 3-3. (a) Color comparison of dye solutions before and after SWCNT dispersion. 1: TB, 2: SWCNT/TB, 3: PR, 4: SWCNT/PR, 5: OII, 6: SWCNT/OII (b) UV-visible-NIR absorbance spectrum of SWCNT/dye. Absorbance surge at ~700 nm for SWCNT/TB is due to the absorbance of TB in solution. (c)~ (e) AFM images of SWCNT/TB, SWCNT/PR, SWCNT/OII, respectively.

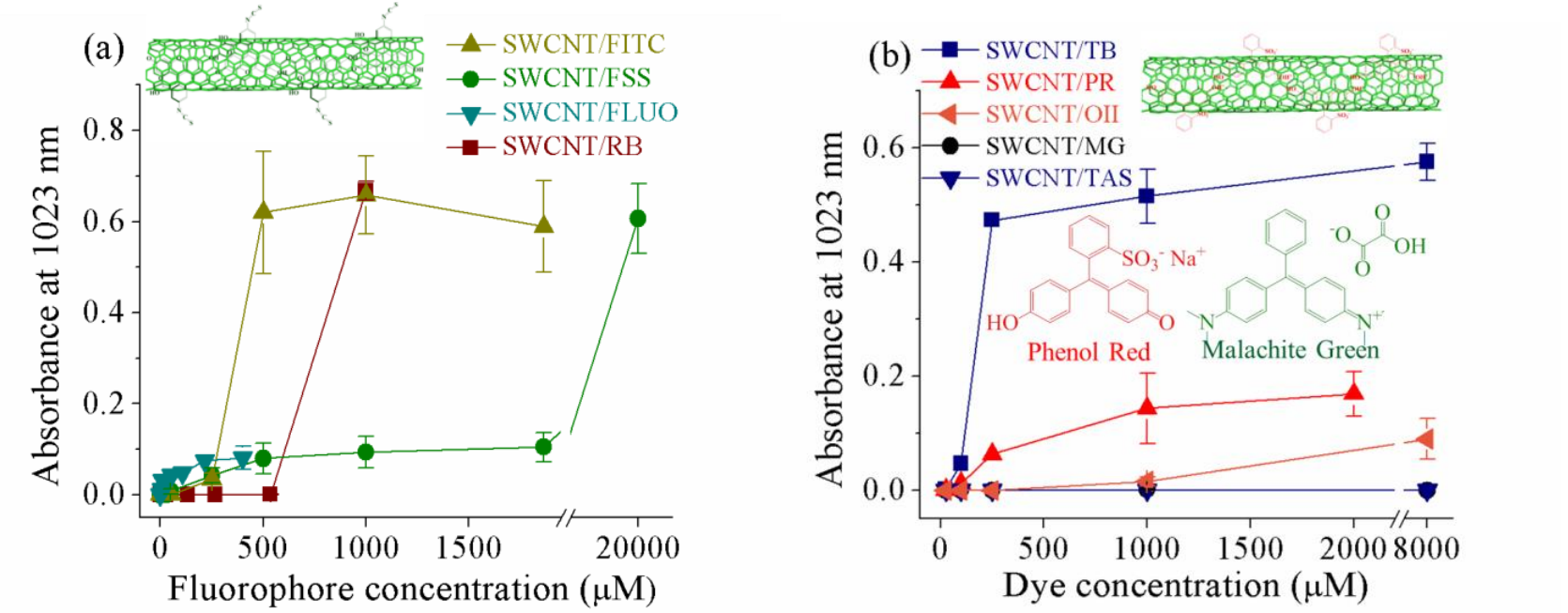

Figure 3-4. (a) [Fluorophore]-dependent dispersion of SWCNTs {Upper right: Schematic cartoon representation of FITC adsorption onto of the surface of (7,5) SWCNTs}. Highest concentrations of fluorophores used to disperse SWCNTs were 400 μM for FLUO, 1 mM for RB, 1.865 mM for FITC and 20 mM for FSS resepectively. (b) [Dye]-dependent dispersion of SWCNTs {Upper right: Schematic cartoon representation of PR adsorption to the surface of (7,5) SWCNTs}. Inset: Chemical structures of PR and MG used in current study. Highest concentrations of dyes used to disperse SWCNTs were 2 mM for PR, and 8 mM for TB, OII, MG and TAS. Under current condition, RB and FLUO have solubility limits of 1 mM and 400 μM, respectively.

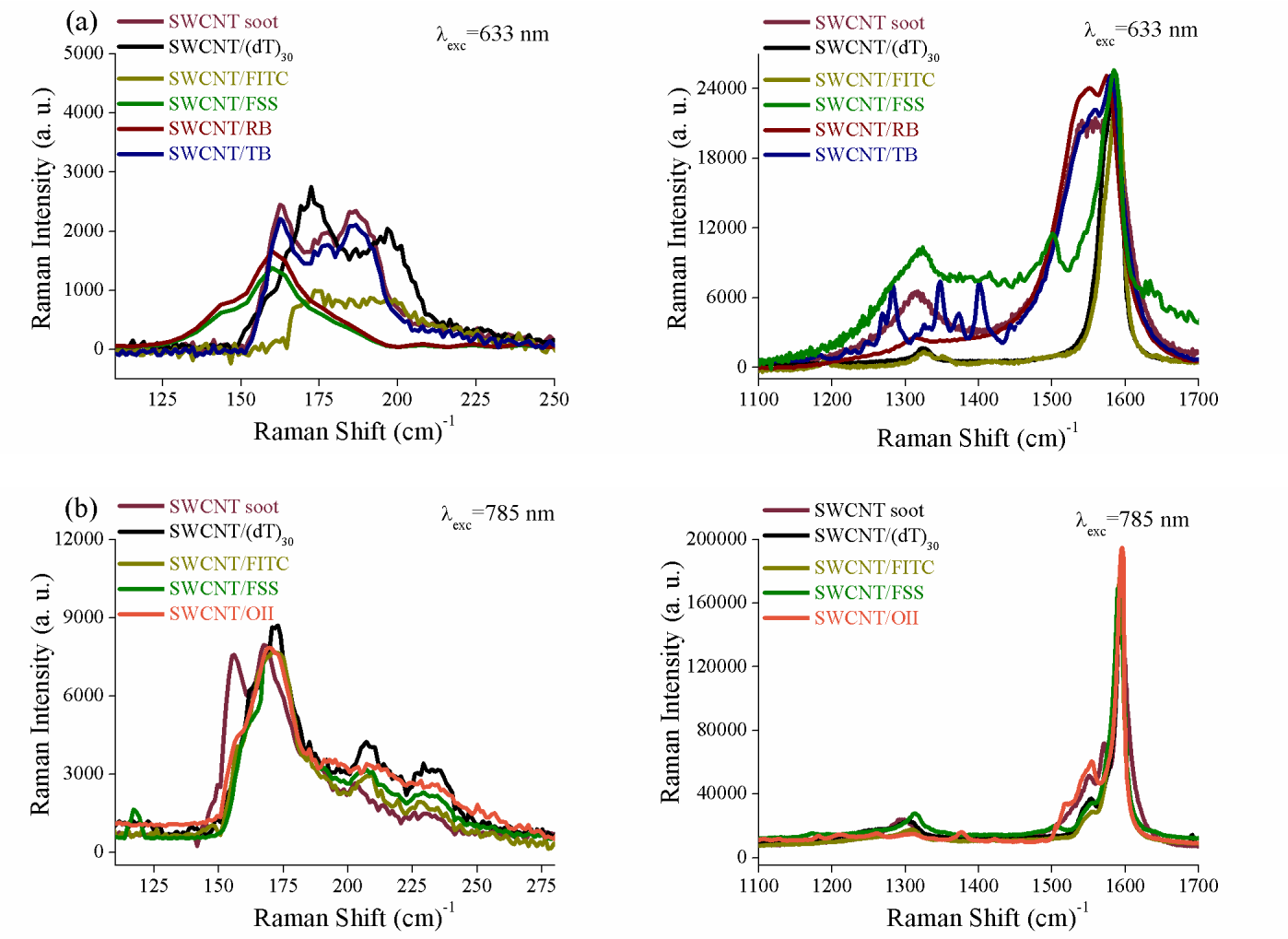

Figure 3-5. RBM (left) and D band (right) Raman spectra of SWCNT/fluorophore and SWCNT/dye with (a) 633 nm (b) 785 nm wavelength laser.

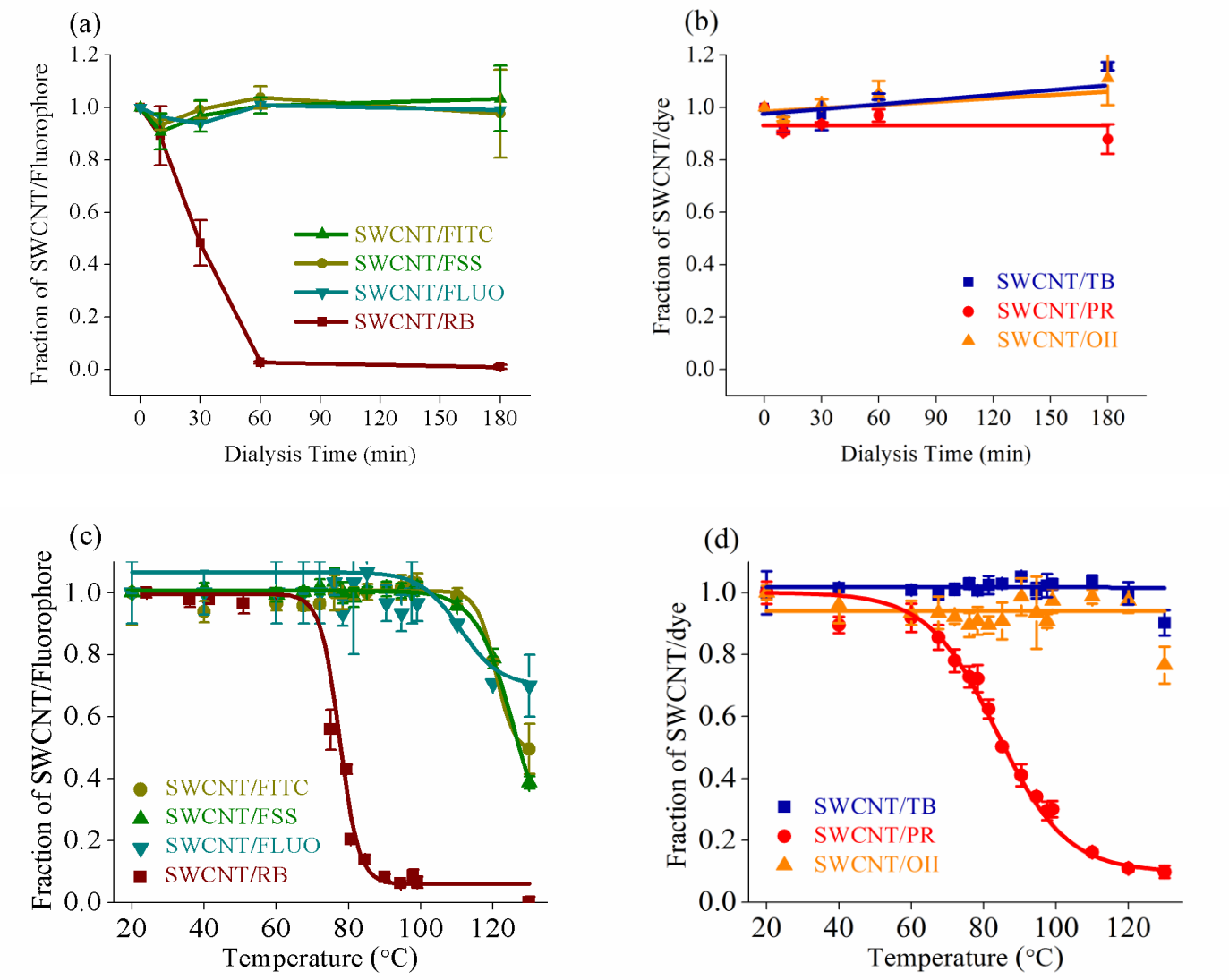
(a)
Fraction of SWCNT/Fluorophore
1.2
1.0
0.8
0.6
0.4
0.2
0.0
0
30
60
90
120
150
180
Dialysis Time (min)
SWCNT/FITC
SWCNT/FSS
SWCNT/FLUO
SWCNT/RB
(b)
Fraction of SWCNT/dye
1.2
1.0
0.8
0.6
0.4
0.2
0.0
0
30
60
90
120
150
180
Dialysis Time (min)
SWCNT/TB
SWCNT/PR
SWCNT/OII
(c)
Fraction of SWCNT/Fluorophore
1.0
0.8
0.6
0.4
0.2
0.0
20
40
60
80
100
120
Temperature (°C)
SWCNT/FITC
SWCNT/FSS
SWCNT/FLUO
SWCNT/RB
(d)
Fraction of SWCNT/dye
1.0
0.8
0.6
0.4
0.2
0.0
20
40
60
80
100
120
Temperature (°C)
SWCNT/TB
SWCNT/PR
SWCNT/OII

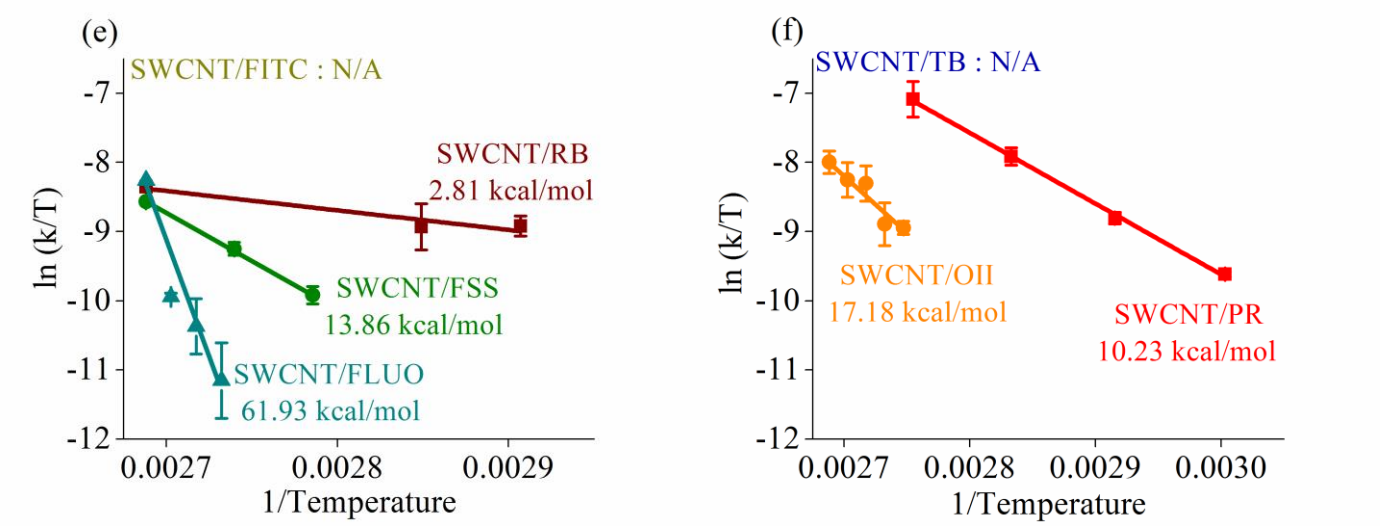

Figure 3-6. Fraction of (a) SWCNT/fluorophores and (b) SWCNT/dye that remained in aqueous solution upon dialysis. Lines only serve as the guide for the eye. Fraction of (c) SWCNT/fluorophore and (d) SWCNT/dye that remained in aqueous solution after incubation at designated temperature for 10 minutes. Sigmoidal model $\{y = A_2 + (A_1 - A_2) / (1 + \exp((x - x_0) / dx))\}$ is used to fit the data in (c) and (d) and the fits are plotted in solid lines. Eyring plots for (e) SWCNT/fluorophore (f) SWCNT/dye derived from kinetic temperature experiments shown in Supplementary figure 3-4.

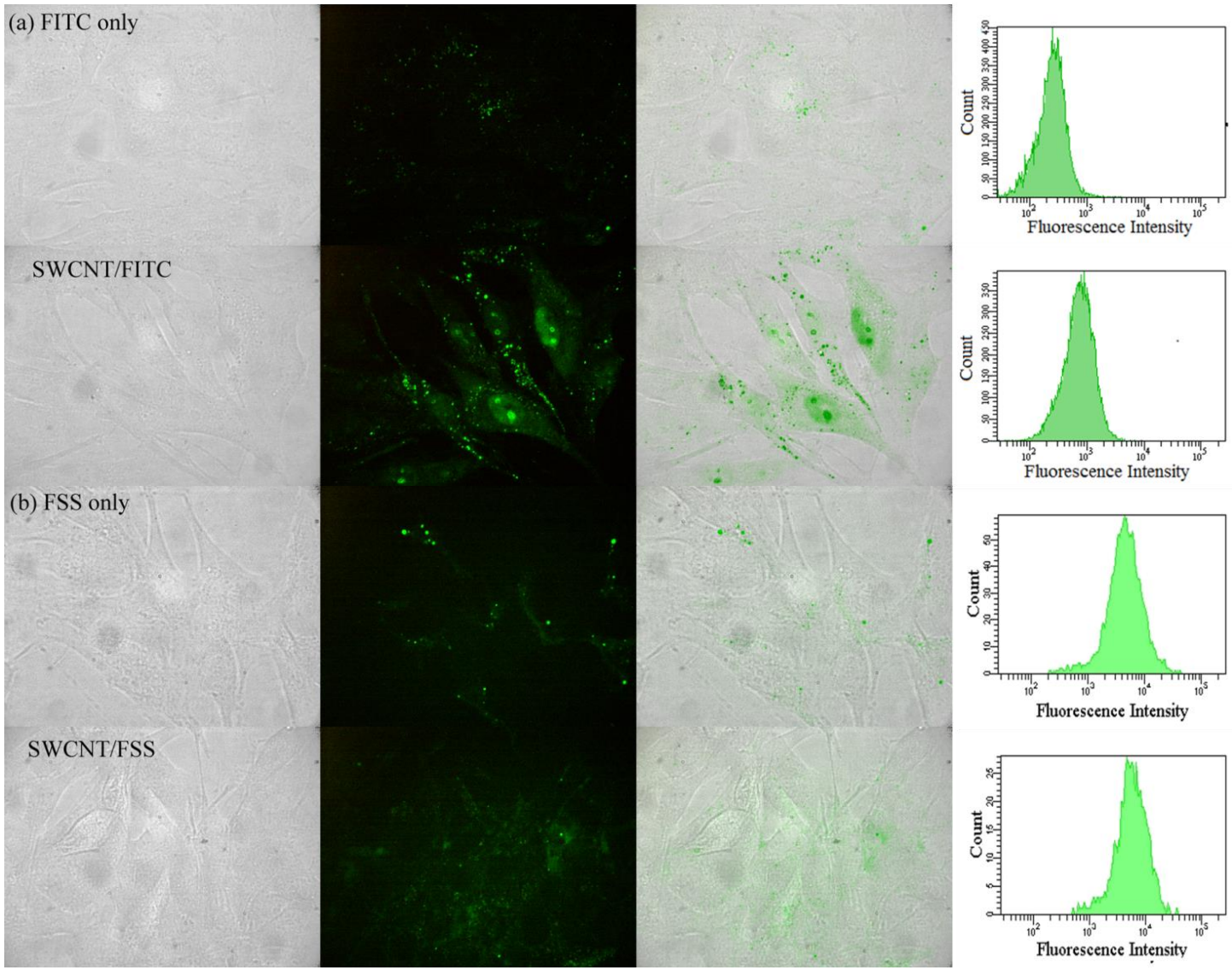
(a) FITC only
SWCNT/FITC
(b) FSS only
SWCNT/FSS
Count
Fluorescence Intensity

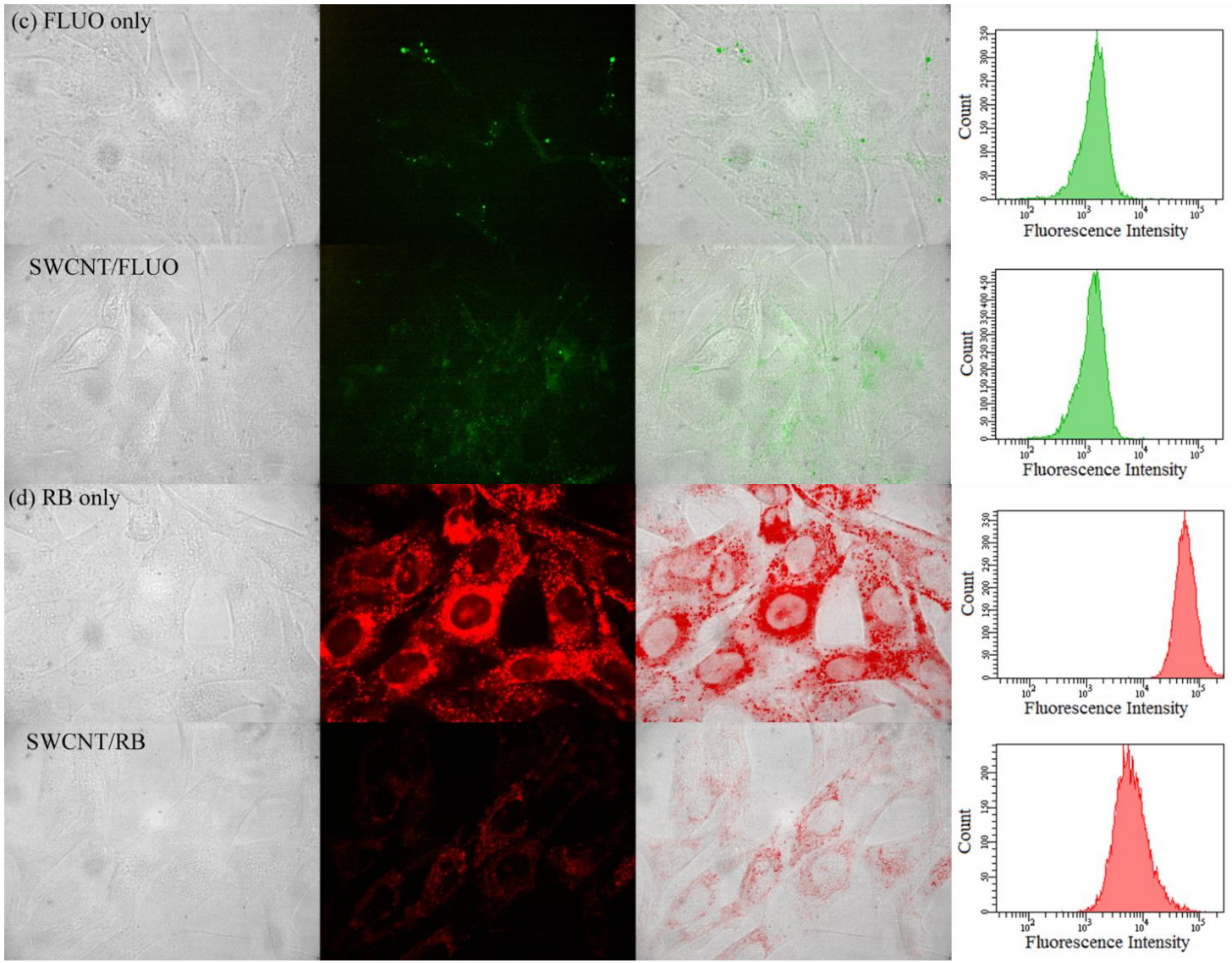
(c) FLUO only
SWCNT/FLUO
(d) RB only
SWCNT/RB
Count
Fluorescence Intensity

Figure 3-7. Bright-field (far left), fluorescence (middle-left) and merged (middle-right) 9L cell images and flow cytometry data (far right) transfected with (a) FITC only (Top), SWCNT/FITC (Bottom), (b) FSS only (Top), SWCNT/FSS (Bottom), (c) FLUO only (Top), SWCNT/FLUO (Bottom), (d) RB only (Top), SWCNT/RB (Bottom). FITC, FSS, FLUO fluorescence were excited with 488 nm laser. RB fluorescence was excited with 561 nm laser. Concentration of fluorophores and SWCNT/fluorophore used to transfect 9L cells were 1 mM except FLUO only and SWCNT/FLUO (400 μM for both). For merged images, the background color of fluorescence images were reversed and then overlaid with bright field images using Adobe Photoshop CS3, version 12.0.4.

3.11 Supporting Information Available

Supporting information is available in the Appendix A

3.12 References

(1) Iijima, S.; Ichihashi, T. *Nature*, **1993**, 363, 603.
(2) Bethune, D. S.; Kiang, C. H.; Devries, M. S.; Gorman, G.; Savoy, R.; Vazquez, J.; Beyers, R. *Nature*, **1993**,363, 605.
(3) Kong, J.; Franklin, N. R.; Zhou, C. W.; Chapline, M. G.; Peng, S.; Cho, K. J.; Dai, H. *Science*, **2000**, 287, 622.
(4) Chen, R. J.; Bangsaruntip, S.; Drouvalakis, K. A.; Kam, N. W. S.; Shim, M.; Li, Y.; Kim, W.; Utz, P. J.; Dai, H. *Proc. Natl. Acad. Sci. U.S.A.*, **2003**, 100, 4984.
(6) Dang, X.; Yi, H.; Ham, M-H.; Qi, J.; Yun, D. S.; Ladewski, R.; Strano, M. S.; Hammond, P. T.; Belcher, A. M. *Nat. Nanotechnol.*, **2011**, 6, 377.
(6) Kongkanand, A.; Martinez Dominguez, R.; Kamat, P. V. *Nano Lett*., **2007**, 7, 676.
(7) Kam, N. W. S.; O'Connell, M.; Wisdom, J. A.; Dai, H. *Proc. Natl. Acad. Sci. U.S.A.*, **2005**, 102, 11600.
(8) Herrero, M. A.; Toma, F. M.; Al-Jamal, K. T.; Kostarelos, K.; K.; Bianco, A.; Ros, T. D.; Bano, F.; Casalis, L.; Scoles, G.; Prato, M. *J. Am. Chem. Soc.*, **2009**, 131, 9843.
(9) Wu, W.; Wieckowski, S.; Pastorin, G.; Benincasa, M.; Klumpp, C.; Briand, J-P.; Gennaro, R.;Prato, M.; Bianco, A. *Angew. Chem. Int. Ed.*, **2005**, 44, 6358.
(10) Su, Z.; Zhu, S.; Donkor, A. D.; Tzoganakis, C.; Honek, J. F. *J. Am. Chem. Soc.*, **2011**, 133, 6874.
(11) Zheng, M.; Jagota, A.; Semke, E. D.; Diner, B. A.; McLean, R. S.; Lustig, S. R.; Richardson, R. E.; Tassi, N. G. *Nat. Mater.*, **2003**, 2, 338.
(12) Zheng, M.; Jagota, A.; Strano, M. S.; Santos, A. P.; Barone, P.; Chou, S. G.; Diner, B. A.; Dresselhaus, M. S.; McLean, R. S.; Onoa, G. B.; Samsonidze, G. G.; Semke, E. D.; Usrey, M.; Walls, D. J. *Science*, **2003**, 302, 1545.
(13) Islam, M. F.; Rojas, E.; Bergey, D. M.; Johnson, A. T.; Yodh, A. G. *Nano Lett.*, **2003**, 3, 269.
(14) Moore, V. C.; Strano, M. S.; Haroz, E. H.; Hauge, R. H.; Smalley, R. E.; Schmidt, J.; Talmon, Y. *Nano Lett.*, **2003**, 3, 1379.
(15) Blanch, A. J.; Lenehan, C. E.; Quinton, J. S. *J. Phys. Chem. B*, **2010**, 114, 9805.
(16) Haggenmueller, R.; Rahatekar, S. S.; Fagan, J. A.; Chun, J.; Becker, M. L.; Naik, R. R.; Krauss, T.; Carlson, L.; Kadla, J. F.; Trulove, P. C.; Fox, D. F.; DeLong, H. C.; Fang, Z.; Kelley, S. O.; Gilman, J. W. *Langmuir*, **2008**, 24, 5070.
(17) Wenseleers, W.; Vlasov, I. I.; Goovaerts, E.; Obraztsova, E. D.; Lobach, A. S.; Bouwen, A. *Adv. Funct. Mater.*, **2004**, 14, 1105.

(18) O'Connell, M. J.; Boul, P. J.; Ericson, L. M.; Huffman, C. B.; Moore, V. C.; Wang, Y. H.; Haroz, E. H.; Kuper, C.; Tour, J.; Ausman, K. D.; Smalley, R. E. *Chem. Phys. Lett.*, **2001**, 342, 265.
(19) Didenko, V. V.; Moore, V. C.; Baskin, D. S.; Smalley, R. E. *Nano Lett.*, **2005**, 5, 1563.
(20) Holt, B. D.; Dahl, K. N.; Islam, M. F. *Small*, **2011**, 7, 2348.
(21) Dieckmann, G. R.; Dalton, A. B.; Johnson, P. A.; Razal, J.; Chen, J.; Giordano, G, M.; Muñoz, E.; Musselman, I. H.; Baughman, R. H.; Draper, R. K. *J. Am. Chem. Soc.*, **2003**, 125, 1770.
(22) Zorbas, V.; Ortiz-Acevedo, A.; Dalton, A. B.; Yoshida, M. M.; Dieckmann, G. R.; Draper, R. K.; Baughman, R. H.; Jose-Yacaman, M.; Musselman, I. H. *J. Am. Chem. Soc.*, **2004**, 126, 7222.
(23) Liu, T. Q.; Gao, L.; Zheng, S. *Nanotechnology*, **2007**, 18, 365702.
(24) Fagan, J. A.; Bauer, B. J.; Hobbie, E. K.; Becker, M. L.; Hight Walker, A. R.; Simpson, J. R.; Chun, J.; Obrzut, J.; Bajpai, V.; Phelan, F. R.; Simien, D.; Huh, J. Y.; Migler, K. B *Adv. Mater.*, **2011**, 23, 338.
(25) Huges, M. E.; Brandin, E.; Glovchenko, J. A. *Nano Lett.*, **2007**, 7, 1191.
(26) Meng, S.; Wang, W. L.; Maragakis, P.; Kaxiras, E Nano Lett. 2007, 7, 2312-2316.
(27) Gao, H.; Kong, Y. *Annu. Rev. Mater. Res.*, **2004**, 34, 123.
(28) Meng, S.; Kaxiras, E. *Biosensing Using Nanomater*., **2009**, 3, 67.
(29) Chen, R. J.; Zhang, Y. J. *J. Phys. Chem. B*, **2006**, 110, 54.
(30) Ahmad, A.; Kurkina, T.; Kern, K.; Balasubramanian, K. *ChemPhysChem*, **2009**, 10, 2251.
(31) Liu, Q.; Chen, B.; Wang, Q.; Shi, X.; Xiao, Z.; Lin, J.; Fang, X. *Nano Lett.*, **2009**, 9, 1007.
(32) Chen, S.; Jiang, Y.; Wang, Z.; Zhang, X.; Dai, L.; Smet, M. *Langmuir*, **2008**, 24, 9233.
(33) Rodriguez, A.; Ovejero, G.; Soltero, J. L.; Mestanza, M.; Garcia, J. *J. Environ. Sci. Health, Part A: Environ. Sci. Eng.*, **2010**, 45, 1642.
(34) Backes, C.; Schmidt, C. D.; Hauke, F.; Boettcher, C.; Hirch, A. *J. Am. Chem. Soc.*, **2009**, 131, 2172.
(35) Ehli, C.; Oelsner, C.; Guldi, D. M.; Mateo-Alonso, A.; Prato, M.; Schmidt, C. D.; Backes, C.; Hauke, F.; Hirsch, A. *Nat. Chem.*, **2009**, 1, 243.
(36) Backes, C.; Mundloch, U.; Ebel, A.; Hauke, F.; Hirsch, A. *Chem. Eur. J.*, **2010**, 16, 3314.
(37) Koh, B.; Park, J. B.; Ximiao, H.; Cheng, W. *J. Phys. Chem. B*, **2011**, 115, 2627.
(38) Bachilo, S. M.; Strano, M. S.; Kittrell, C.; Hauge, R. H.; Smalley, R. E.; Weisman, R. B. *Science*, **2002**, 298, 2361.
(39) Hammon, M. A.; Itkis, M. E.; Niyogi, S.; Alvaraez, T.; Kuper, C.; Menon, M.; Haddon, R. C. *J. Am. Chem. Soc.*, **2001**, 123, 11292.
(40) Itkis, M. E.; Perea, D. E.; Niyogi, S.; Richard, S. M.; Hamon, M. A.; Hu, H.; Zhao, B.; Haddon, R. C. *Nano Lett.*, **2003**, 3, 309.
(41) Waldorff, E.I.; Waas, A.M.; Friedmann, P.P.; Keidar, M. *J. Appl. Phys.*, **2004**, 95, 2749.
(42) Freiman, S.; Hooker, S.; Migler, K.; Arepalli, S. NIST Special Publication. **2008**, 960.

(43) Dresselhaus, M. S.; Dresselhaus, G.; Saito, R.; Jorio, A. *Phys. Rep.*, **2005**, 409, 47.
(44) Maultzsch, J.; Telg, H.L Reich, S.; Thomsen, C. *Phys. Rev. B*, **2005**, 72, 205438.
(45) Strano, M. S.; Doorn, S. K.; Haroz, E. H.; Kittrell, C.; Hauge, R. H.; Smalley, R. E. *Nano Lett.*, **2003**, 3, 1091.
(46) Albertorio, F.; Hughes, M. E.; Golovchenko, J. A.; Branton, D. *Nanotechnology*, **2009**, 20, 395101.

Chapter 4

Degree of Surface Damage of Single-Walled Carbon Nanotubes upon Sonication

4.1 Background

Sonication is fundamental step for dispersing SWCNTs in aqueous solution[1-5]. However, there is a possibility that radicals which are produced during the sonication can damage surface of carbon nanotubes[6,7], changing its physical as well as optical properties. Therefore, studies on possible damages of carbon nanotube surface upon sonication is urgently required for further researches on SWCNT dispersion.

4.2 Rationale and Significance

Studies have been suggest that oxygen radical as well as other radicals can be produced during the regular sonication process. Since, the production of radicals can damage surface of SWCNTs during dispersion, it is necessary to conduct systematic test on SWCNT surface damage upon sonication. We adopted raman spectroscopy to measure the potential damages of SWCNTs upon sonication[8-11]. SWCNTs have specific D band

and G band which arise from the degree of carbon-carbon bonding. D band is responsible for sp^3 hybridized bond, while G band is responsible for sp^2 hybridized bond. Since entire carbon bonding of structurally perfect SWCNTs are consist of sp^2 hybridized bonds, we can estimate degree of SWCNT surface damages by comparing D band and G band intensity of SWCNT samples. Results from this study can provide insights on degree of SWCNT damages as well as stiffness of SWCNT surface upon sonication.

4.3 Abstract

Surface of SWCNTs can be damaged upon regular sonication process. We assessed degree of surface damage of SWCNTs upon sonication. We evaluated degree of surface damage of carbon nanotubes with variety of different conditions. Data is suggesting that routine sonication process does not induce noticeable damages of SWCNT surface.

4.4 Introduction

SWCNTs can be dispersed in aqueous solution with the assistance of sonication. However, sonication can produce radicals, which can potentially damages surface of SWCNTs. This surface damage can change optical and physical properties of SWCNTs, therefore significant attention should be required. However, not many studies have been conducted in order to systematically evaluate degree of SWCNT surface damages upon sonication. In addition, recent study is suggesting that routine sonication process can significantly damage surface of SWCNTs[12]. Therefore, here we tried to systematically

evaluate degree of SWCNT surface damage upon sonication in order to validate appropriateness of sonication process.

4.5 Methods

Raman spectroscopy 10 μL of each carbon nanotube samples were placed on top of cover glass. Raman spectra of each samples were measured by Renishaw inVia raman microscope (Renishaw, UK).

4.6 Results and discussion

Raman spectra of functionalized SWCNTs Figure 4-1 shows strong D band peak from both functionalized SWCNT soots. This data is suggesting that both carboxylic as well as amide functionalized carbon nanotube have significant degree of surface damages as they intended to be produced. Therefore, these two samples can serve as positive control.

Raman spectra of SWCNTs dispersed with elevated level of O_2 We thought about possibility that elevated O2 level may enhance surface damage of SWCNT upon sonication. However, figure 4-2 is showing that there is minimal effect of O2 level on functionalization of SWCNT surface. We also test whether high concentration of OH (which can be turn in to OH·) can induce damage on SWCNT surface. However, our Raman data suggests that high concentration of OH does not induce surface

functionalization of SWCNTs. We observed limited dispersion of SWCNTs in 100 mM NaOH and no dispersion of SWCNTs in 1 M NaOH.

Raman spectra of SWCNT soot and SWCNT/$(dT)_{30}$ dispersed with sonication When we compare the Raman spectra of SWCNT soot and SWCNT dispersed with $(dT)_{30}$ in ddH_2O, we cannot conclude that sonication is inducing SWCNT surface damage due to the minimal peak intensity form D band region (Figure 4-3). We can see minimal changes in peaks intensities. (Also, low I_D/I_G ratio)

Raman spectra of SWCNTs dispersed with antioxidants We dispersed SWCNT in ddH2O in the presence of antioxidants (Figure 4-4) to see whether SWCNTs can be dispersed in ddH2O in the presence of antioxidants. Hines proposed that sonication can induce surface damages of SWCNT surface, and in the presence of antioxidants, SWCNTs cannot be dispersed in aqueous solution. However, our Raman spectral data shows that SWCNTs can be dispersed in aqueous solution with a similar degree to that of without antioxidant (Figure 4-5). Also, we don't see distinguishable changes in D band and G band peak intensities. (Also, I_D/I_G ratio).

Raman spectra of SWCNTs dispersed with no O_2 Also, we further tested the effect of removing the O_2 (by vacuum + Ar purging) on SWCNT dispersion. If Hines' argument is true, then we should not see the SWCNT dispersion since SWCNT surface cannot be functionalized in this condition. However, we still able to disperse SWCNT when there is minimal or no level of O_2 (Figure 4-6), therefore our data suggests that

surface functionalization is not a driving force for ssDNA mediated dispersion of SWCNT upon sonication.

4.7 Conclusion

Data suggests that covalent bonding of ssDNA {$(dT)_{30}$} to SWCNT surface upon surface functionalization is not a major factor of ssDNA mediated dispersion of SWCNTs, since we observed minimal surface functionalization upon sonication. Also, we were still able to see the dispersion of SWCNTs in the presence of antioxidant which is oppose to Hines' argument. The researcher's view on covalent linkage mediated dispersion of SWCNT does not seems right as their assumption, based on (a) the absence of dispersion of carbon nanotubes by T30 in the presence of free radical inhibitors, (b) the details of the structure of T30 dispersed SWCNTs by SPM59, (c) Raman and XPS data, and (d) the specific hybridization of T30 associated SWCNTs with A30 without loss of dispersion, it is apparent that "sonication leads to the generation of covalent linkages between oligonucleotides and SWCNTs" was not effective on our experimental system.

4.8 Acknowledgements

We thank Dr. Adam Matzger in Department of Chemistry, University of Michigan for sharing their instruments as well as insightful comments on manipulating and analyzing Raman spectra.

4.9 Tables

SWCNTs	I_D/I_G ratio
<Positive Control>	
SWCNT-COOH soot	0.261
SWCNT-$CONH_2$ soot	0.040
SWCNT/$(dT)_{30}$ with ↑O_2 in ddH_2O	0.008
SWCNT/$(dT)_{30}$ in 10 mM NaOH	0.008
SWCNT soot	0.007
SWCNT/$(dT)_{30}$ in ddH_2O	0.007
<Negative Control>	
SWCNT/(dT)30 in ddH2O with Ascorbic acid	0.010
SWCNT/(dT)30 in ddH2O with Trolox	0.011
SWCNT/(dT)30 + Ascorbic acid + Ar purging in ddH2O	0.015
SWCNT/(dT)30 + Trolox + Ar purging in ddH2O	0.015

Table 4-1. SWCNTs and corresponding I_D/I_G ratio.

4.10 Figures

SWCNT-COOH soot

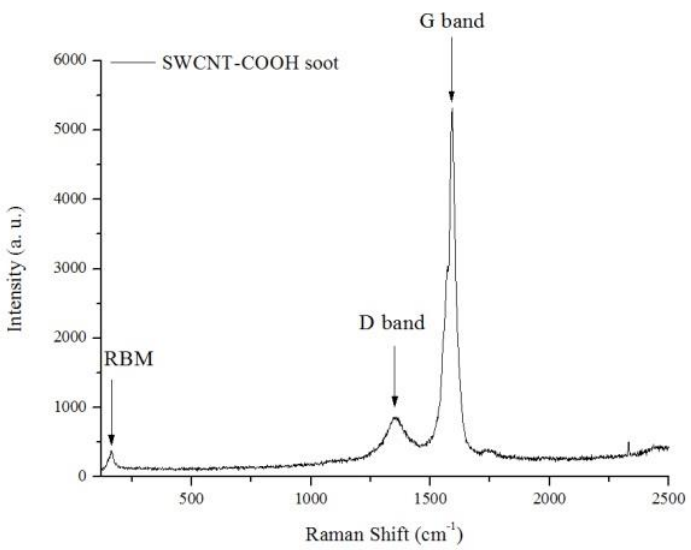

SWCNT-$CONH_2$ soot

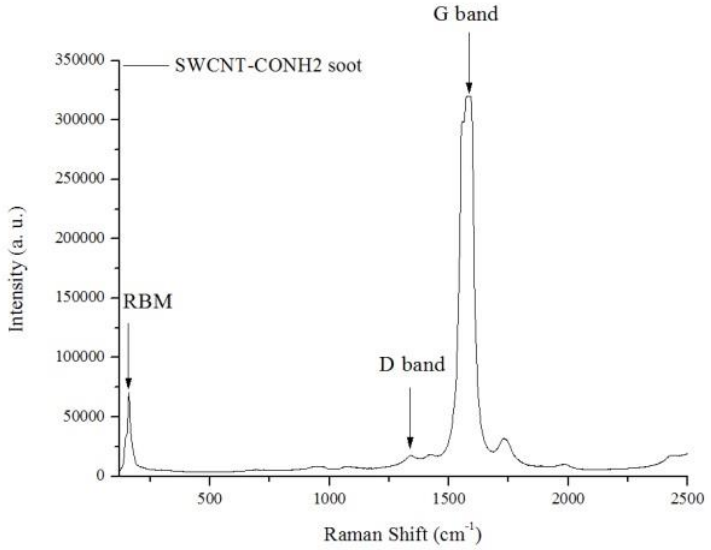

Figure 4-1. Raman spectra of functionalized SWCNTs.

SWCNT/$(dT)_{30}$ with ↑O_2 in ddH_2O SWCNT/$(dT)_{30}$ in 10 mM NaOH SWCNT/$(dT)_{30}$ in 100 mM NaOH

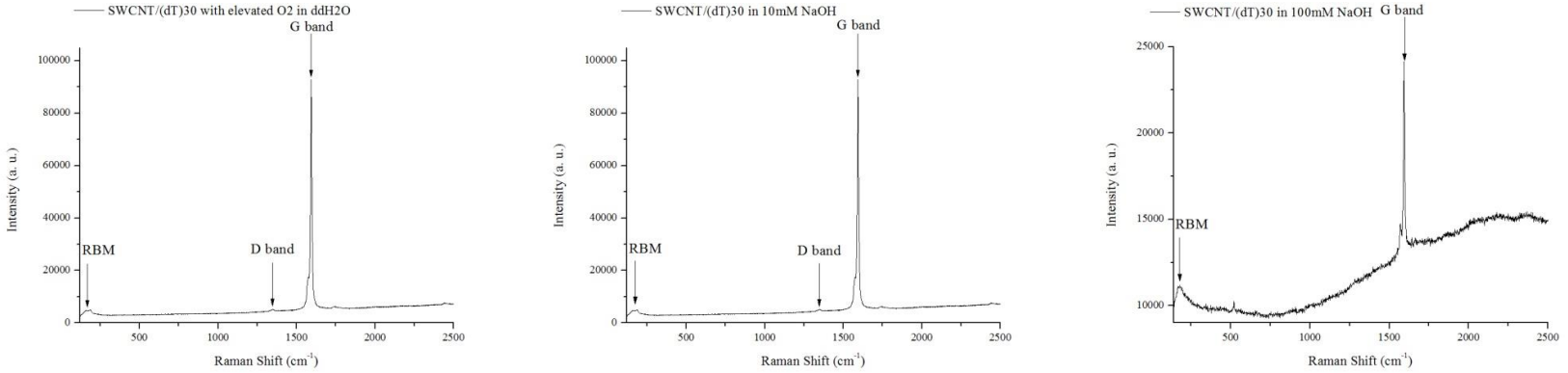

Figure 4-2. Raman spectra of SWCNT/$(dT)_{30}$ with elevated level of O_2 in ddH_2O and 10 mM NaOH.

SWCNT soot

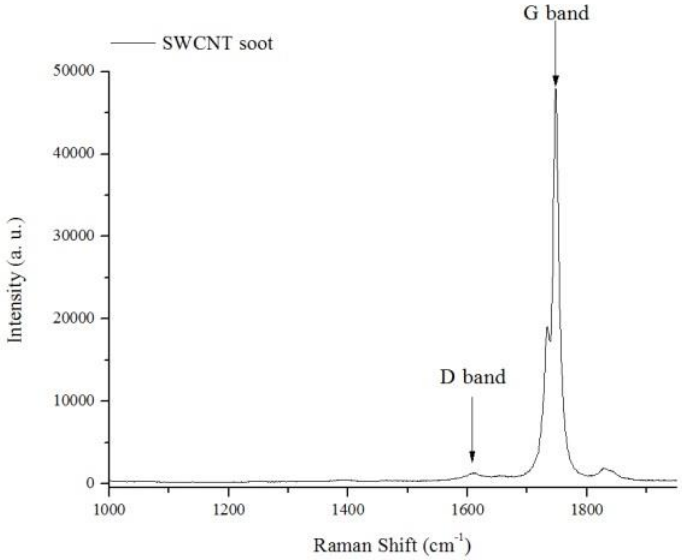

SWCNT/$(dT)_{30}$ in ddH_2O

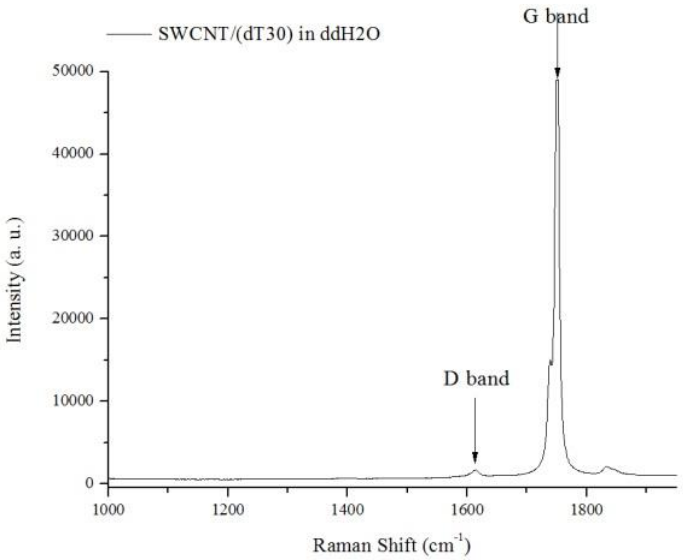

Figure 4-3. Raman specra of SWCNT soot and SWCNT/$(dT)_{30}$ in ddH_2O.

Ascorbic acid (CAS#: 50-81-7)

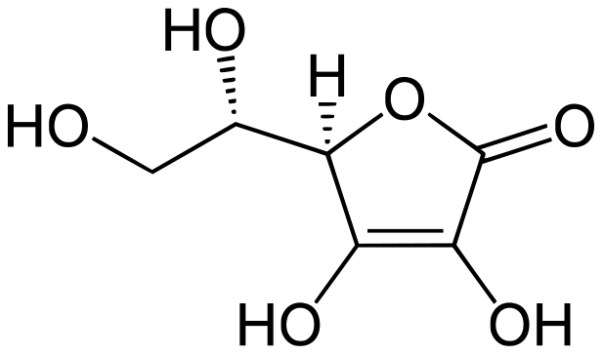

Trolox (CAS#: 53188-07-1)

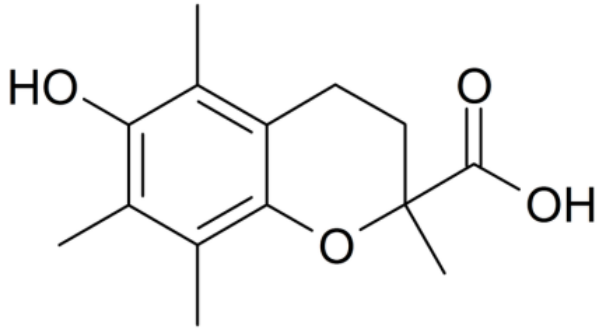

Figure 4-4. Chemical structure of ascorbic acid and trolox.

SWCNT/$(dT)_{30}$ in ddH_2O with AA

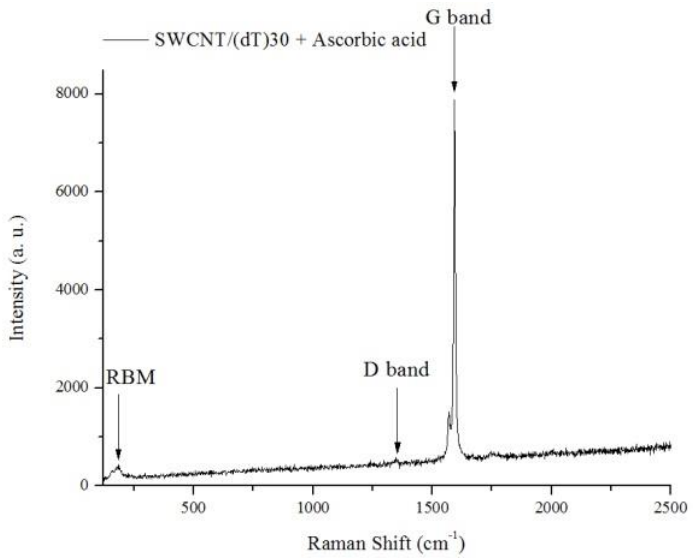

SWCNT/$(dT)_{30}$ in ddH_2O with Trolox

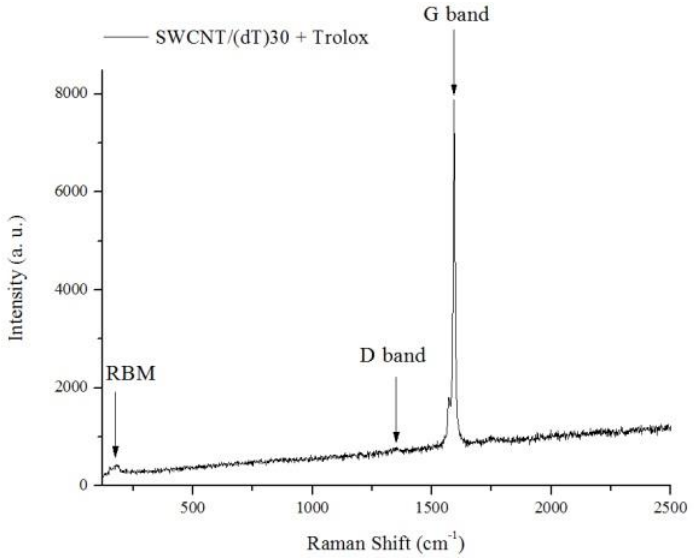

Figure 4-5. Raman Spectra of SWCNT/$(dT)_{30}$ in ddH_2O with ascorbic acid and trolox.

SWCNT/$(dT)_{30}$ + AA + Ar purging in ddH_2O

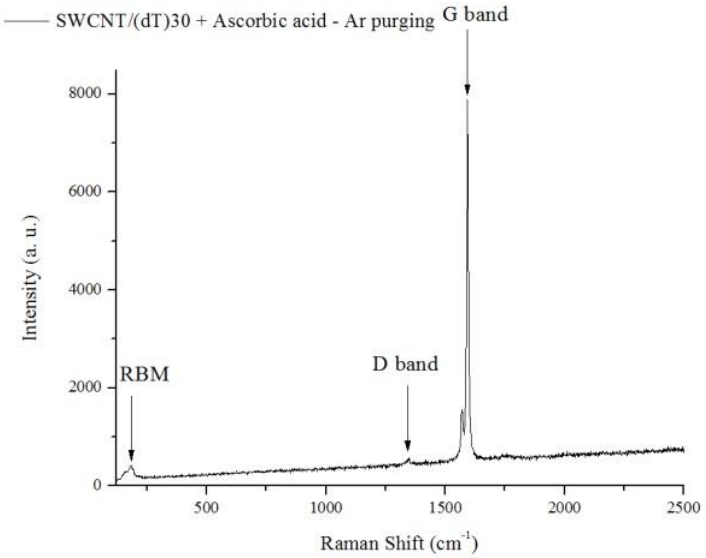

SWCNT/$(dT)_{30}$ + Trolox + Ar purging in ddH_2O

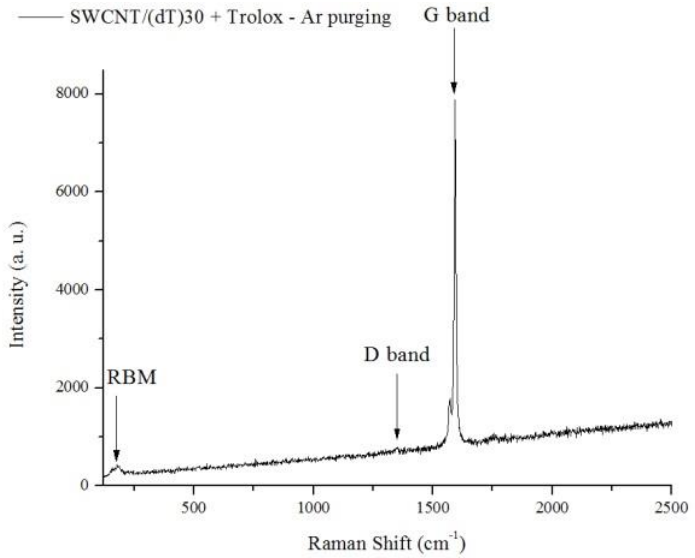

Figure 4-6. Raman spectra of SWCNT/$(dT)_{30}$ with ascorbic acid and trolox with argon purging in ddH_2O.

4.11 References

(1) Park, C.; Ounaises, Z.; Wantson, K. A.; Crooks, R. E.; Smith Jr. J.; Lowther, S. E.; Connell, J. W.; Siochi, E. J.; Harrison, J. S.; St Clair, T. L. *Chem. Phys. Lett.*, **2002**, 364, 303.

(2) Huang, W.; Lin, Y.; Taylor, S.; Gaillard, J.; Rao, A. M.; Sun, Y-P. *Nano Lett.*, **2002**, 2, 231.

(3) Zheng, M.; Jagota, A.; Semke, E. D.; Diner, B. A.; Mclean, R. S.; Lustig, S. R.; Richardson, R. E.; Tassi, N. G. *Nat. Mater.*, **2003**, 2, 338.

(4) Strano, M. S.; Moore, V. C.; Miller, M. K.; Allen, M. J.; Haroz, E. H.; Kittrell, C.; Hauge, R. H.; Smalley, R. E. *Nanosci. Nanotech.*, **2003**, 3, 81.

(5) Tan, Y.; Resasco, D. E. *J. Phys. Chem. B,* **2005**, 109, 14454.

(6) Elia, P.; Azoulay, A.; Zeiri, Y. *Ultrasonic Sonochem.,* **2012**, 19, 314.

(7) Milowska, K.; Gabryelak, T. *Biomol. Eng.*, **2007**, 24, 263.

(8) Dresselhaus, M. S.; Dresselhaus, G.; Jorio, A.; Souza Filho, A. G.; Pimenta, M. A.; Saito, R. *Acc. Chem. Res.,* **2002**, 35, 1070.

(9) Dresselhaus, M. S.; Dresselhaus, G.; Jorio, A.; Souza Filho, A. G.; Samsonidze, G.G.; Saito, R. *Nanosci. Nanotech.,* **2003**, 3, 19.

(10) Jorio, A.; Saito, R.; Hafner, J. H.; Lieber, C. M.; Hunter, M.; McClure, T.; Dresselhaus, G.; Dresselhaus M. S. *Phys. Rev. Lett.*, **2001**, 86, 1118.

(11) Dresselhaus, M. S.; Dresselhaus, G.; Saito, R.; Jorio, A. *Phys. Rep.*, **2005**, 409, 47.

(12) Hines, B. D. D. Purdue Ph.D Dissertation, **2009**.

Chapter 5

Single-Walled Carbon Nanotubes Clearance and Toxicity Issues in Relation to Aggregation Status

5.1 Background

Individually dispersed SWCNTs are used to deliver genes or drugs due to its excellent properties of getting inside of the cells with low or no toxicity[1-3]. However, not much attention has been made on possible aggregation of individually dispersed SWCNTs inside biological systems. Our studies on chapter 6 are showing that individually dispersed SWCNTs can be aggregated during transfection due to the presence of various salts in blood or transfection reagent which mediate charge neutralization of the surface of SWCNTs. Since sizes of aggregated form of SWCNTs including diameter and length significantly differ to that of individually dispersed SWCNTs, its influence on pharmacologic as well as toxic profile cannot be overlooked. Therefore, in this chapter, various reports on toxicity and clearance profiles of individually dispersed SWCNTs as well as aggregated SWCNTs will be summarized and discussed in detail. In addition, the importance of controlling aggregation status of SWCNTs will be discussed.

5.2 Rationale and Significance

Most of the studies of SWCNTs using as gene or drug delivery tools uses individually dispersed carbon nanotubes[4-6]. Dispersed SWCNTs can be stabilized in aqueous system and also easy to attach cargo molecules[7-9]. However, our studies are showing that dispersed SWCNTs can be aggregated in biological system due to the charges on various salts. Since, different pharmacologic as well as toxic profile of aggregated SWCNTs are expected compare to dispersed SWCNTs, it is important to investigate relationship between aggregation status of SWCNTs and clearance as well as toxicity induced by SWCNTs.

5.3 Abstract

Individually dispersed SWCNTs are used for delivering drugs or gene inside of cells and biological systems. However, dispersed SWCNTs can be aggregated by presence of various charged salts which induces neutralization of the surface charge of SWCNTs. Diameter and length of aggregated carbon nanotubes can be 10 ~ 10,000 fold greater than that of individually dispersed SWCNTs, which can influence clearance as well as toxicity. Studies are showing that clearance of aggregated SWCNTs are slower than dispersed SWCNTs and it tend to accumulate in the biological system.

5.4 Discussion

Studies on individually dispersed SWCNTs clearance are suggesting that their blood clearance half-life are average 1.65 hours. However, when the SWCNTs become aggregated (becoming larger), blood clearance half-life became 12.5 hours. Therefore, we can deduce that longer and larger SWCNT aggregates tend to stay longer inside of biological system. Studies on SWCNT accumulation after administration are also suggesting that individually dispersed SWCNTs are not accumulated while SWCNT aggregates tend to accumulate in liver spleen and lung. (Table 5-1) In addition, studies on SWCNT toxicity suggest that SWCNT aggregates are inducing lung inflammation and fibrosis while individually dispersed SWCNTs does not show any noticeable toxicity. Therefore we can deduce that SWCNTs in aggregated form and dispersed form have both advantages and disadvantages as delivery tool. Advantages of using aggregated SWCNTs as potential delivery tool is that they have relatively longer half-life (> 12 hours) compare to individually dispersed SWCNTs because they are not easily taken up by macrophages or going through urinary excreting system or biliary excreting system as dispersed SWCNTs. However, using aggregated SWCNTs have significant disadvantage over dispersed SWCNTs since they are not easily excreted from the body, so that they are gradually accumulated in the body causing inflammatory or fibrotic responses. Individually dispersed SWCNTs have advantages in terms of clearance which result in lower accumulation in biological system compare to aggregated SWCNTs. However, they have shorter half-life (> 2 hours) which makes them not a suitable delivery tool in terms of their prolonged efficacy.

Due to the advantages as well as disadvantages of aggregated and dispersed SWCNTs as delivery tool, it is required to developing method to control aggregation status of SWCNTs inside biological systems.

5.5 Conclusion

Previous studies on SWCNT clearance and toxicity are showing that aggregated form of SWCNTs are having longer clearance time and higher chance to accumulate inside of the body which can cause toxicity. Since, both aggregated as well as individually dispersed SWCNTs have advantages and disadvantages in terms of using as drug or gene delivery tool, it is highly necessary to develop method to control aggregation status of SWCNTs during delivery process.

5.6 Tables

Research articles	Nanotube types	Length (μm)	Diameter (nm)	route	Dose (μg)	$t_{1/2}$* (hr)	toxicity	Accumulation
Dispersed (small) carbon nanotubes								
Nano Lett. 2010, 10,1664	CNT/ Pluronic	~1	1	intra-tracheal	40	-	None	none
PNAS, 2008, 105, 1410	CNT/PEG	~0.1	1	i.v.	20	-	None	none
Nanomedicine 2010,5,1535	CNT/PEG	0.04-0.4	0.8-1.4	i.v.	100	-	None	none
PNAS, 2006, 103,3357	CNT-DTBP	0.3-1	1	i.v.	60	3	None	none
Nano. Res. 2009, 85, 120	CNT/Paclitaxel PEG	0.1	1-2	i.v.		1.1	None	accumulation in liver and spleen
Nat.Nanotechnol. 2007, 2, 47	CNT/PEG	0.1	1-5	i.v.	50	0.5-2	None	none
Am. J. Path. 2011, 178, 2587	Small CNTs	1-5	15	intra-pleural	5	Fast	none	none
Aggregated (large) carbon nanotubes								
Nano. Res. Lett. 2012,2,473	CNT-functional group	1-10	10	i. v.	50	2	none	accumulation in lung
Nano Lett. 2010, 10,1664	CNT/ Pluronic	~20	>10	intra-tracheal	40	-	inflammation	accumulation in lung
Nuc.Med. Bio. 2007, 34, 579.	CNT-Glucosamine	10-100	20-40	i.p.	0.5 (mCi)	5.5	no severe toxicity	none
Am. J. Path. 2011, 178, 2587	Large CNTs	50	20-100	intra-pleural	5	Slow	acute inflammation with fibrosis	accumulation in lung
JACS, 2012, 134,10664	CNT /DSPE mPEG	-	20-50	i.v.	60	>30	none	none

*Blood circulation half-life

Table 5-1. Pharmacokinetic and toxicological profile of various SWCNTs.

5.7 References

(1) Kam, N. W. S.; Jessop, T. C.; Wender, P. A.; Dai, H. *J. Am. Chem. Soc.*, **2004**, 126, 6850.

(2) Bhirde, A. A.; Patel, V.; Gavard, J.; Zhang, G.; Sousa, A. A.; Masedunkas, A.; Leapman, R. D.; Weigert, R.; Gutkind, J. S.; Rusling, J. F. *ACS Nano.*, **2009**, 3, 307.

(3) Singh, R.; Pantarotto, D.; McCarthy, D.; Chaloin, O.; Hoebeke, J.; Partidos, C. D.; Briand, J-P.; Prato, M.; Bianco, A.; Kostarelos, K. *J. Am. Chem. Soc.*, **2005**, 127, 4388.

(4) Klumpp, C.; Kostarelos, K.; Prato, M.; Bianco, A. *Biochimica et Biophysica Acta*, **2006**, 1758, 404.

(5) Gao, L.; Nie, L.; Wang, T.; Qin, Y.; Guo, Z.; Yang, D.; Yan, X. *Chembiochem*, **2006**, 7, 239.

(6) Singh, R.; Pantarotto, D.; McCarthy, D.; Chaloin, O.; Hoebeke, J.; Partidos, C. D.; Briand, J-P.; Prato, M.; Bianco, A.; Kostarelos, K. *J. Am. Chem. Soc.*, **2005**, 127, 4388.

(7) Bandyopadhyaya, R.; Nativ-Roth, E.; Regev, O.; Yerushalmi-Rozen, R. *Nano Lett.*, **2002**, 2, 25.

(8) Matarredona, O.; Rhoads, H.; Li, Z.; Harwell, J. H.; Balzano, L.; Resasco, D. E. *J. Phys. Chem. B*, **2003**, 107, 13357.

(9) Sinani, V. A.; Gheith, M. K.; Yaroslavov, A. A.; Rakhyanskaya, A. A.; Sun, K.; Mamedov, A. A.; Wicksted, J. P.; Kotov, N. A. *J. Am. Chem. Soc.*, **2005**, 127, 3463.

(10) Mutulu, G. M.; Budinger, G. R. S.; Green, A. A.; Urich, D.; Soberanes, S.; Chiarella, S. E.; Alheid, G. F.; McCrimmon, D. R.; Szleifer, I.; Hersam, M. C. *Nano Lett.*, **2010**, 10, 1664.

(11) Liu, Z.; Davis, C.; Cai, W.; He, L.; Chen, X.; Dai, H. *Proc. Natl. Acad. Sci. U.S.A.*, **2008**, 105, 1410.

(12) Bhirde, A. A.; Patel, S.; Sousa, A. A.; Patel, V.; Molinolo, A. A.; Ji, Y.; Leapman, R. D.; Gutkind, J. S.; Rusling, J. F. *Nanomedicine*, **2010**, 10, 1535.

(13) Singh, R.; Pantarotto, D.; Lacerda, L.; Pastorin, G.; Klumpp, C.; Prato, M.; Bianco, A.; Kostarelos, K. *Proc. Natl. Acad. Sci. U.S.A.*, **2006**, 103, 3357.

(14) Liu, Z.; Tabakman, S.; Welsher, K.; Dai, H. *Nano Res.*, **2009**, 85, 120.

(15) Liu, Z.; Cai, W.; He, L.; Nakayama, N.; Chen, K.; Sun, X.; Chen, X.; Dai, H. *Nat. Nanotechnol.*, **2007**, 2, 47.

(16) Murphy, F. A.; Poland, C. A.; Duffin, R.; Al-Jamal, K. T.; Ali-Boucetta, H.; Nunes, A.; Byrne, F.; Prina-Mello, A.; Volkov, Y.; Li, S.; Mather, S. J.; Bianco, A.; Prato, M.; Macnee, W.; Wallace, W. A.; Kostarelos, K.; Donaldson, K. *Am. J. Pathol.*, **2011**, 178, 2587.

(17) Wei, Q.; Zhan, L.; Juanjuan, B.; Jing, W.; Jianjun, W.; Taoli, S.; Yi'an, G.; Wangsuo, W. *Nanoscale Res. Lett.*, **2012**, 23, 473.

(18) Guo, J.; Zhang, X.; Li, Q.; Li, W. *Nucl. Med. Biol.*, **2007**, 34, 579.

(19) Robinson, J. T.; Hong, G.; Liang, Y.; Zhang, B.; Yaghi, O. K.; Dai, H. *J. Am. Chem. Soc.*, **2012**, 134, 10664.

Chapter 6

Carbon Nanotube Aggregation Mechanism and Reversion of Carbon Nanotube Aggregates

The contents in this Chapter is in submission to Journal of American Chemical Society with title of "Carbon Nanotube Aggregation Mechanism and Reversion of Carbon Nanotube Aggregates" (Koh, B., Cheng, W.). My contribution to this paper was design and conduct all the experiments and analysis of experimental data and the writing of the manuscript.

6.1 Background

Despite of possibility of SWCNTs being aggregated during *in vitro* as well as *in vivo* transfection, SWCNT aggregation and its mechanism of aggregation is poorly understood. In addition, it is important to find method to re-disperse SWCNT aggregates when they are formed during transfection. Therefore, we designed and conducted experiment on SWCNT aggregation upon addition of various reagents and investigated mechanism of SWCNT aggregation. We also explored method to re-disperse SWCNT aggregates with breaking connection between SWCNTs by adding disulfide bond reducing agents and enzymes.

6.2 Rationale and Significance

In previous chapter, toxicity of SWCNT aggregates during *in vivo* delivery was discussed. Even though SWCNT have good ability of delivering molecules inside of the cells or biological entities, it is still unclear whether they will form aggregates and cause toxicity during delivery process. Therefore, in this section we studied possible aggregation of SWCNTs during *in vitro* as well as *in vivo* delivery. SWCNT aggregation mechanism was also investigated, since it is important to understand the process during aggregation. In addition, it is important to have method to re-disperse SWCNT aggregates when SWCNT aggregates are formed. Re-dispersing method of SWCNT aggregates were also studied in order to successfully re-disperse SWCNT aggregates when they are formed.

6.3 Abstract

Because of their ability to either penetrate cell membranes or to be endocytosed into cells with relatively low or no toxicity, individually dispersed SWCNTs are considered to be effective carriers of gene or drug molecules. In contrast, studies have suggested that an aggregated form of SWCNTs induces a toxic response *in vivo*, including accumulation in the lung and spleen and induces inflammation and fibrosis, thus limiting their use as a potential delivery tool. Even though the dispersion status of SWCNTs is important for their use as drug/gene carriers, few studies have been carried out describing the potential aggregation of SWCNTs during delivery. Here we studied the

potential aggregation of SWCNTs during cellular delivery and the requirements of SWCNT aggregation. We also examined the mechanism of SWCNT aggregation during cellular delivery. Our study suggests that neutralization of the surface charge induced by charged molecules is responsible for the aggregation of SWCNTs, and this aggregation mechanism of SWCNTs by charged molecules is similar to the DNA condensation mechanism induced by multivalent cations. Lastly, methods for dispersing SWCNT aggregates during cellular delivery were explored. Overall, our studies suggests that SWCNT aggregates can form during cellular delivery, however, they can be re-dispersed, thus preventing accumulation and toxicity.

6.4 Introduction

Due to its unique electrical, mechanical and thermal properties, SWCNTs[1,2] considered as one of the most versatile nano-materials including potential usage in nano-electronics[3,4], cancer treatment[5] and drug and molecule delivery[6]. Individually dispersed SWCNTs have been intensively studied as drug/molecular carrier, since they have ability to either directly penetrate[7-9], or to be endocytosed inside the cells[10-12] with low or no toxicity. However, studies have been suggested that SWCNTs aggregates tend to accumulate inside body causing fibrosis and inflammation[13]. Therefore, it is important to study the aggregation and dispersion of SWCNT during the drug delivery. Many careful studies had been conducted in order to disperse SWCNTs[14-19] as well as controlling aggregation status of SWCNTs by switching a solution pH[20-24], light induced[25-27], changing the oxidation and reduction state of dispersants[28-31], using foldamers[32], via

temperature changes[20,23] and via salt addition[33-35], however not much attention has been made on aggregation of SWCNTs during cellular delivery. We studied possible aggregation of SWCNTs during delivery as well as aggregation of SWCNTs mediated by salts and polyamines were monitored which can be present in animal or human body. Relationship between SWCNT aggregation and SWCNT zeta potential changes were analyzed in order to find a mechanism of SWCNT aggregation. Re-dispersion of SWCNT aggregates mediated by salts, polyamines, were explored in order to reverse SWCNT aggregate formation during *in vitro* or *in vivo* delivery. Especially, enzymatic reversion of SWCNT aggregates were studied which can be applied for controlling aggregation status of SWCNTs during *in vitro* as well as *in vivo* delivery.

6.5 Materials and Methods

Aggregation of SWCNTs in cell culture media. AD SWCNTs (Helix Materials Solution, TX) were dispersed in de-ionized water (ddH_2O, Synergy UV, Millipore, MA) with 1 hr sonication in the presence of short single stranded DNA (ssDNA), $(dT)_{30}$, (TTT TTT TTT TTT TTT TTT TTT TTT TTT TTT, Integrated DNA Technologies, IA), 1,2-distearoyl-*sn*-glycero-3-phosphoethanolamine-N-[amino(polyethylene glycol)-2000] ammonium salt (DSPE-PEG, Avanti Polar Lipids, AL), Pluronic F 108 (Pluronic, BASF) in sonicator (Ultrasonic Processor S-4000, Misonix, Farmingdale, NY, ~15 W, bath was prevent from overheat by adding an ice). P3-SWNTs (SWCNT-COOH, Carbon solutions, CA) were dispersed in ddH_2O with the same procedure described above. We adjusted concentration of dispersed SWCNTs as ~0.02 μg/μL for the consistency throughout the

experiments. 1 µg of dispersed SWCNTs were agitated with cell culture media {90 % ATCC Dulbecco's Modified Eagle Medium (DMEM) + 10 % Fetal Bovine Serum (FBS)} in total volume of 100 µL volume. After 30 minutes of agitation at 200 rpm (Excella E-24R benchtop incubator shakers, New Brunswick Scientific Co, NJ), samples were collected followed by centrifugation at 17,000 g for 90 minutes (Legend Pro 17, Thermo Fisher Scientific, MA). Supernatant was collected after centrifugation and fraction of individual SWCNTs remain in solution was measured with UV-visible-IR spectrophotometer (Shimadzu UV-1800, Kyoto, Japan). All reagents were purchased from Sigma-Aldrich (MO) unless specified.

Charge neutralization and aggregation of SWCNTs. Individually dispersed SWCNTs were agitated in the presence of varying concentration of NaCl, $CaCl_2$, $MgCl_2$, $FeCl_3$, spermidine, spermine, Poly-L-Lysine (PLL) and DEAE-Dextran. (total volume fixed, for 30 minutes at 200 rpm). After agitation, samples were centrifuged for 30 minutes at 17,000 g and supernatants were collected for UV-visible-IR absorbance measurement. Zetal potential of SWCNTs were measured after each treatment in Zetasizer ZS90 (Malvern, UK). For EDTA and NaCl mediated re-dispersion of SWCNT aggregates experiment, we induced aggregation of SWCNTs with 1 mM spermine and spermidine, and further agitate samples with EDTA and NaCl. For agarose gel experiment, 20 µL of 0.02 µg/µL SWCNT samples were aggregated with spermidine, spermine, PLL and DEAE-Dextran and loaded onto 0.6 % agarose gel and ran for 1 hr at 100 V (Powerpac basic, Bio-rad). For atomic force microscopy experiment, 15 µL of re-dispersed SWCNT samples with spermidine, spermine, PLL and DEAE-Dextran were

deposited into either untreated mica or PLL coated mica surface. Samples were then incubated for 15 minutes, washed with 500 μL of ddH_2O for 3 times and then air-dried with N_2. Samples were analyzed with tapping-mode AFM (Veeco Dimension Icon AFM, Veeco, NY) with a silicon AFM probe (RTESP, Veeco, NY), and collected AFM images were analyzed by Nanoscope analysis software (Veeco, NY). All reagents were purchased from Sigma-Aldrich (MO) unless specified.

SWCNT aggregation mechanism. AD SWCNTs were dispersed with $(dT)_{30}$, fluorescein isothiocyanate (FITC, EMD chemicals, NJ), rhodamine B isothiocyanate (RB), crystal violet (CV) and PLL with the same procedure described above. Individually dispersed SWCNT samples were then aggregated by addition of salts and fraction of dispersed SWCNTs as well as its zeta potential changes were monitored with the procedure and instruments described above. For SWCNT aggregation experiment with monovalent and multivalent cations, SWCNT/$(dT)_{30}$ and SWCNT-COOH were aggregated in the presence of designated concentration of potassium chloride (KCl) and spermidine, spermine, PLL and DEAE-Dextran. Changes in SWCNT/$(dT)_{30}$ aggregates size were monitored by brief centrifugation (10 minutes at 17,000 g) after incubation of 0, 1 and 6 hours with 1 mM of $CaCl_2$. 15 μL of collected SWCNT/$(dT)_{30}$ after designated incubation time with $CaCl_2$ were then analyzed with AFM with same procedure described above. For electrolyte concentration dependent SWCNT aggregation kinetic studies, 36 μl of designated concentration of $CaCl_2$ and $MgCl_2$ were added to 3.564 mL of SWCNT/$(dT)_{30}$ and agitated for in benchtop shaker. At designated time points (5, 15, 60, 120, 360 and 720 minutes) after brief vortexing (Vortex Mixer, Thermo Fisher Scientific),

600 µl of incubated samples were collected and centrifuged for 30 minutes at 17,000g in order to remove aggregated SWCNTs. Fraction of individual SWCNTs remain in solution were estimated relative to concentration of SWCNTs before incubation. For DNA length dependent SWCNT aggregation kinetic studies, 1 µl of 200 mM of $CaCl_2$ (final concentration 2 mM) was added and vortexed briefly (1 second) to 99 µl of SWCNTs dispersed with three different length of ssDNA [30 nt ssDNA $\{(dT)_{30}\}$, 200 nt ssDNA with random sequence (Integrated DNA Technologies) and ~2,000 nt ssDNA (extracted from calf thymus)]. SWCNT samples were then transferred to spectrophotometer for the kinetic analysis of aggregate formation. We used the fact that visible light (~500 nm wavelength) is scattered when the SWCNT aggregate is formed. Aggregation kinetics of SWCNT were monitored by measuring absorbance at 500 nm wavelength for every 5 seconds. All reagents were purchased from Sigma-Aldrich (MO) unless specified.

Re-dispersion of aggregated SWCNTs. After inducing aggregation of SWCNT/$(dT)_{30}$, SWCNT-COOH and SWCNT/FITC with determined concentration of salts (5 mM of $CaCl_2$ and $MgCl_2$, 500 µM of $FeCl_3$ for SWCNT/$(dT)_{30}$, 1 mM $CaCl_2$ and $MgCl_2$, 100 µM $FeCl_3$ for SWCNT-COOH, 5 mM $CaCl_2$ for SWCNT/FITC and SWCNT/FSS, 20 mM $CaCl_2$ for SWCNT/RB, SWCNT/CV), designated concentration of ethylenediamine tetraacetic acid (EDTA) was added and agitated in shakers for 30 minutes at 200 rpm. Zeta potential of SWCNT samples were measured after each treatment. Samples were then centrifuged for 30 minutes at 17,000 g and supernatant were collected for absorbance measurement. We determined fraction of individually

dispersed SWCNTs remained in solution relative to reference samples underwent same agitation procedures with same volume of ddH_2O. In order to determine the visible-IR absorbance changes after inducing aggregation and re-dispersion, AD SWCNTs, CVD SWCNTs (SES research, Richardson, TX) and HiPCO SWCNTs (Super purified grade, Unidym, CA) were dispersed in the presence of $(dT)_{30}$ and agitated for 30 minutes with 5 mM of $CaCl_2$ in order to induce aggregation. SWCNT samples were then followed by agitation in the presence of 20 mM EDTA for re-dispersion. For comparison, each AD SWCNT/$(dT)_{30}$, CVD SWCNT/$(dT)_{30}$ and HiPCO SWCNT/$(dT)_{30}$ samples were went through same procedures as $CaCl_2$ and EDTA treated samples but with ddH_2O. UV-visible-IR absorbance were recorded and plotted in parallel for side-by-side comparison. For Dithiothreitol (DTT) and 2-Mercaptoethanol (BME) mediated re-dispersion experiment, SWCNT/$(dT)_{30,}$ SWCNT-COOH and SWCNT/FITC aggregates induced by 20 mM, 5 mM and 10 mM of cystamine dihydrochloride (CD) and 1,6-diaminohexane (DH) respectively, were agitated in the presence of DTT and BME for 30 minutes at 200 rpm. Samples were then collected, centrifuged (for 30 minutes at 17,000 g) and fraction of individual SWCNTs remain in solution were estimated using the procedure described above. All reagents were purchased from Sigma-Aldrich (MO) unless specified.

Enzymatic reversion of bridged SWCNT aggregates. For enzyme mediated re-dispersion of SWCNT aggregates experiment, SWCNT/$(dT)_{30,}$ SWCNT-COOH and SWCNT/FITC were aggregated by addition of customized sequence of polypeptide (KAAAAAAAAK, Pierce Protein, IL. 1 mM for SWCNT/$(dT)_{30,}$ 0.5 mM for SWCNT-COOH, and 2 mM for SWCNT/FITC respectively) with 5 minutes agitation at 200rpm

and then further incubated with designated concentration of trypsin for 6 hours at 37 ℃. Zeta potential of SWCNTs and fraction of individually dispersed SWCNTs remain in solution was determined by vis-IR absorbance spectra. SWCNT/PLL, SWCNT/CV and SWCNT/RB samples were aggregated with polypeptide (EAAAAAAAAE, Pierce Protein, IL) and then further incubated with proteinase K for re-dispersion. For inhibition of enzyme activity as a control experiment, SWCNT aggregates induced by polypeptide (KAAAAAAAAK) were treated with trypsin inhibitor and SWCNT aggregates induced by polypeptide (EAAAAAAAAE) were treated with PMSF. Trypsin and proteinase K were then added to SWCNT aggregates to monitor the re-dispersion of SWCNTs respectively. All reagents were purchased from Sigma-Aldrich (MO) unless specified.

6.6 Results and discussion

Aggregation of SWCNTs in cell culture media. We first tested whether SWCNT can be aggregated in the presence of cell culture media, because it is likely the surrounding circumstances during the transfection process. We used four different types of dispersed carbon nanotubes, SWCNT dispersed by 30-mer single-stranded DNA {SWCNT/$(dT)_{30}$}, SWCNT with carboxylic functional moieties (SWCNT-COOH), SWCNT dispersed by DSPE-PEG (SWCNT/DSPE-PEG) and SWCNT dispersed by Pluronic F 108 (SWCNT/Pluronic) for monitoring the aggregation (Molecular structure of all dispersants as well as other important reagents are shown in supplementary chart 6-1). Aggregation profiles of each SWCNTs are showing that SWCNT/$(dT)_{30}$, SWCNT-COOH and SWCNT/DSPE-PEG were all aggregated in the presence of cell culture

media but not SWCNT/Pluronic (Figure 6-1). Structural difference between SWCNT/$(dT)_{30}$, SWCNT-COOH, SWCNT/DSPE-PEG and SWCNT/Pluronic is that former SWCNTs are carrying multiple negative charges because of negatively charged phosphate backbone on $(dT)_{30}$, carboxylic functional group and negative charges on phosphatidyl groups on DSPE-PEG respectively, while pluronic molecule does not carry any charges. These suggests that electrostatic interaction between negative charges on SWCNT/$(dT)_{30}$, SWCNT-COOH , SWCNT/DSPE-PEG and components in cell culture media is inducing aggregation of SWCNTs.

Charge neutralization and aggregation of SWCNTs. Given the complexity of cell culture media, it is difficult to point out which component is responsible for the aggregation of SWCNTs. We assumed that electrostatic interaction between negative charges on SWCNT/$(dT)_{30}$, SWCNT-COOH , SWCNT/DSPE-PEG and metallic cations in salts present in cell culture media mediates aggregation of SWCNTs due to charge neutralization of SWCNTs. Therefore, we tested aggregation of four different types of SWCNTs in the presence of various salts (Na^+, Ca^{2+}, Mg^{2+}, and Fe^{3+} with Cl^- counter ion) to monitor the aggregation of SWCNTs. Experimental data suggests that SWCNT/$(dT)_{30}$, SWCNT-COOH and SWCNT/DSPE-PEG aggregated as we increased concentration of salts as Niyogi et al.[33-34] previously observed. As Nepal and Geckeler[21] previously reported the relationship between SWCNT zeta potential and aggregation status of SWCNTs, we monitored the relationship between SWCNT aggregation and zeta potential changes. Data suggest that negatively charged SWCNT/$(dT)_{30,}$ SWCNT-COOH (-39.9 ± 12.2 mV, -47.9 ± 14.4 mV respectively) became neutralized (-6.8 ± 13.1 mV, -7.9 ± 12.1

mV, respectively) as SWCNT aggregated by increasing concentration of salts {Figure 6-2. (b)}. We observed aggregation and re-dispersion of SWCNT/DSPE-PEG as we increased the concentration of salts with minimal changes on zeta potential {Figure 6-2. (c)}. We speculated that with low concentration of salts, long chain of hydrophobic PEG can be stacked on hydrophilic DSPE moiety exposing negative charges on phosphatidyl group. Negative charges on phoshatidyl group interact with cations inducing aggregation of SWCNT/DSPE-PEG. However, at high concentration of salts, this long chain of hydrophobic PEG cannot stack on DSPE moiety thus negative charges on phoshpatidyl group cannot be exposed to interact with cations. Another hypothesis is that under lower concentration of salt, electrostatic interaction between negative charges on DSPE and cation induces aggregation of SWCNTs, while long chain of PEG hinders electrostatic interaction between negative charges and cations at high concentration of salts. Overall, this data suggest that addition of cations neutralize the charges of slipping plane of SWCNTs, resulting in increased attraction between SWCNTs thus promoting aggregation. Fe^{3+} showed most efficient neutralization of SWCNTs, followed by Ca^{2+}, Mg^{2+} and Na^{+}. This result suggests that multivalent cations (Fe^{3+}) have more capability of reducing electronic repulsion between individual SWCNTs compare to mono or divalent cations {Figure 6-2. (a), (b) and (c)}. We also monitored potential aggregation of SWCNTs with polyamines (Spermidine, Spermine) and cationic polymers {Poly-L-Lysine (PLL) and DEAE-Dextran} in order to further prove the relationship between SWCNT aggregation and its zeta potential changes. SWCNTs {SWCNT/$(dT)_{30,}$ SWCNT-COOH and SWCNT/DSPE-PEG} aggregated as it became neutralized by addition of polyamines and cationic polymers (Supplementary figure 6-1 and Supplementary figure 6-2). However,

we observed re-dispersion followed by re-aggregation as we increased concentration of polyamines and cationic polymers. Our explanation is that at low concentration, polyamines bind to SWCNTs intermolecularly, serve as bridge connecting surrounding SWCNTs. However, at intermediate concentration, polyamines bind to SWCNTs intramolecularly, so that individual SWCNTs can remain in solution as dispersed (Supplementary figure 6-1). We anticipated that even higher concentration of polyamines favor intermolecular binding to SWCNTs inducing SWCNT aggregates. Second possibility is that intermediate concentration of polyamines screen the electrostatic interaction between individual SWCNTs and polyamine so that charge of individual SWCNTs were retained thus remain in solution as dipsersed. This explanation is further supported by our experiment with SWCNT/$(dT)_{30}$ and EDTA, NaCl. EDTA and NaCl induces dispersion and re-aggregation of SWCNTs aggregates induced by polyamines, and we hypothesized that EDTA and NaCl screen the electrostatic interaction between SWCNT and polyamines (Supplementary figure 6-3). Pelta et al.[36] also described DNA re-solubilization in the presence of high concentration of multivalent cations due to the screening of the short range electrostatic attraction, which support our hypothesis. SWCNTs aggregated with cationic polymers showing similar aggregation and re-dispersion except zeta potential of SWCNTs changed from negative values to positive values (Supplementary figure 6-2). We suspect that those cationic polymers with average > 1000 positively charged moieties continuously adsorbed on the negatively charged surface of SWCNTs until all negatively charged SWCNTs moieties are covered with cationic polymers. Agarose gel experimental data shows that individually dispersed SWCNTs with 1 mg/mL PLL as well as 100 mg/mL DEAE-Dextran migrated toward

anode while SWCNTs with spermine or spermidine migrated toward cathode suggesting reversal of SWCNT surface charge from negative to positive (Supplementary figure 6-4). AFM images of SWCNTs also suggesting that SWCNTs with 1 mg/mL PLL as well as 100 mg/mL DEAE-Dextran adsorbed onto negatively charged untreated mica surface, while SWCNTs with polyamines adsorbed onto positively charged PLL treated mica surface (Supplementary figure 6-5). However, as we increase the concentration of cationic polymers even greater extent, cationic polymers interact with individual SWCNTs intermolecularly, inducing re-aggregation of SWCNTs. No aggregation of SWCNT/Pluronic were observed at any circumstances. We speculate that since pluronic molecule does not carry any charges, no electrostatic interaction occurred after we added charged molecules.

SWCNT aggregation mechanism. Together with SWCNT/$(dT)_{30}$ and SWCNT-COOH, we dispersed SWCNT using negatively charged Fluorescein isothiocyanate (FITC) and positively charged Rhodamine B (RB), Crystal Violet (CV), Poly-L-Lysine (PLL) and monitored relationship between SWCNT aggregation and zeta potential changes (Supplementary figure 6-6). We directly plotted fraction of individual SWCNTs remain with its zeta potential changes in order to see the relationship between SWCNT aggregation and their zeta potential changes (Figure 6-3). Data is suggesting that when 82 % of charges of SWCNTs become neutralized, SWCNTs were fully aggregated. This reminds DNA condensation study by Bloomfield[37,38] and other groups[39-41] that when ~ 90% of DNA charges were neutralized by addition of cations, DNA were condensed. Studies by Korolev et al.[42,43] further studied DNA condensation in the presence of both

monovalent and multivalent cations and ended up with simple thermodynamic model of DNA condensation by oligocationic ligands. We induced aggregation of SWCNT/$(dT)_{30}$ and SWCNT-COOH in the presence of both monovalent Potassium chloride, KCl) and multivalent cations (Spermidine, spermine, PLL and DEAE-Dextran) and monitored the aggregation of SWCNTs. Our data is suggesting that both SWCNT/$(dT)_{30}$ and SWCNT-COOH aggregation with either spermine or spermidine are depending on concentration of KCl while their aggregation with either PLL and DEAE-Dextran are not depending on KCl concentration (Supplementary figure 6-7 and Supplementary figure 6-8). This is similar to what Korolev et al.[42,43] observed with DNA condensation in the presence of both monovalent and multivalent cations, that multivalent cations with >10 valencies compete with KCl to bind to the DNA while multivalent cations with >30 valencies preferentially bind to the DNA inducing condensation without affected by concentration of KCl. We estimated number of negative charges on SWCNT/$(dT)_{30}$ based on careful studies on ssDNA wrapping around SWCNTs[44,45]. We also estimated number of carboxylic group on SWCNT-COOH based on the estimation of negative charges on each individual SWCNT/$(dT)_{30}$. Results from these experiments suggests that partial neutralization of SWCNT surface charge induces aggregation of individually dispersed SWCNTs. We also observed growth of SWCNT aggregates size during SWCNT aggregation. As Fedorov et al.[35] previously conducted careful studies on salt concentration dependent SWCNT aggregates size control, we took a sample of SWCNT/$(dT)_{30}$ after designated time point incubated with $CaCl_2$ and analyzed SWCNT aggregates size changes by taking images with atomic force microscopy (AFM). Before incubation with $CaCl_2$, average height and length of SWCNT/$(dT)_{30}$ were 1.89 nm and

588.40 nm respectively (Supplementary figure 6-9). However, after 1 hr and 6 hours of incubation with $CaCl_2$, average height and diameter of SWCNTs increase to 4.10 nm, 797.27 nm and 8.01 nm, 1462.44 nm respectively. Based on our observation, we propose that cations are first neutralizing the surface charge of SWCNTs forming small aggregates, followed by further aggregation resulting in large aggregates. In addition, we conducted SWCNT aggregation kinetic studies in order to monitor how fast SWCNTs aggregates depending on salt concentration (Supplementary figure 6-10). High concentration of Ca^{2+} and Mg^{2+} induced faster aggregation of SWCNT/$(dT)_{30}$. Therefore, concentrations of cation not only determine the fraction of SWCNTs aggregated but also rate of aggregation. In addition, we monitored aggregation rate of SWCNTs dispersed with different length of DNA upon addition of $CaCl_2$. We used three different length of DNA [30 nt {$(dT)_{30}$}, 200 nt and ~2000 nt long] to disperse SWCNTs. Data suggests that SWCNTs dispersed with ~2,000 nt ssDNA showed fastest aggregation rate followed by 200 nt ssDNA and 30 nt ssDNA. (Supplementary figure 6-11). We speculate that negative charge density on SWCNT dispersed by 2,000 nt ssDNA is higher than SWCNT with 200 nt ssDNA or 30 nt SSDNA, so that each individual SWCNTs dispersed by 2,000 nt ssDNA having more chance to interact with cations which results in faster aggregation.

Re-dispersion of SWCNT aggregates. Since surface charge neutralization of SWCNTs with addition of cationic molecules induces aggregation of SWCNTs, we were curious to see whether chelation of these positively charged metal cations can re-disperse SWCNT aggregates. We induced aggregation of negatively charged SWCNTs with metal

cations and further incubated with metal chelating reagent, EDTA. Addition of EDTA induces re-dispersion of SWCNT aggregates (Figure 6-5). Negative charges on SWCNTs were recovered during re-dispersion which suggests that EDTA successfully chelated metal cations. We proposed that chelating of metal cations blocks binding of metal cations to SWCNTs inducing re-dispersion {Supplementary figure 6-12. (a)}. This can be further supported by the fact that minimal changes of visible-IR absorbance of SWCNTs was observed after inducing aggregation and re-dispersion by adding Ca^{2+} and EDTA compare to that of individual SWCNTs without incubation {Supplementary figure 6-12.(b)}. We also want to point out that 1: 1~10 ratio of cations: EDTA mediates re-dispersion but even greater concentration of EDTA does not induces re-dispersion of SWCNT-COOH aggregates {Figure 6-5. (b)}. This is probably because one molecule of EDTA carries two Na^{+} , and even though EDTA can chelate those metal cations, presence of Na^{+} can induces aggregation of SWCNT-COOH. In addition, concentration of EDTA required to re-disperse SWCNTs is higher than that of metal cations which was required to fully aggregate SWCNT/$(dT)_{30.}$ This data suggests that even though EDTA can form 1:1 complex with metal ions, there can be some steric hinderance due to the crowded SWCNTs which can potentially block binding of EDTA to metal ions. Since we observed charge neutralization mediated aggregation of SWCNTs, we were curious to see whether spacer molecules which have two positive charges at the ends linked by carbon or disulfide chains can mediated aggregation of SWCNTs acting as a “bridge” between SWCNTs. We choose cystamine dihydrochloride (CD) and 1,6-diaminohexane (DH) molecules, one composed entirely with hydrocarbon with the other composed with hydrocarbon and disulfide bond. We confirmed that CD and DH mediate aggregation of

SWCNTs (Supplementary figure 6-13). In order to prove concept of CD and DH molecules acting as "bridge" between SWCNTs, we further incubated SWCNT aggregates with disulfide reducing reagents DTT and BME to see whether reducing disulfide bond can mediate re-dispersion of SWCNTs. We observed that negatively charged SWCNTs aggregated with CD were re-dispersed in the presence of DTT and BME (Figure 6-6). Control experiment with SWCNTs aggregated by DH showed no re-dispersion (Supplementary figure 6-14). These results suggest that both CD and DH play a role as "bridge" between nearby SWCNTs to induce aggregation. Once we break bond in middle of bridge, we were able to see the re-dispersion of SWCNTs. Recovery of zeta potential of SWCNTs to negatively charged state after reducing disulfide bond in CD further suggests that CD and DH molecule mediates aggregation of SWCNTs by connecting nearby SWCNTs (Figure 6-6).

Enzymatic reversion of bridged SWCNT aggregates. Since we observed that the molecules with two positive charges separated by both hydrocarbons or disulfide bond can induce aggregation of SWCNTs, we tested whether customized peptide with two positive (or negative) charges separated by peptide bonds can induce aggregation of SWCNTs. Negatively charged SWCNTs {SWCNT/$(dT)_{30}$, SWCNT-COOH and SWCNT/FITC} were aggregated in the presence of polypeptide {KAAAAAAAAK, Supplementary figure 6-15. (a)}. Positively charged SWCNTs (SWCNT/PLL, SWCNT/CV and SWCNT/RB) were also aggregated by peptide {EAAAAAAAAE, Supplementary figure 6-15. (b)}. After inducing aggregation of SWCNTs, we incubated SWCNT aggregates in the presence of enzymes (trypsin for KAAAAAAAAK and

proteinase K for EAAAAAAAAE). We observed enzyme dependent re-dispersion of SWCNTs (Figure 6-7). Since, trypsin and proteinase K can hydrolyze the peptide bond between lysine (K), alanine (A) and glutamic acid (E), alanine (A) respectively, we deduce that trypsin and proteinase K mediate dispersion of SWCNT aggregates by breaking the polypeptide bridge in between SWCNTs. ~80% of SWCNT/$(dT)_{30}$ and SWCNT-COOH aggregates were re-dispersed with trypsin, while SWCNT/FITC can only reach ~ 55 % re-dispersion. Based on the study that FITC adsorbs to SWCNTs less strongly compare to ssDNA {$(dT)_{30}$} and covalently attached carboxylic functional group on SWCNTs[17], we think that electrostatic interaction between negative charges on FITC and positive charges on polypeptide mediates dissociation of FITC from SWCNTs inducing less re-dispersion. We observed >50 % re-dispersion of SWCNT/CV and SWCNT/RB aggregates by proteinase K with the same reason. Increase in SWCNT aggregates size during incubation with polypeptide {Supplementary figure 6-16. (a)} and decreased re-dispersion with trypsin after inducing SWCNT aggregation with longer agitation time {Supplementary figure 6-16. (b)} also suggest that degree of SWCNT packing is important on re-dispersion of SWCNTs. Lastly, in order to prove whether trypsin or proteinase K are responsible for re-dispersion of SWCNTs, we incubated SWCNT aggregates with enzyme inhibitors {trypsin inhibitor, proteinase K inhibitor (DMSF)} and then further incubated with enzymes (trypsin, proteinase K). In all cases, trypsin inhibitor and DMSF totally blocked re-dispersion, which suggests that trypsin and proteinase K mediate re-dispersion of SWCNT aggregates (Figure 6-7).

6.7 Conclusion

Here we present aggregation of SWCNTs with cell culture media, salts and polyamines which can be present in animal or human body. Our data suggests that SWCNTs can be aggregated during *in vitro* as well as *in vivo* delivery. We found that partial neutralization of charges (~82 %) can induce aggregation of SWCNTs which suggest that there is strong relationship between SWCNT aggregation and SWCNT charge status. We also found that the aggregation of SWCNTs can be described by a mathematical model of DNA condensation in the presence of cations. In addition, aggregated SWCNTs by metallic cations, bridging molecules (Cystamine Dihydrochloride, Customized polypeptides) can be re-dispersed in the presence of metal chelating agents, disulfide bond reducing agents and restriction enzyme. Our method of re-dispersing aggregated SWCNTs could potentially be used to controlling aggregation status of SWCNTs inside biological system.

6.8 Acknowledgements

We thank Dr. Victor Yang in Department of Pharmaceutical Science, University of Michigan, Dr. Raoul Kopelman and Dr. Adam Matzger in Department of Chemistry, University of Michigan for manipulating and sharing the use of their instruments. We thank Cheng lab member Dr. Michael DeSantis, for helping on manipulation of the software.

6.9 Figures

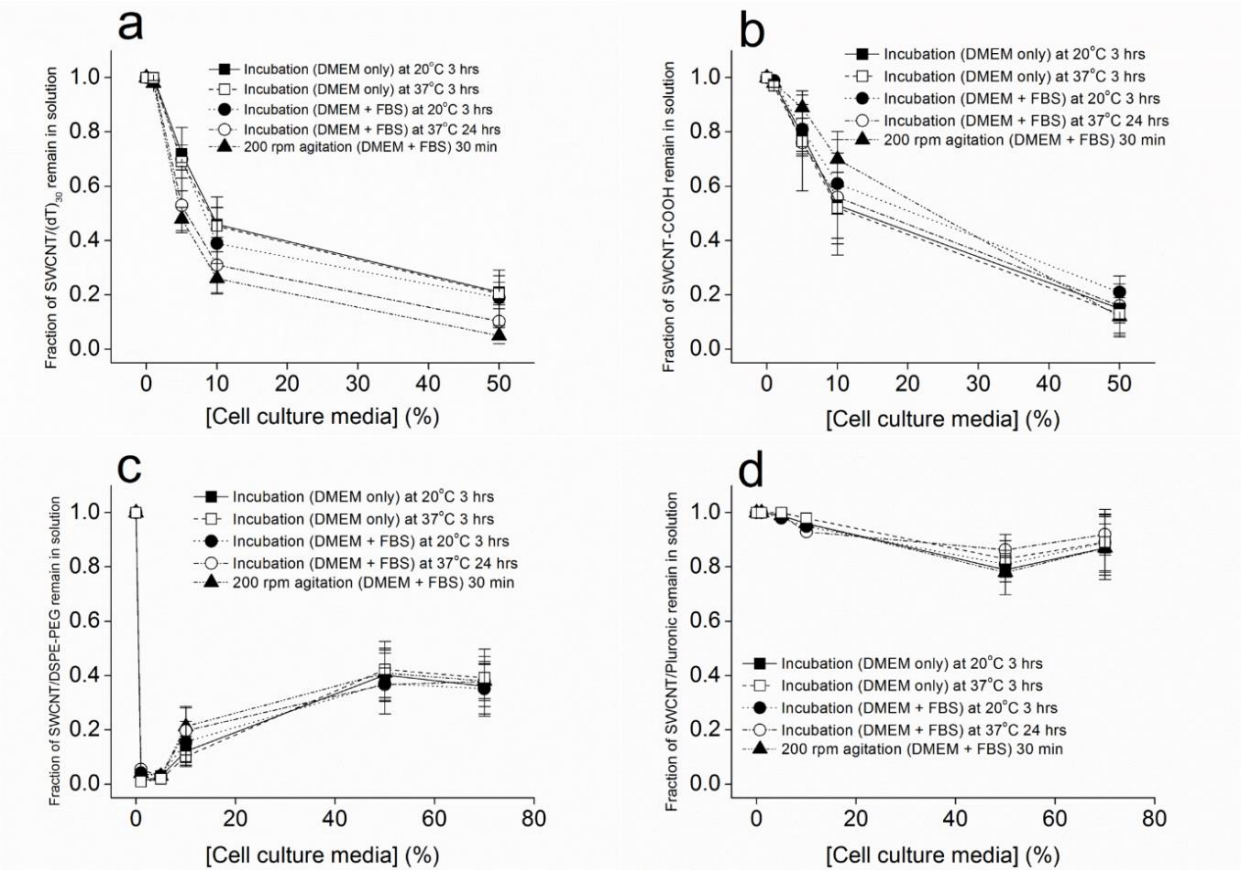

Figure 6-1. Aggregation of (a) SWCNT/$(dT)_{30}$ (b) SWCNT-COOH (c) SWCNT/DSPE-PEG and (d) SWCNT/Pluronic in the presence of cell culture media*. [Cell culture media] represent % volume of cell culture media relative to total volume of dispersed SWCNT + Cell culture media.

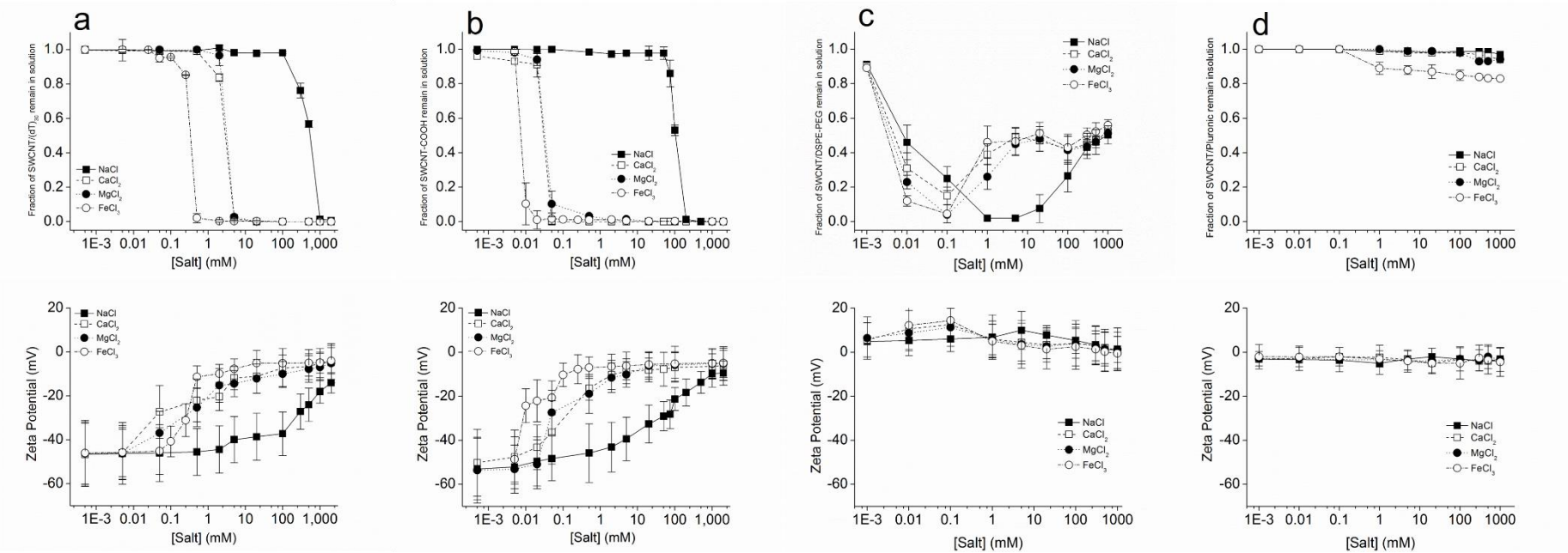

Figure 6-2. Fraction of individual (a) SWCNT/$(dT)_{30,}$ (b) SWCNT-COOH, (c) SWCNT/DSPE-PEG and (d) SWCNT/Pluronic remained in solution (upper panel) with NaCl, $MgCl_{2,}$ $CaCl_2$ and $FeCl_3$ and its zeta potential changes (lower panel).

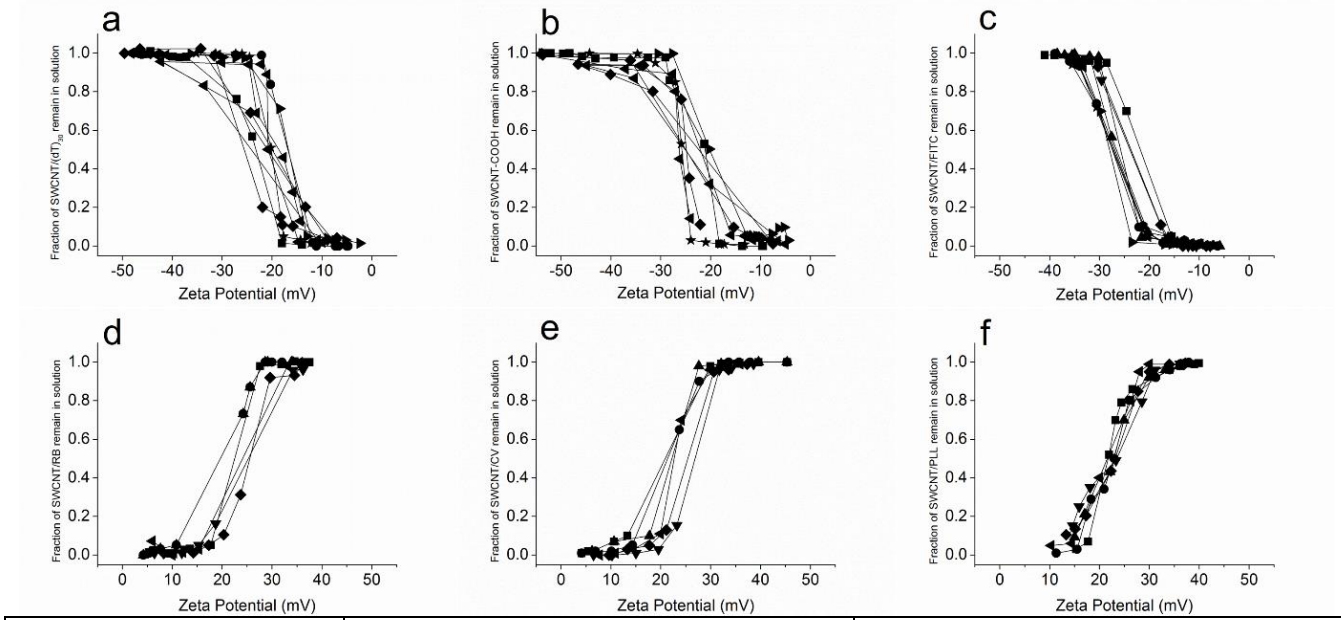

SWCNT type	Original zeta potential (mV)	Zeta potential at SWCNT fully aggregated (mV)
SWCNT/$(dT)_{30}$	-39.9 ± 12.2	-6.8 ± 13.1 (82.1 %)*
SWCNT-COOH	-47.9 ± 14.4	-7.9 ± 12.1 (83.5 %)*
SWCNT/FITC	-38.7 ± 10.6	-8.6 ± 12.1 (77.8 %)*
SWCNT/RB	34.6 ± 11.6	4.7 ± 7.1 (86.4 %)*
SWCNT/CV	41.6 ± 16.6	5.3 ± 6.5 (87.4 %)*
SWCNT/PLL	39.6 ± 15.4	9.9 ± 8.9 (75.0 %)*

*% Zeta potential neutralized compare to original zeta potential

Figure 6-3. Fraction of individually dispersed (a) SWCNT/$(dT)_{30}$ (b) SWCNT-COOH (c) SWCNT/FITC (d) SWCNT/RB (e) SWCNT/CV (f) SWCNT/PLL with zeta potential changes.

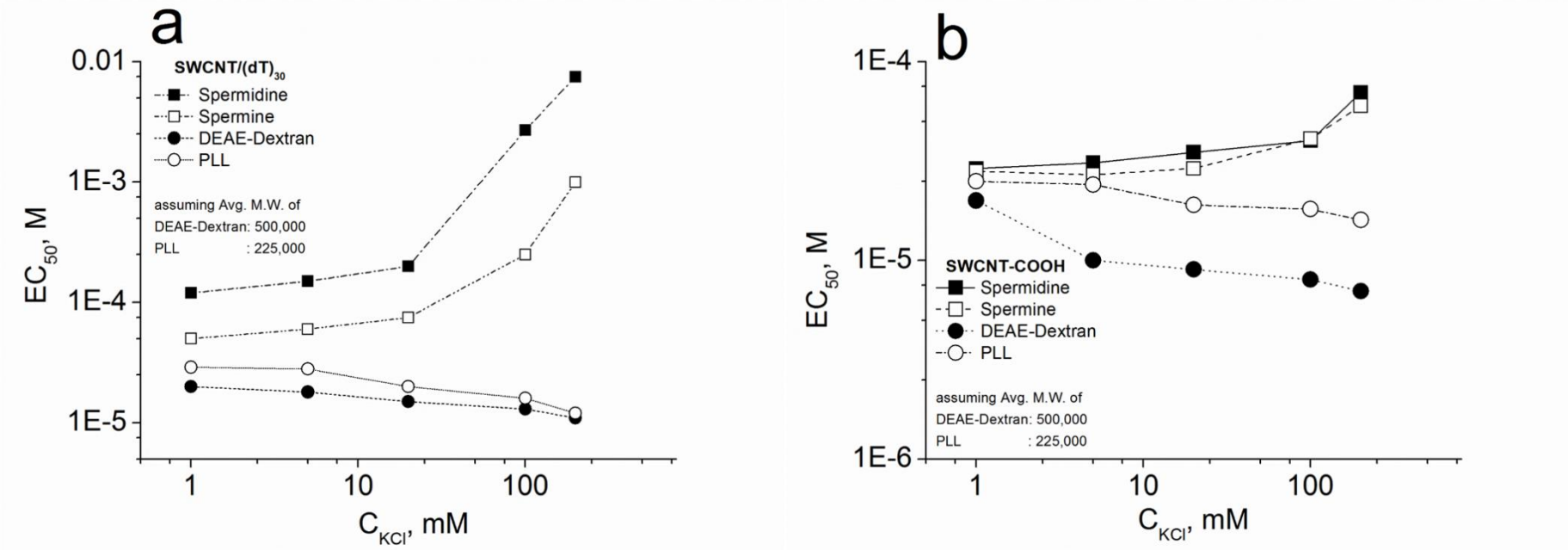

Figure 6-4. KCl concentration dependence of SWCNT aggregation by cationic ligands.

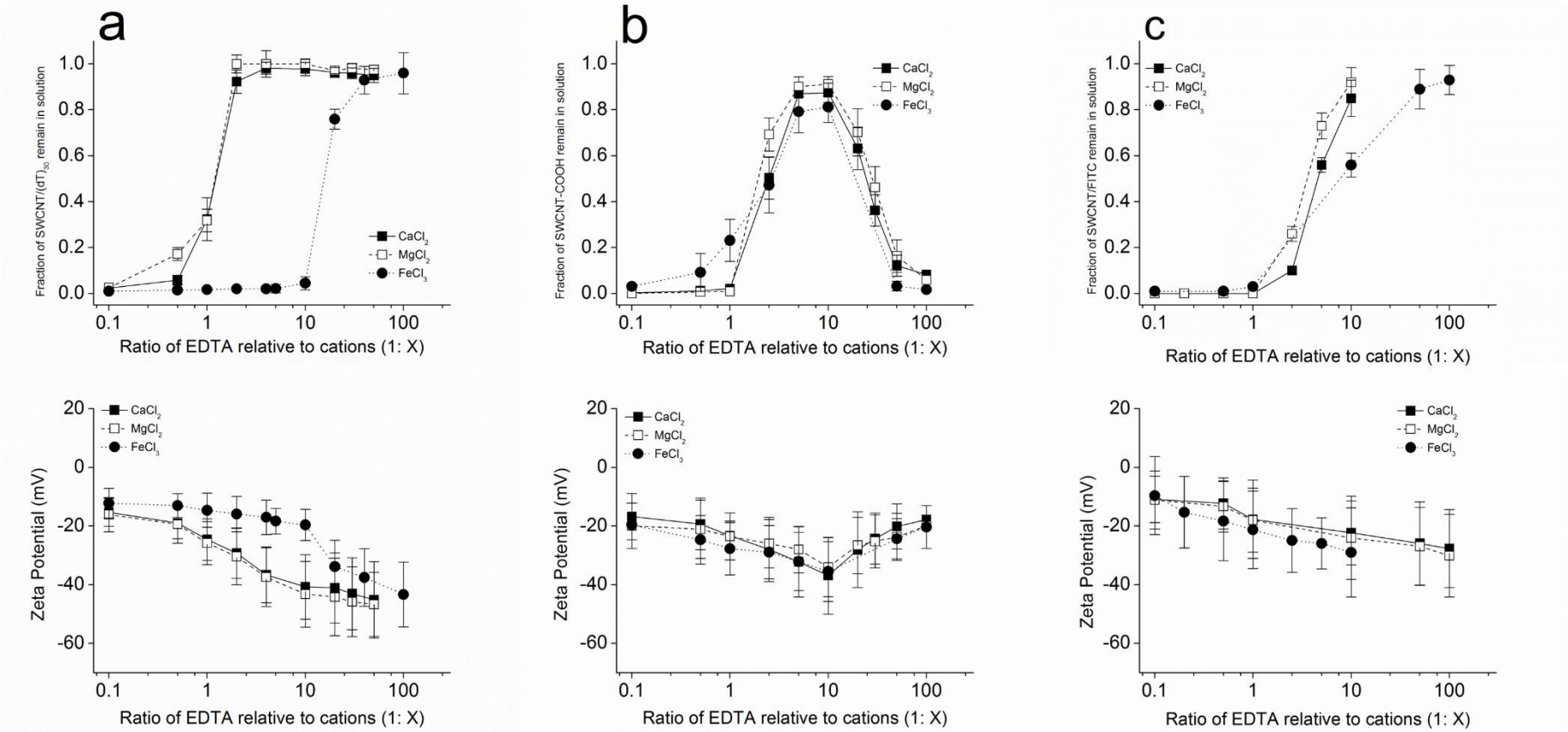

Figure 6- 5. EDTA mediates re-dispersion of (a) SWCNT/$(dT)_{30}$ (b) SWCNT-COOH and (c) SWCNT/FITC aggregates in the presence of metal cations.

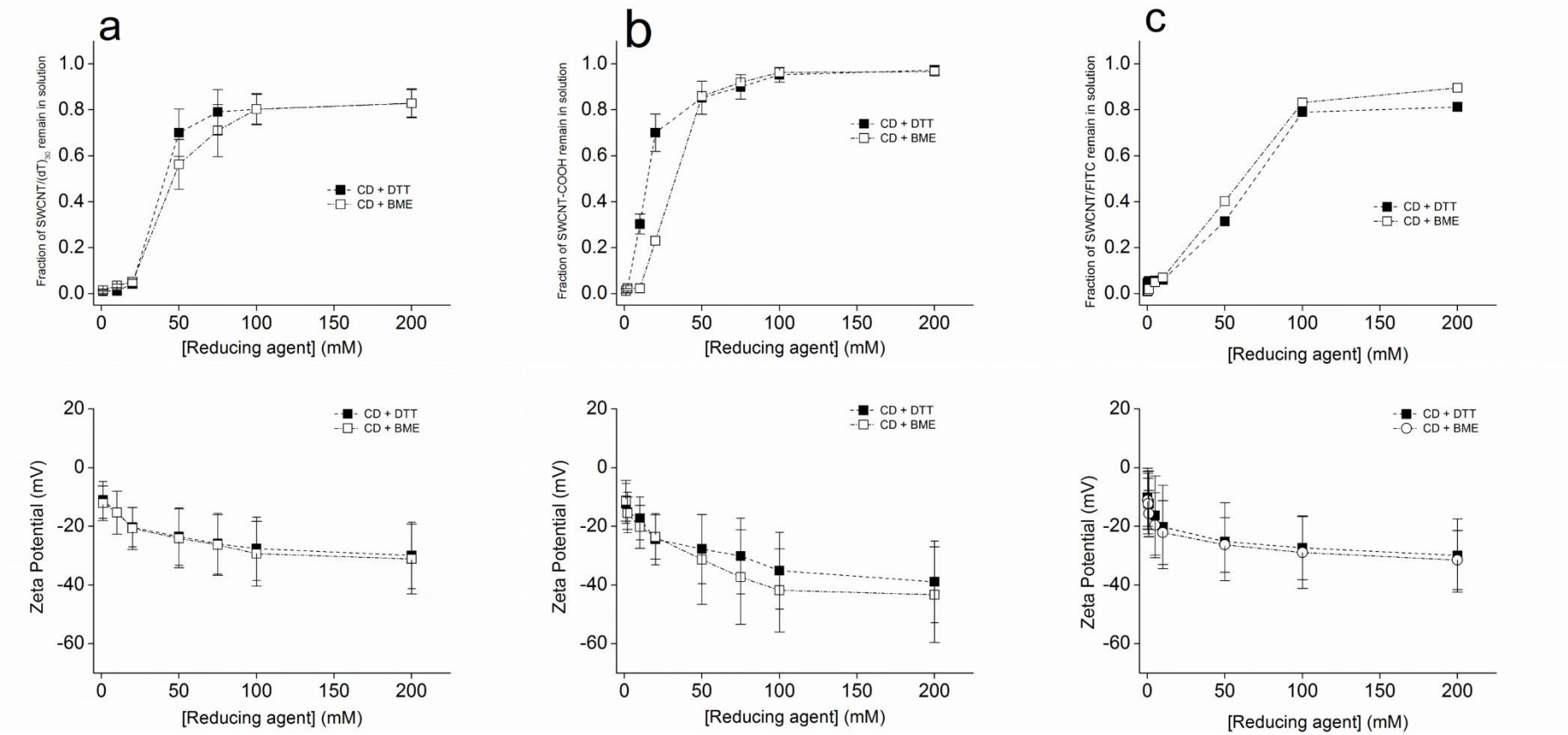

Figure 6-6. Spermine and spermidine concentration dependent aggregation and re-dispersion of (a) SWCNT/$(dT)_{30,}$ (b) SWCNT-COOH with its zeta potential changes.

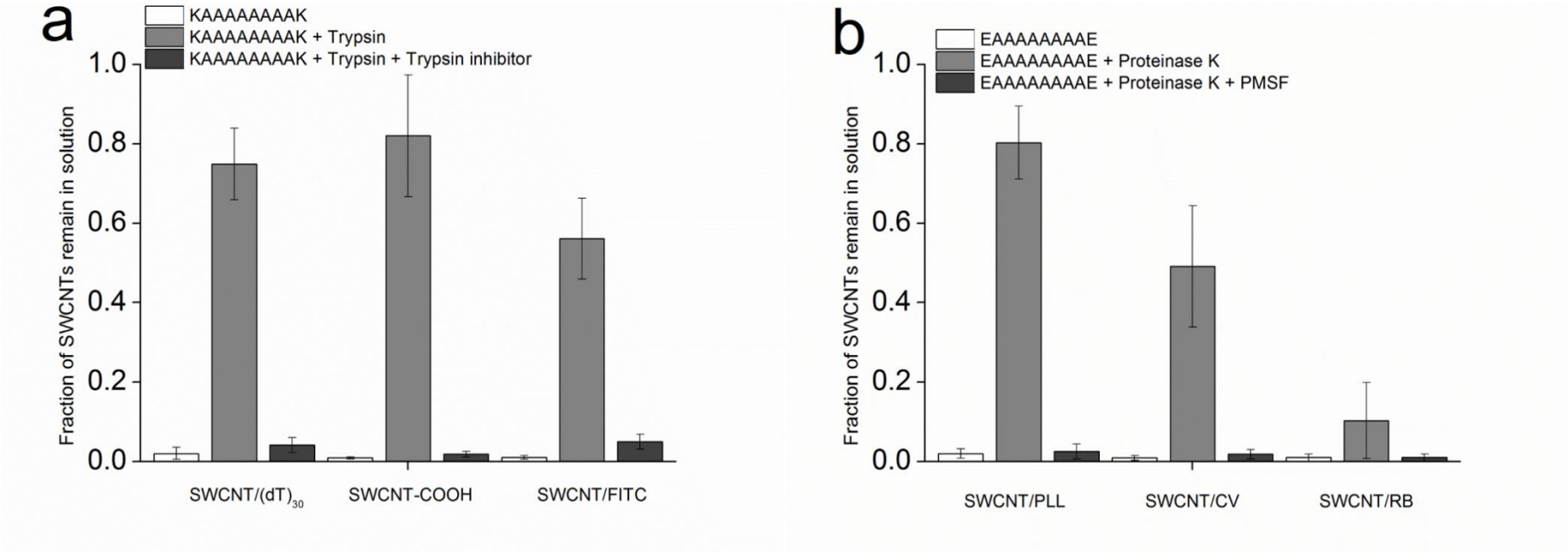

Figure 6-7. (a) Trypsin concentration dependent re-dispersion of SWCNTs (b) Kinetic experiment on trypsin dependent re-dispersion of SWCNTs (c) Buffer type and Trypsin inhibitor influence on re-dispersion of SWCNTs.

6.10 Supporting Information Available

Supporting information is available in the Appendix B

6.11 References

(1) Iijima, S.; Ichihashi, T. *Nature*, **1993**, 363, 603.
(2) Bethune, D. S.; Kiang, C. H.; Devries, M. S.; Gorman, G.; Savoy, R.; Vazquez, J.; Beyers, R. *Nature*, **1993**, 363, 605.
(3) Chen, R. J.; Bangsaruntip, S.; Drouvalakis, K. A.; Kam, N. W. S.; Shim, M.; Li, Y. M.; Kim, W.; Utz, P. J.; Dai, H. *Proc. Natl. Acad. Sci. U.S.A.*, **2003**, 100, 4984.
(4) Dang, X.; Yi, H.; Ham, M-H.; Qi, J.; Yun, D. S.; Ladewski, R.; Strano, M. S.; Hammond, P. T.; Belcher, A. M. *Nat. Nanotechnol.*, **2011**, 6, 377.
(5) Kam, N. W. S.; O'Connell, M.; Wisdom, J. A.; Dai, H. *Proc. Natl. Acad. Sci. U.S.A.*, **2005**, 102, 11600.
(6) Wu, W.; Wieckowski, S.; Pastorin, G.; Benincasa, M.; Klumpp, C.; Briand, J-P.; Gennaro, R.; Prato, M.; Bianco, A. *Angew. Chem. Int. Ed.*, **2005**, 44, 6358.
(7) Pantarotto, D.; Singh, R.; McCarthy, D.; Erhardt, M.; Briand, J-P.; Prato, M.; Kostarelos, K.; Bianco, A. *Angew. Chem.*, **2004**, 116, 5354.
(8) Singh, R.; Pantarotto, D.; McCarthy, D.; Chaloin, O.; Hoebeke, J.; Partidos, C. D.; Briand, J-P.; Prato, M.; Bianco, A.; Kostarelos, K *J. Am. Chem. Soc.*, **2005**, 127, 4388.
(9) Herrero, M. A.; Toma, F. M.; Al-Jamal, K. T.; Kostarelos, K.; Bianco, A.; Ros, T. D.; Bano, F.; Casalis, L.; Scoles, G.; Prato, M. *J. Am. Chem. Soc.*, **2009**, 131, 9843.
(10) Liu, Z.; Chen, K.; Davis, C.; Sherlock, S.; Cao, Q.; Chen, X.; Dai, H. *Cancer Res.*, **2008**, 68, 6652.
(11) Kam, N. W. S.; Liu, Z.; Dai, H. *Angew. Chem. Int. Ed.*, **2006**, 45, 577.
(12) Kam, N.W.S.; Dai, H. *J. Am. Chem. Soc.*, **2005**, 127, 6021.
(13) Mutlu, G. M.; Budinger, R. S.; Green, A. A.; Urich, D.; Soberanes, S.; Chiarella, S. E.; Alheid, G. F.; McCrimmon, D. R.; Szleifer, I.; Hersam, M. C. *Nano Lett.*, **2010**, 10, 1664.
(14) Zheng, M.; Jagota, A.; Semke, E. D.; Diner, B. A.; McLean, R. S.; Lustig, S. R.; Richardson, R. E.; Tassi, N. G. *Nat. Mater.*, **2003**, 2, 338.
(15) Backes, C.; Schmidt, C. D.; Hauke, F.; Boettcher, C.; Hirch, A. *J. Am. Chem. Soc.*, **2009**, 131, 2172.
(16) Koh, B.; Park, J. B.; Ximiao, H.; Cheng, W. *J. Phys. Chem. B*, **2011**, 115, 2627.
(17) Koh, B.; Kim, G.; Yoon, H.; Park, J. B.; Kopelman, R.; Cheng, W. *Langmuir*, **2012**, 28, 11676.
(18) Fagan, J. A.; Bauer, B. J.; Hobbie, E. K.; Becker, M. L.; Hight Walker, A. R.;

Simpson, J. R.; Chun, J.; Obrzut, J.; Bajpai, V.; Phelan, F. R.; Simien, D.; Huh, J. Y.; Migler, K. B. *Adv. Mater.*, **2011**, 23, 338.
(19) Itkis, M. E.; Perea, D. E.; Niyogi, S.; Richard, S. M.; Hamon, M. A.; Hu, H.; Zhao, B.; Haddon, R. C. *Nano Lett.*, **2003**, 3, 309.
(20) Wang, D.; Chen, L. *Nano Lett.*, **2007**, 7, 1480.
(21) Nepal, D.; Geckeler, K. E. *Small*, **2006**, 2, 406.
(22) Zhang, J.; Wang, A. *J. Colloid Interface Sci.*, **2009**, 334, 212.
(23) Grunlan, J. C.; Liu, L.; Kim, Y. S. *Nano Lett.*, **2006**, 6, 911.
(24) Wang, Y.; Xu, H.; Zhang, X. *Adv. Mater.*, **2009**, 21, 2849.
(25) Rodgers, T.; Shoji, S.; Sekkat, Z.; Kawata, S. *Phys. Rev. Lett.*, **2008**, 101, 127402.
(26) Chen, S.; Jiang, Y.; Wang, Z.; Zhang, X.; Dai, L.; Smet, M. *Langmuir*, **2008**, 24, 9233.
(27) Matsuzawa, Y.; Kato, H.; Ohyama, H.; Nishide, D.; Kataura, H.; Yoshida, M. *Adv. Mater.*, **2011**, 23, 3922.
(28) Lemasson, F.; Tittmann, J.; Hennrich, F.; Stürzl, N.; Malik, S.; Kappes, M. M.; Mayer, M. *Chem. Commun*., **2011**, 47, 7428.
(29) Nobusawa, K.; Ikeda, A.; Kikuchi, J.; Kawano, S.; Fujita, N.; Shinkai, S. *Angew. Chem. Int. Ed.*, **2008**, 47, 4577.
(30) Liang, S.; Chen, G.; Peddle, J.; Zhao, Y. *Chem. Commun.*, **2012**, 48, 3100.
(31) Ding, Y.; Chen, S.; Xu, H.; Wang, Z.; Zhang, X.; Ngo, T. H.; Smet, M. *Langmuir*, **2010**, 26, 16667.
(32) Zhang, Z.; Che, Y.; Smaldone, R. A.; Xu, M.; Bunes, B. R.; Moore, J. S.; Zang, L. *J. Am. Chem. Soc.*, **2010**, 132, 14113.
(33) Niyogi, S.; Boukhalfa, S.; Chikkannanavar, B.; McDonald T. J.; Heben, M. J.; Doorn, S. K. *J. Am. Chem. Soc.*, **2007**, 129, 1898.
(34) Niyogi, S.; Densmore, C. G.; Doorn, S. K. *J. Am. Chem. Soc.*, **2009**, 131, 1144.
(35) Fedorov, M. V.; Arif, R. N.; Frolov, A. I.; Kolar, M.; Romanova, A. O.; Rozhin, A. G. *Phys. Chem. Chem. Phys*., **2011**, 13, 12399.
(36) Pelta, J.; Livolant, F.; Sikorav, J-L. *J. Biol. Chem*., **1996**, 271, 5656-5662.
(37) Bloomfield, V. A. *Biopolymers*, **1997**, 44, 269.
(38) Wilson, R. W.; Bloomfield, V. A. *Biochemistry*, **1979**, 18, 2192.
(39) Eickbush, T. H.; Moudrianakis, E. N. *Cell*, **1978**, 13, 295.
(40) Lang, D. *J. Mol. Biol.*, **1978**, 78, 247.
(41) Rauspaud, E.; Olvera de la Cruz, M.; Sikorav, J.-L.; Livolant, F. *Biophys. J*., **1998**, 74, 381.
(42) Korolev, N.; Berezhnoy, N. V. ; Eom, K. D.; Tam, J. P.; Nordenskiold, L. A *Nucleic Acid Res*., **2009**, 37, 7137.
(43) Korolev, N.; Lyubartsev, A. P.; Nordenskiold, L. *Adv. Colloid Interface Sci*., **2010**, 158, 32.
(44) Campbell, J. F.; Tessmer, I.; Thorp, H. H.; Erie, D. A. *J. Am. Chem. Soc*., **2008**, 130, 10648.
(45) Yarotski, D. A.; Kilina, S. V.; Talin, A. A.; Treitiak, S.; Prezhdo, O. V.; Balatsky, A. V.; Taylor, A. J. *Nano Lett.*, **2009**, 9, 12.

Chapter 7

Final Discussion

7.1 Overview of Results

Data from optimization of SWCNT dispersion study is suggesting that mild sonication with extensive centrifugation can produce individually dispersed SWCNTs with highest degree of dispersion. Our study is suggesting that SWCNT dispersants have two common properties: 1. having hydrophobic moiety which can adsorb to the surface of SWCNTs, 2: having hydrophilic moieties but not necessarily charged moieties which allows to be stabilized in aqueous solution. In addition, data is showing that SWCNT surface cannot be damaged upon sonication process. Therefore, sonication process can be adopted for dispersion of SWCNTs. It is observed that individually dispersed SWCNTs can be aggregated during cell transfection experiment due to the opposite charges in either cell culture media or in blood. It is suggested that this aggregated form of SWCNTs can be toxic due to the low clearance and accumulation inside body. Therefore, understanding the SWCNT aggregation mechanism as well as searching methods to re-disperse aggregated SWCNTs are important. Our data is suggesting that when the surface charges of dispersed SWCNTs become neutralized, SWCNTs start to aggregate. One

other observation is that SWCNTs can be re-dispersed when surface charges of aggregated SWCNTs recovered to original state. Inducing SWCNT aggregation by polypeptide then adding restriction enzyme were able to disperse aggregated SWCNTs. This approach can be applied for controlling aggregation status of SWCNTs during transfection experiment.

7.2 Interpretation of Results

SWCNTs can be dispersed with sonication in the presence of dispersants[1-4]. Sonication allows SWCNT bundles to be separated momentarily and the dispersants can adsorb to each individual SWCNT's surface during the moment of separation. This relates to the structural requirements for SWCNT dispersants. SWCNT dispersants must have hydrophobic moieties which allows adsorption (stacking) onto the surface of SWCNTs[5-7]. However, adsorption of dispersant on the surface of SWCNTs does not mean it can be dispersed in aqueous solution. Dispersants also should have hydrophilic moieties which can face aqueous environment without forming colloid. Our SWCNT dispersion experiment with fluorophores and dye molecules is also supporting this requirement of SWCNT dispersants. However, our data is suggesting that not all the fluorophores or dye molecules can disperse SWCNTs. Therefore, being amphiphilic molecules but with specific chemical structure is required for successful SWCNT dispersants. Another important issues in SWCNT dispersion is that whether sonication can induce surface damages of SWCNTs, which can change its fundamental properties[8-10]. We conducted Raman spectroscopic analysis of SWCNT surface and our data is

suggesting that sonication with conventional sonicator does not induce damages on SWCNT surface[11-13]. Therefore, sonication step can be regularly adopted for the dispersion of SWCNTs. SWCNT aggregation is another important issues when we want to develop as potential delivery tools[14-18]. It has been suggested that SWCNT aggregates does not easily secreted starts to accumulate inside of the body[19,20]. This can result inflammatory response and eventual damages on the specific organs where it accumulates[21-23]. Therefore, controlling aggregation status of SWCNTs are important as we want to use it as therapeutic purposes. Our experimental data is suggesting that individually dispersed SWCNTs can be aggregated when the surface charge is became neutralized. Individually dispersed SWCNTs with either positive or negative surface charges can be attracted by counterions and neutralization of the surface charges as well as aggregation seems to occur. This mechanism of SWCNTs can be further validated by other experimental results, addition of chelating agents of counterions can mediate dispersion of aggregated SWCNTs. We also observed SWCNT surface charge recovery as they dispersed. By using this fact, we also try to induce aggregation of SWCNTs with customized polypeptide with counter charges on each ends. Aggregation of SWCNTs with this polypeptide was re-dispersed by addition of restriction enzyme which can digest polypeptide bonds in this customized polypeptide. This data is suggesting that it is possible to control aggregation status of SWCNTs even inside of biological system using polypeptide and enzymes inside of biological system.

7.3 Issues to be Resolved

We found similarity in between mechanism of SWCNTs aggregation and DNA condensation related to their changes in surface charges. However, mathematical model of describing SWCNT aggregation were still under investigation. In addition, our experimental data suggests that aggregation status of SWCNTs can be controlled by using specific aggregation and dispersion agents. However, even though many pharmacokinetic as well as toxicological profiles of SWCNTs have been studied, it is still not clear how the SWCNTs inside biological system can be cleared and its dependency on aggregation status of SWCNTs. In addition, our proposed model of controlling aggregation status of SWCNTs inside of biological system using polypeptide and enzyme is still not validated *in vivo* system.

7.4 Future Direction

Mathematical model describing SWCNT aggregation is currently under development. In addition, in order to further develop carbon nanotubes as therapeutics, systematic studies on SWCNT clearance and its toxicological profile should be conducted. Our experimental data suggests that SWCNTs can be aggregated during cellular *in vitro* as *in vivo* transfection experiment. Therefore, SWCNT mediated delivery studies should concern possible aggregation during experiment. In addition, enzymatic model of re-dispersion of aggregated SWCNTs can be further supported by *in vitro* as well as *in vivo* studies as we want to use as controlling aggregation status of SWCNTs.

7.5 Overarching Conclusion

SWCNTs can be used as a potential drug/DNA carrier due to their ability to enter cells with relatively low or no toxic effects. Dispersion of SWCNTs in aqueous solution is essential to prevent toxicity, but few systematic studies have been conducted on optimizing SWCNT dispersion, and few have investigated the structural requirements of SWCNT dispersants. Therefore, we designed and conducted experiments to find the optimal conditions for successful SWCNT dispersion. We also investigated the structural requirements of effective SWCNT dispersants. Since the aggregation of SWCNTs during cellular delivery can cause serious adverse effects on biological systems, our study addresses fundamental issues of SWCNT aggregation: (1) how SWCNTs aggregate and (2) how to control the aggregation of SWCNTs.

We investigated both the mechanistic and experimental phenomena of SWCNT aggregation and dispersion. More therapeutically applicable, we developed a successful model for re-dispersing SWCNT aggregates using enzymes, which can potentially be used as a method to control the aggregation of SWCNTs inside biological entities.

However, despite our findings, there are still many obstacles to the further development of SWCNTs as successful drug/DNA carriers. First of all, its exact clearance mechanism and toxic profiles are still not clearly understood. Secondly, our model for controlling the aggregation status of SWCNTs was not tested in vivo. Therefore, further development requires followup studies on (1) controlling the aggregation status of SWCNTs in vitro and in vivo, and (2) identifying the pharmacokinetic profile of SWCNTs inside biological entities.

In summary, we conducted systematic and mechanistic studies of SWCNT aggregation and dispersion. Hopefully, our results can serve as a step forward in (1) understanding SWCNT aggregation and dispersion as well as in (2) developing SWCNTs for further application in drug/DNA delivery.

7.6 References

(1) Rastogi, R.; Kaushal, R.; Tripathi, S. K.; Sharma, A. L.; Kaur, I.; Bharadwaj, L. M. *J. Coll. Int. Sci.*, **2008**, 328, 421.
(2) Chatterjee, T.; Yurekli, K.; Hadjiev, V. G.; Krishnamoorti, R. *Adv. Func. Mater.*, **2005**, 15, 1832.
(3) Matsuura, K.; Saito, T.; Okazaki, T.; Ohshima, S.; Yumara, M.; Iijima, S. *Chem. Phys. Lett.*, **2006**, 429, 497.
(4) Zheng, M.; Jagota, A.; Semke, E. D.; Diner, B. A.; Mclean, R. S.; Lustig, S. R.; Richardson, R. E.; Tassi, N. G. *Nat. Mater.*, **2003**, 2, 338.
(5) Moulton, S. E.; Minett, A. I.; Murphy, R.; Ryan, K. P.; McCarthy, D.; Coleman, J. N.; Blau, W. J.; Wallace, G. G. *Carbon*, **2005**, 4, 1879.
(6) Yan, L. Y.; Poon, Y. F.; Chan-Park, M. B.; Chen, Y.; Zhang, Q. *J. Phys. Chem. C*, **2008**, 112, 7579.
(7) Zou, J. Liu, L.; Chen, H.; Khondaker, S. I.; McCullough, R. D.; Huo, Q.; Zhai, L. *Adv. Mater.*, **2008**, 20, 2055.
(8) Zhao, W.; Song, C.; Pehrsson, P. E. *J. Am. Chem. Soc.*, **2002**, 124, 12418.
(9) Vink, T. J.; Gilles, M.; Kriege, J. C.; van der Laar, H. W. J. *J. Appl. Phys. Lett.*, **2003**, 83, 3552.
(10) Kim, J. A.; Seong, D. G.; Kang, T. J.; Youn, J. R. *Carbon*, **2006**, 44, 1898.
(11) Grossiord, N.; Loos, J.; van Laake, L.; Maugey, M.; Zakri, C.; Koning, C. E.; Hart, A. J. *Adv. Func. Mater.*, **2008**, 18, 3226.
(12) Sham, M-L.; Kim, J-K. *Carbon*, **2006**, 44, 768.
(13) Hines, B. D. D. Purdue Ph.D Dissertation, **2009**.
(14) Qu, G.; Bai, Y.; Zhang, Y.; Jia, Q.; Zhang, W.; Yan, B. *Carbon*, **2009**, 47, 2060.
(15) Simon-Deckers, A.; Gouget, B.; Mayne-L'Hermite, M.; Herlin-Boime, N.; Reynaud, C.; Carriere, M. *Toxicology*, **2008**, 253, 137.
(16) Liu, Z.; Chen, K.; Davis, C.; Sherlock, S.; Cao, Q.; Chen, X.; Dai, H. *Cancer. Res.*, **2008**, 68, 662.
(17) Liu, Z.; Cai, W.; He, L.; Nakayama, N.; Chen, K.; Sun, X.; Chen, X.; Dai, H. *Nat. Nanotechnol.*, **2007**, 2, 47.
(18) Schmidt, R. H.; Kinloch, I. A.; Burgess, A. N.; Windle, A. H. *Langmuir*, **2007**, 23, 5707.

(19) Maitani, Y.; Nakamura, Y.; Kon, M.; Sanada, E.; Sumiyoshi, K.; Fujine, N.; Asakawa, M.; Kogiso, M.; Shimizu, T. *Int. J. Nanosci.*, **2013**, 8, 315.
(20) Chang, J.; Shiral Fernando, K. A.; Monica Veca, L.; Sun, Y-P.; Lamond, A. I.; Lam, Y. W.; Cheng, S. H. *ACS Nano*, **2008**, 2, 2085.
(21) Bhattacharya, K.; Andon, F. T.; El-Sayed, R.; Fadeel, B. *Adv. Drug Deliv. Rev.*, **2013**, In press
(22) Yang, S-T. Wang, X.; Jia, G.; Gu, Y.; Wang, T.; Nie, H.; Ge, C.; Wang, H.; Liu, Y. *Toxicol. Lett.*, **2008**, 181, 182.
(23) Warheit, D. B.; Laurence, B. R.; Reed, K. L.; Roach, D. H.; Reynolds, G. A. M. Webb, T. R. *Toxicol. Sci.*, **2004**, 77, 117.

Appendices

Appendix A

Supporting Information in Chapter 3

Supplemental Figures and tables

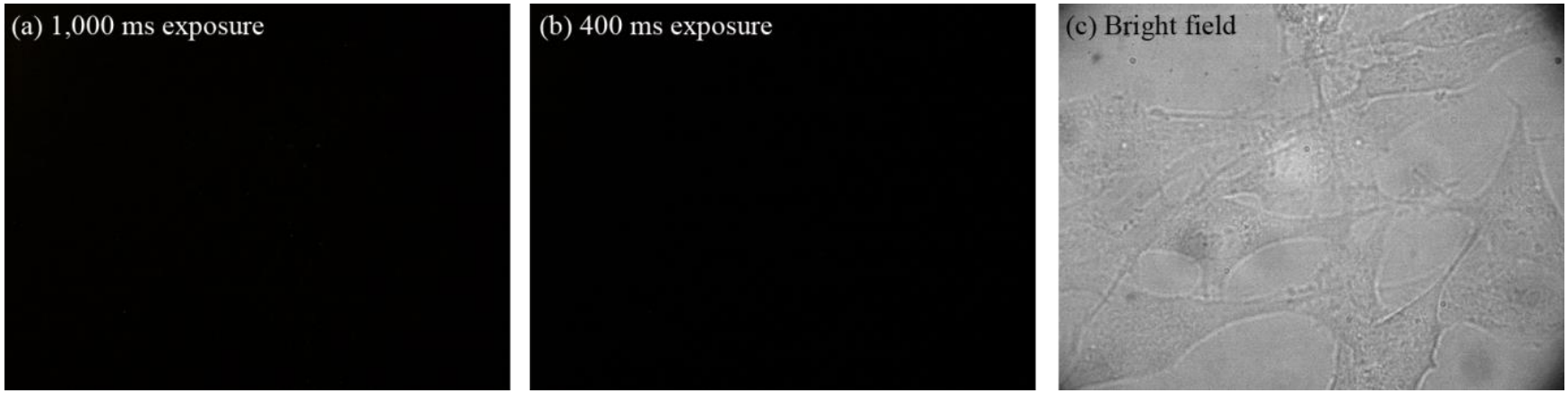

Supplementary Figure 3-1. Measuring autofluorescence from the cells. Cell images in fluorescent mode with (a) 1,000 ms exposure time, (b) 400 ms exposure time and (c) corresponding bright field images. No autofluorescence was detected at either of the two exposure times.

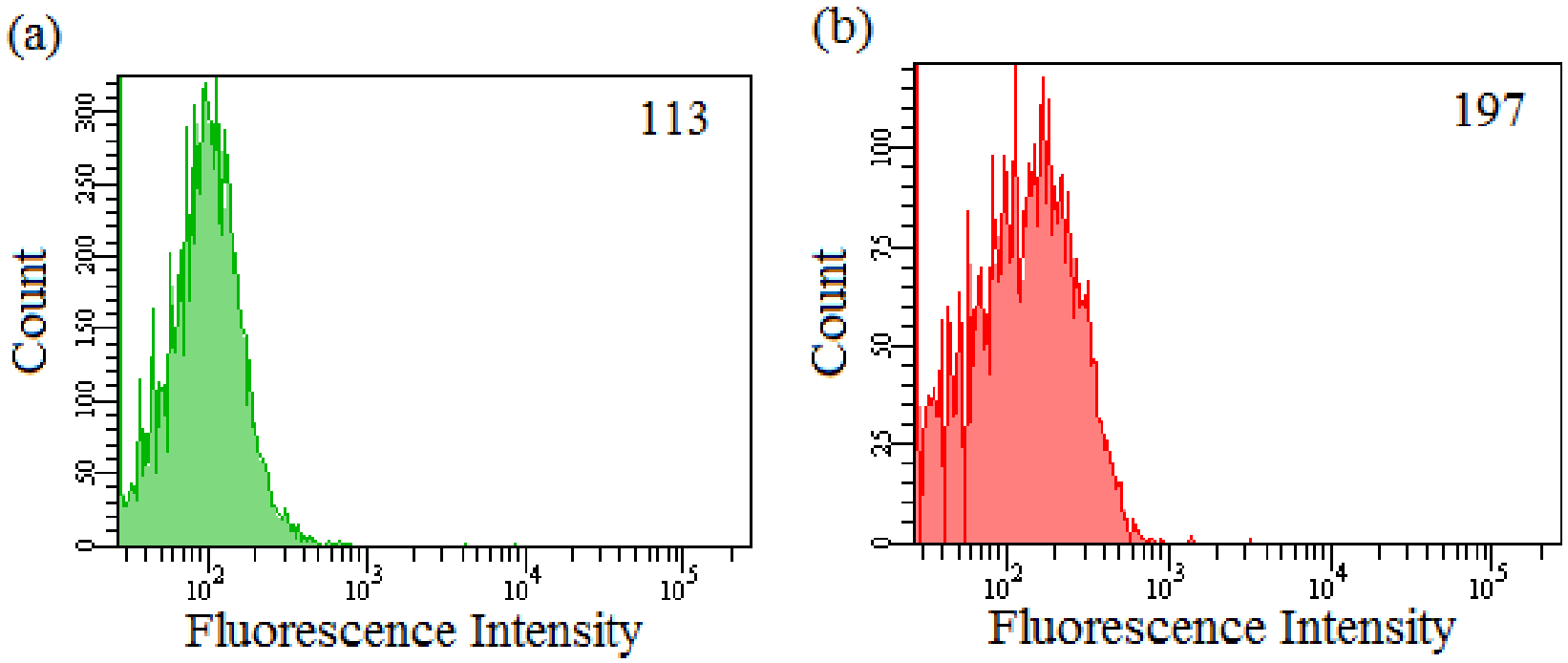

Supplementary figure 3-2. Cell autofluorescence measured using flow cytometry with (a) 488 nm excitation laser and (b) 561 nm excitation laser.

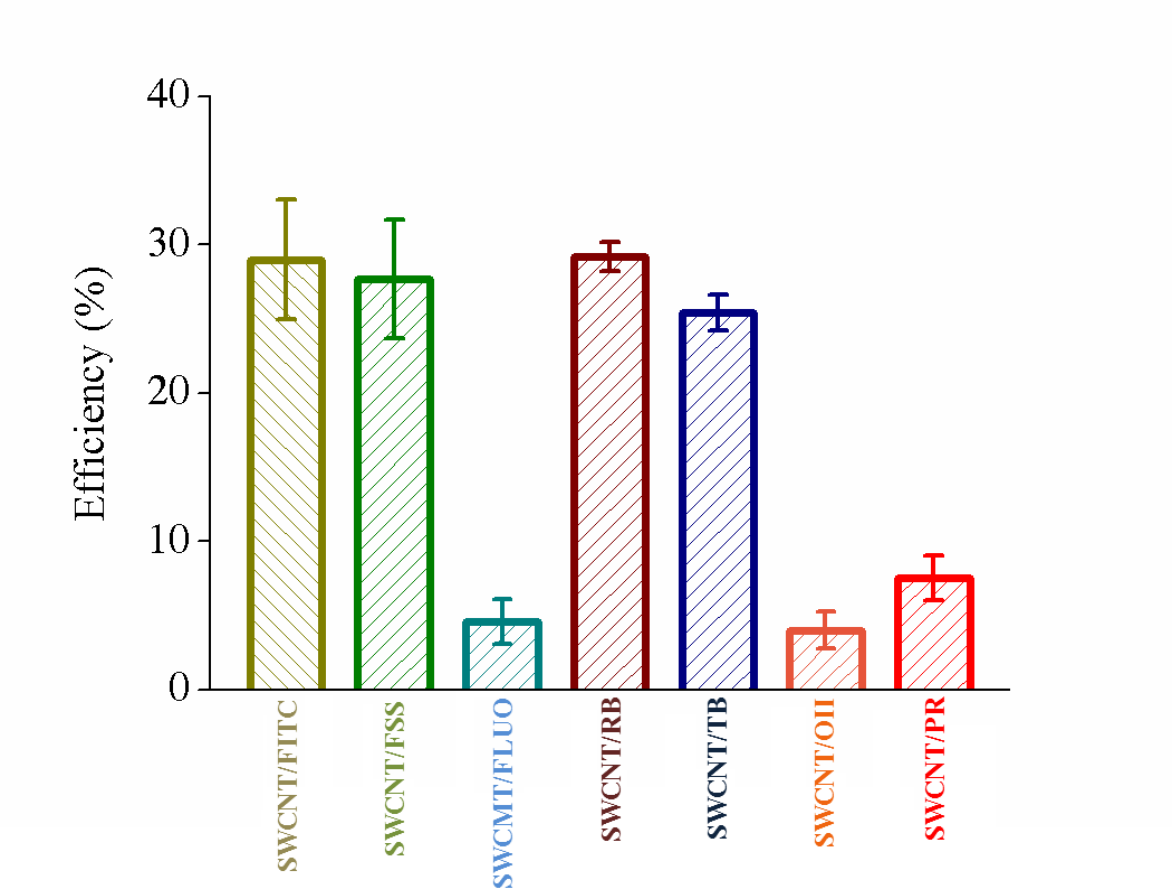

Supplementary figure 3-3. The efficiency of SWCNT dispersion by specified fluorophore or dye molecules in aqueous solution. The efficiency is measured as the fraction of SWCNTs present in the aqueous phase relative to the total input dry material.

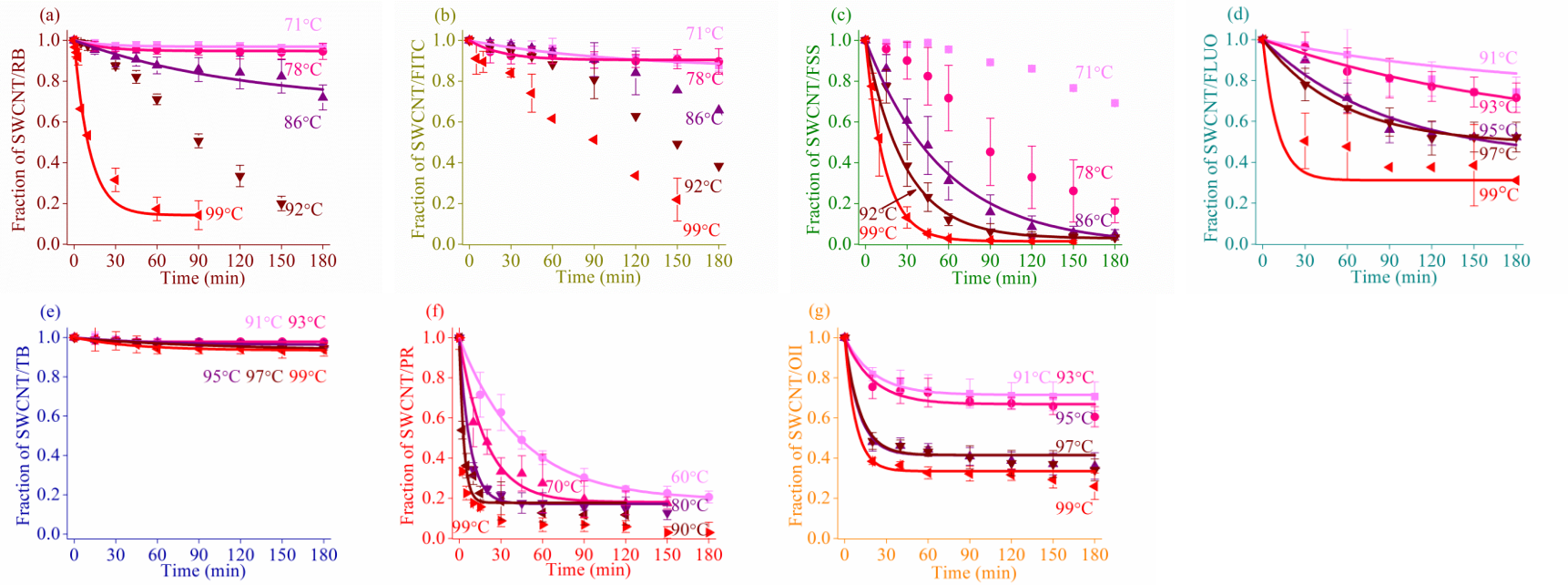

Supplementary figure 3-4. Temperature-dependent aggregation of each SWCNT/Fluorophore or SWCNT/dye sample. (a)~(g) Fraction of SWCNT/RB, SWCNT/FITC, SWCNT/FSS, SWCNT/FLUO , SWCNT/TB, SWCNT/PR and SWCNT/OII that remained in solution after incubation for designated length of time at various temperatures. Solid lines are fits to single-exponential decay function $\{y = A_1*\mathrm{Exp}(-x/t_1) + y_0\}$. The rate constants obtained from these fitted progress curves were further used for Eyring analysis as shown in figure 5 (e), which include 71 ℃, 78 ℃, and 99 ℃ for SWCNT/RB; 86 ℃, 92 ℃, and 99 ℃ for SWCNT/FSS; 93 ℃, 95 ℃, 97 ℃, and 99 ℃ for S SWCNT/FLUO; 60 ℃, 70 ℃, 80 ℃, and 90 ℃ for SWCNT/PR and 91 ℃, 93 ℃, 95 ℃, 97 ℃, and 99 ℃ for SWCNT/OII. The calculated activation enthalpy values were listed in Table 3-1.

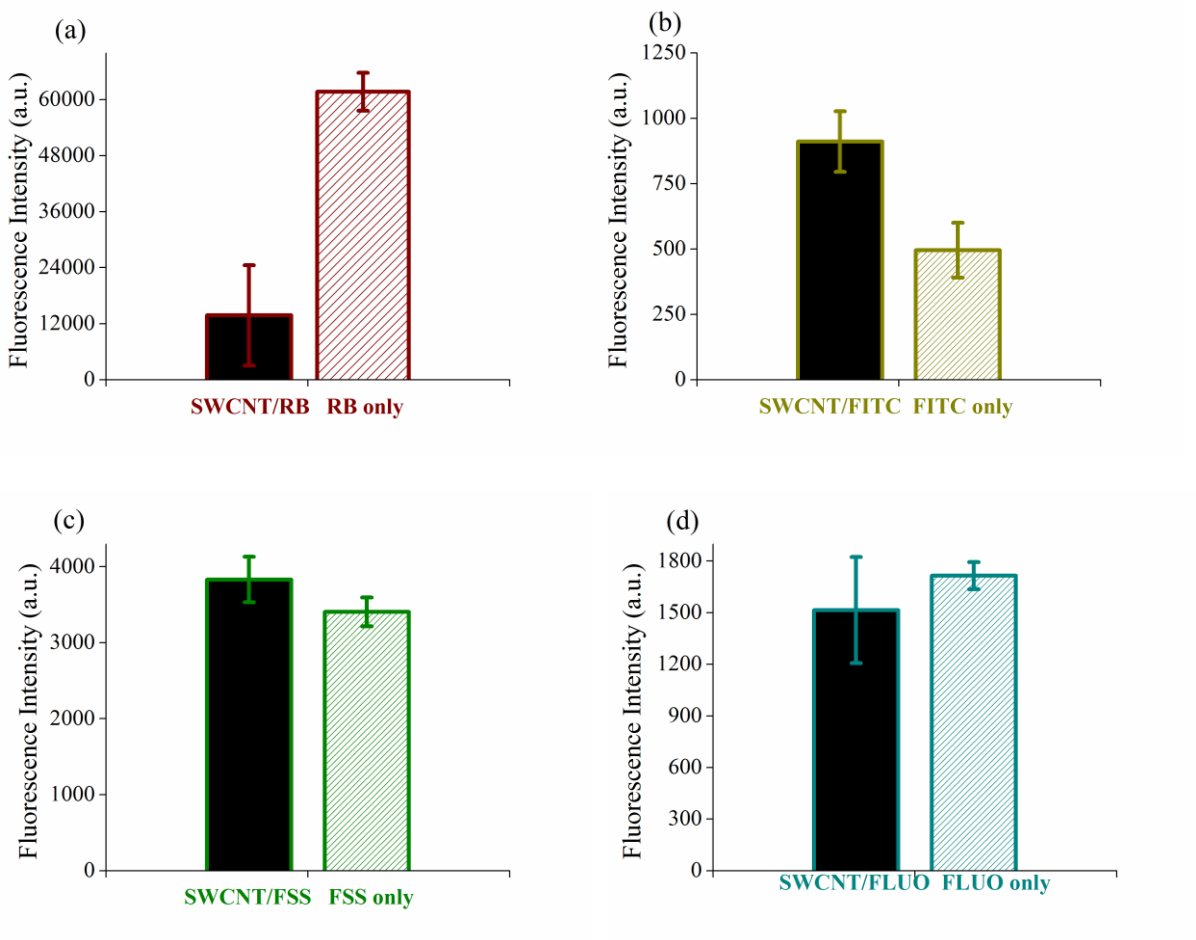

Supplementary figure 3-5. Summary of geometric mean values of cell fluorescence intensity from flow cytometry experiments for 9L cells transfected with various reagents. Cells transfected with FITC only, SWCNT/FITC, FSS only, SWCNT/FSS, FLUO only, SWCNT/FLUO were excited with 488 nm laser, while cells transfected with RB only and SWCNT/RB were excited with 561 nm laser.

	Surface area of SWCNTs (nm^2)	Maximal projection area of each dispersant molecule ($Å^2$)	# of dispersant molecules required to cover single SWCNT surface	Saturation concentration of SWCNTs (nM)	Concentration of dispersant molecules required to cover all SWCNTs (μM)	Critical concentration of dispersant molecules (μM)
SWCNT/ FITC	5364	99.71	5380	66.9	355.1	250
SWCNT/ FSS	4429	88.51	5004	63.1	297.9	N.A.
SWCNT/ FLUO	6688	83.16	8843	9.75	85.3	N.A.
SWCNT/RB	6095	138.47	4402	64.5	248.9	500
SWCNT/TB	3615	195.56	1849	60.0	98.7	200
SWCNT/OII	5244	99.07	5294	18.9	86.8	N.A.
SWCNT/PR	4778	82.66	5781	10.6	49.4	100

Supplementary Table 3-1. Comparison between theoretical concentration of dispersant molecules required to cover SWCNT surface and the critical concentration measured in this study (Figure 3). In this estimation, the surface area of SWCNT was estimated using the average length and height of each SWCNT sample listed in Table 3-1. The maximal projection area of each dispersant molecule was estimated using ChemAxon™ Marvin Version 5.9.3. The number of dispersant molecules required to cover a single SWCNT surface was estimated by taking the ratio between column 2 and 3. The saturation concentration of SWCNTs was estimated based on results shown in figure 3. The critical concentrations of dispersant molecules were directly read off figure 3 as the experimental concentration of dispersant molecules required before more than 50% of the saturation concentration of SWNCT was dispersed. This concentration was well defined for FITC, RB, TB and PR based on the dispersion profile shown in figure 3.

SWCNTs	I_D/I_G ratio at 633 nm	I_D/I_G ratio at 785 nm
SWCNT/$(dT)_{30}$	0.025	0.027
SWCNT/FITC	0.041	0.029
SWCNT/FSS	-	0.046
SWCNT/FLUO	-	-
SWCNT/RB	0.026	-
SWCNT/TB	-	-
SWCNT/OII	-	0.011
SWCNT/PR	-	-

Supplementary Table 3-2. Intensity ratio between Raman D and G bands for dispersed SWCNT samples. This ratio was not available for FLUO and PR dispersed samples due to high background present in the Raman spectra.

SWCNT/Fluorophore	Fluorophore Conc. (mM)	Solution	Zeta Potential (mV)
SWCNT/FITC	1	10 mM PB	-35.10 ± 5.03
SWCNT/FSS	1	ddH_2O	-30.21 ± 6.09
SWCNT/FLUO	0.4	ddH_2O	-35.62 ± 3.89
SWCNT/RB	1	ddH_2O	37.72 ± 2.08

Supplementary Table 3-3. SWCNT/Fluorophore complexes and their zeta potential values. All samples were ~8 fold diluted for the measurement.

Appendix B

Supporting Information in Chapter 6

Supplemental charts and figures

<Negatively charged dispersants>

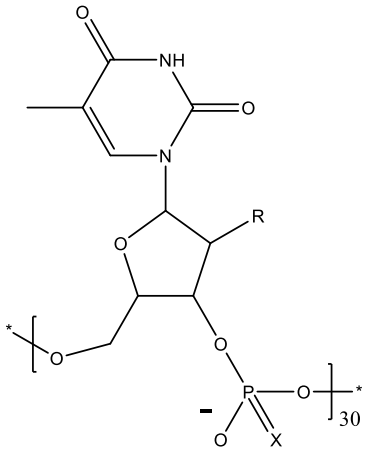

ssDNA {$(dT)_{30}$}

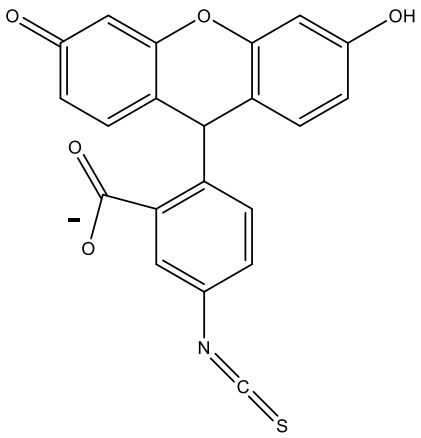

Fluorescein isothiocyanate (FITC)

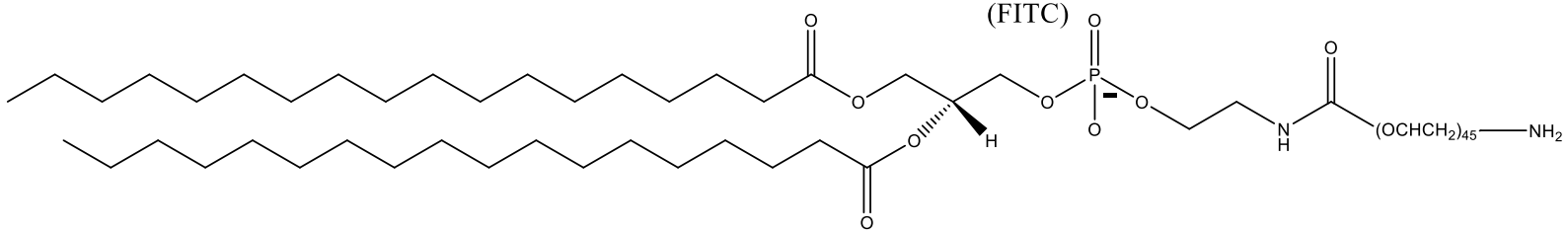

DSPE-PEG(2000) Amine (DSPE-PEG)

<Positively charged dispersants>

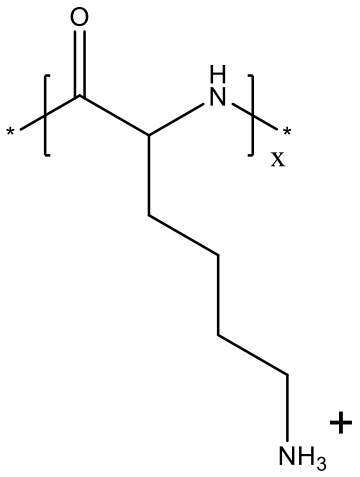

Poly-L-Lysine (PLL)

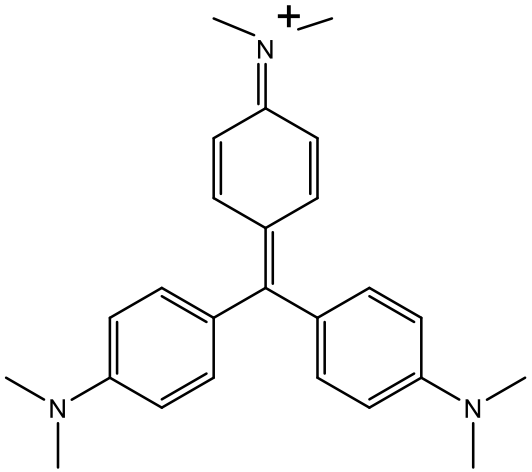

Crystal Violet (CV)

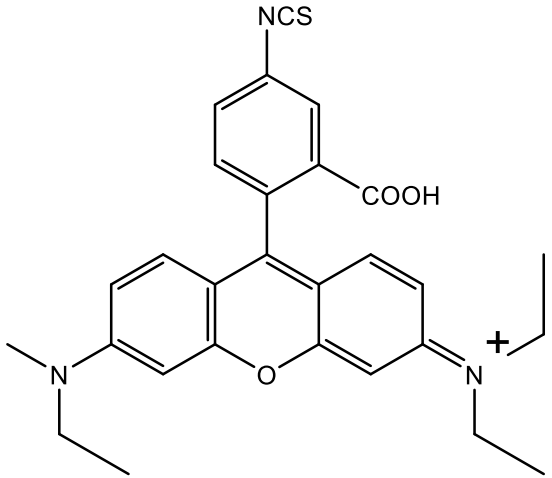

Rhodamine B (RB)

<Non-charged dispersants>

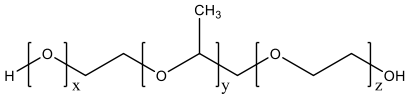

Pluronic F

<Bridge molecules>

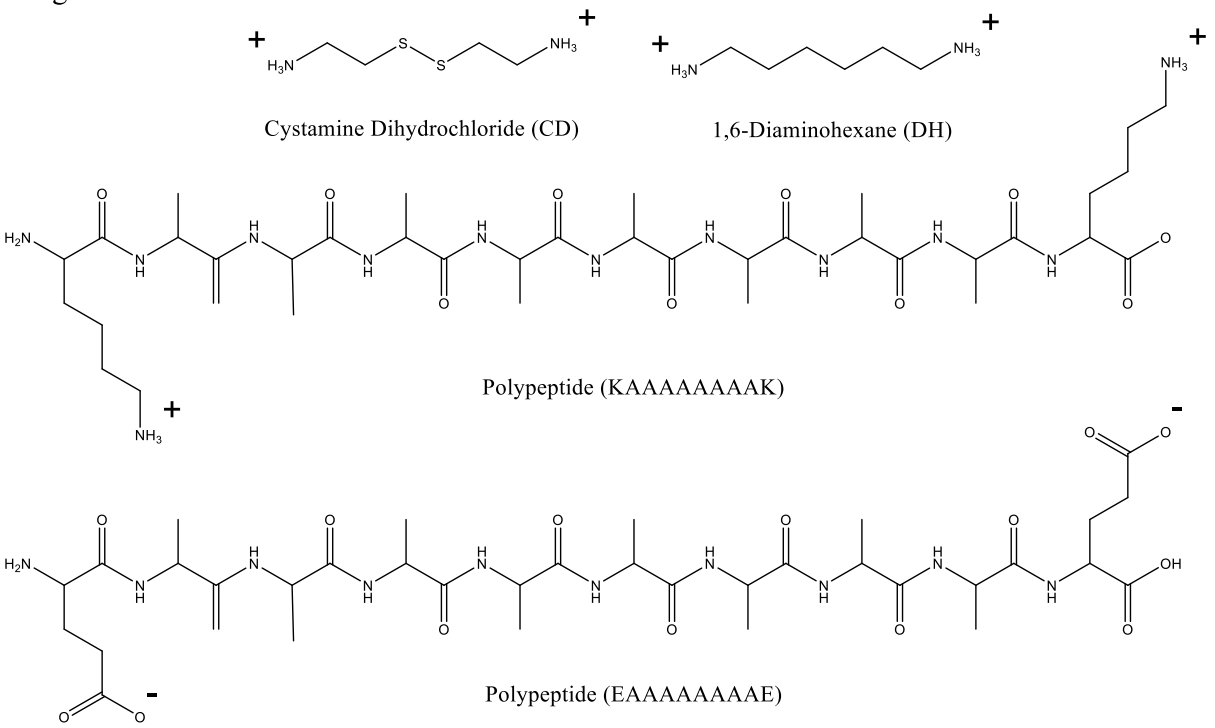

Supplementary Chart 6-1. List of negatively charged, positively charged and non-charged dispersants used to disperse SWCNTs and bridge molecules used to induce aggregation of SWCNTs.

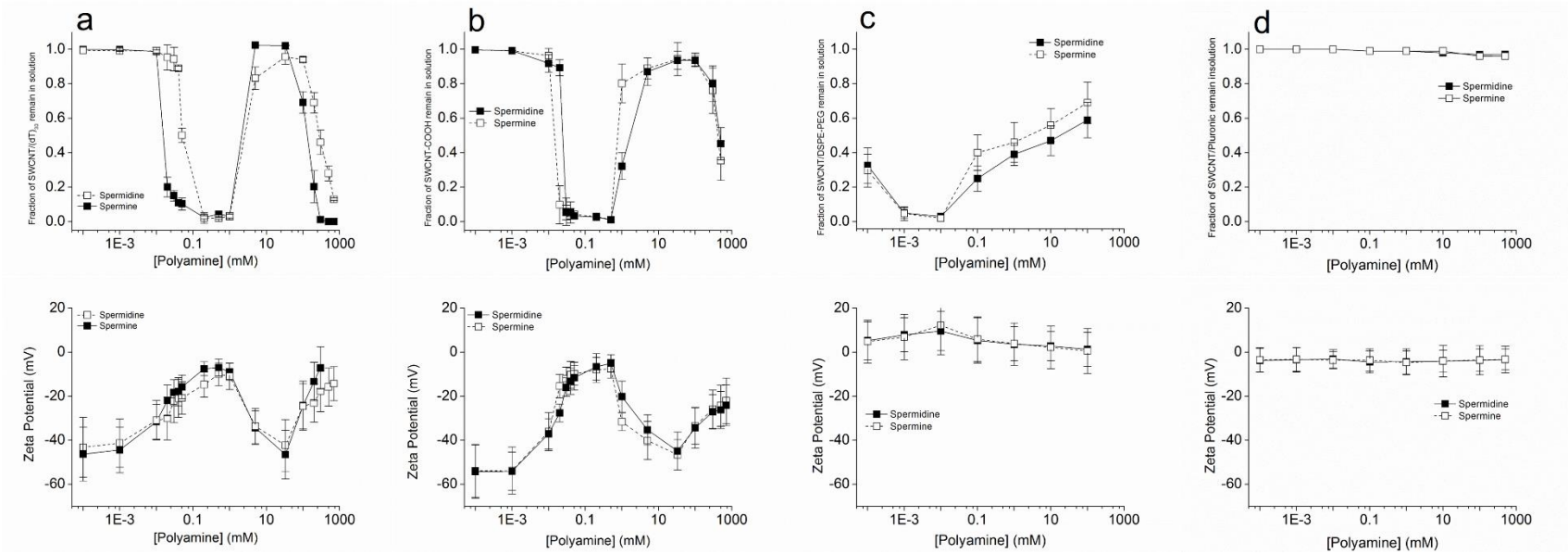

Supplementary figure 6-1. Spermine and spermidine concentration dependent aggregation and re-dispersion of (a) SWCNT/$(dT)_{30}$, (b) SWCNT-COOH, (c) SWCNT/DSPE-PEG and (d) SWCNT/Pluronic with its zeta potential changes.

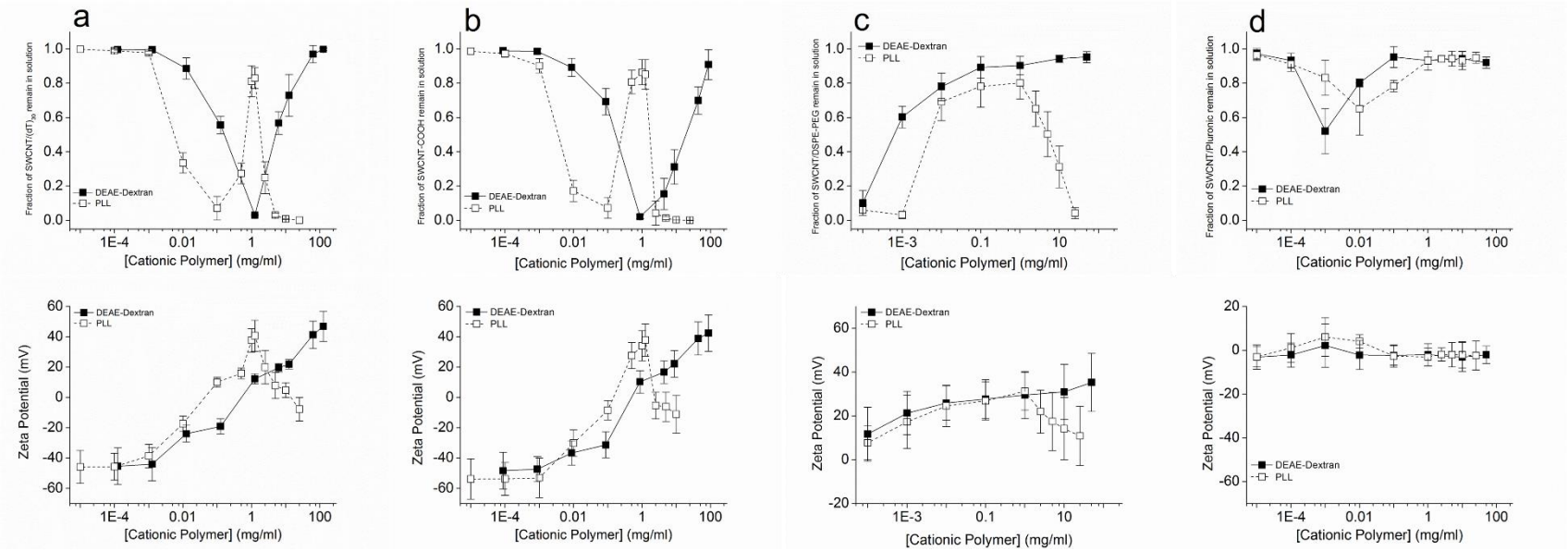

Supplementary figure 6-2. Poly-L-Lysine and DEAE-Dextran concentration dependent aggregation and re-dispersion of (a) SWCNT/$(dT)_{30,}$ (b) SWCNT-COOH, (c) SWCNT/DSPE-PEG and (d) SWCNT/Pluronic with its zeta potential changes.

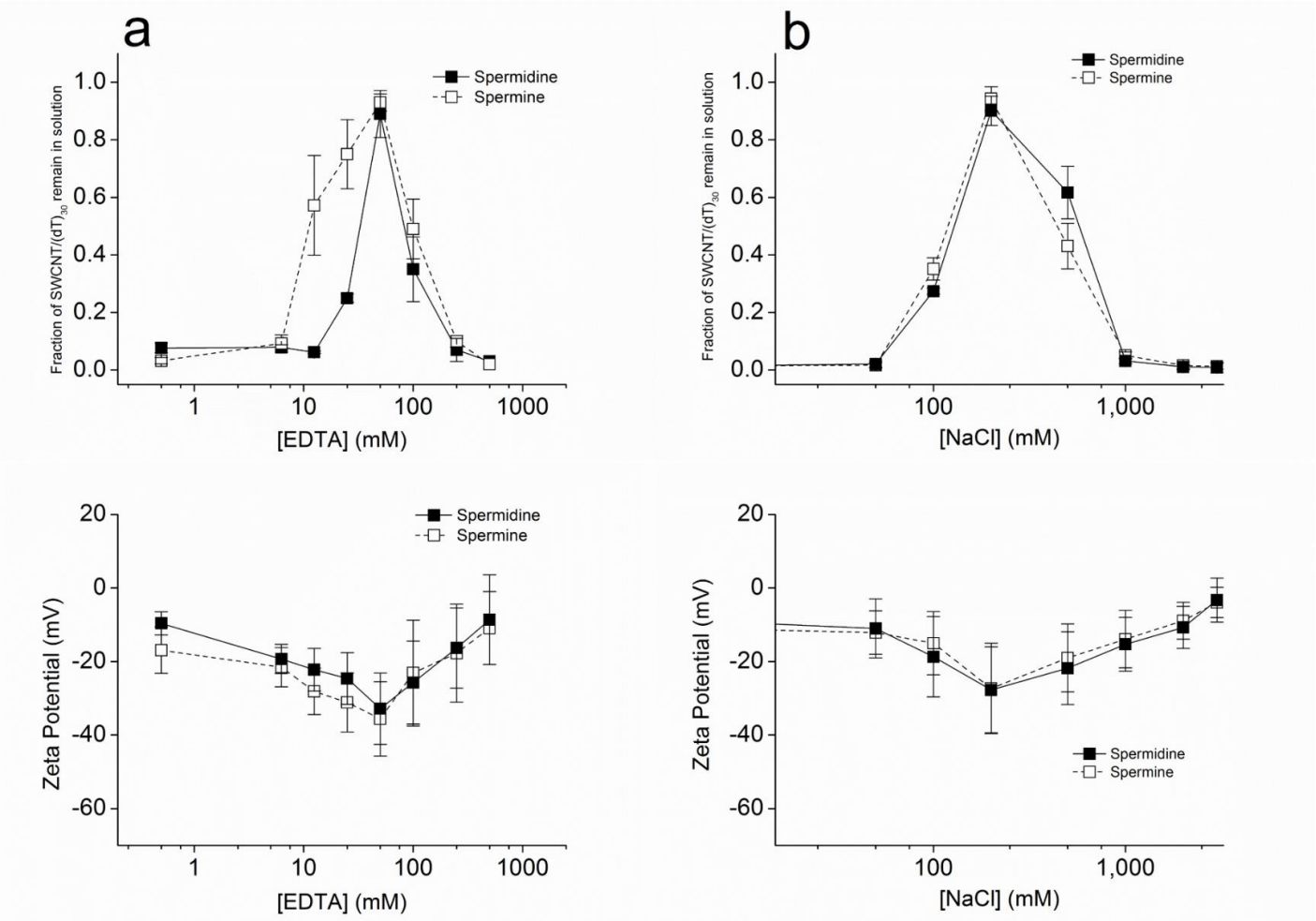

Supplementary figure 6-3. Re-dispersion of SWCNT/$(dT)_{30}$ aggregates induced by polyamines with (a) EDTA and (b) NaCl.

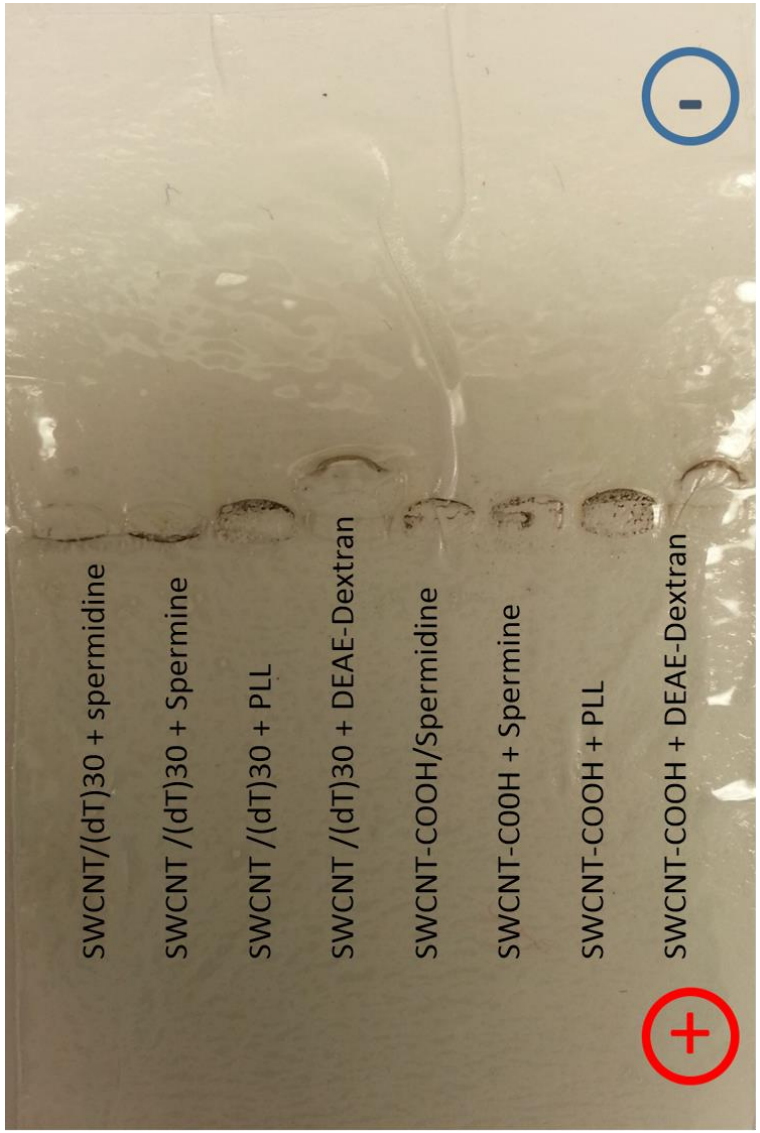

Suppelemntary figure 6-4. Charge reversal of SWCNT/$(dT)_{30}$ and SWCNT-COOH upon addition of PLL and DEAE-Dextran.

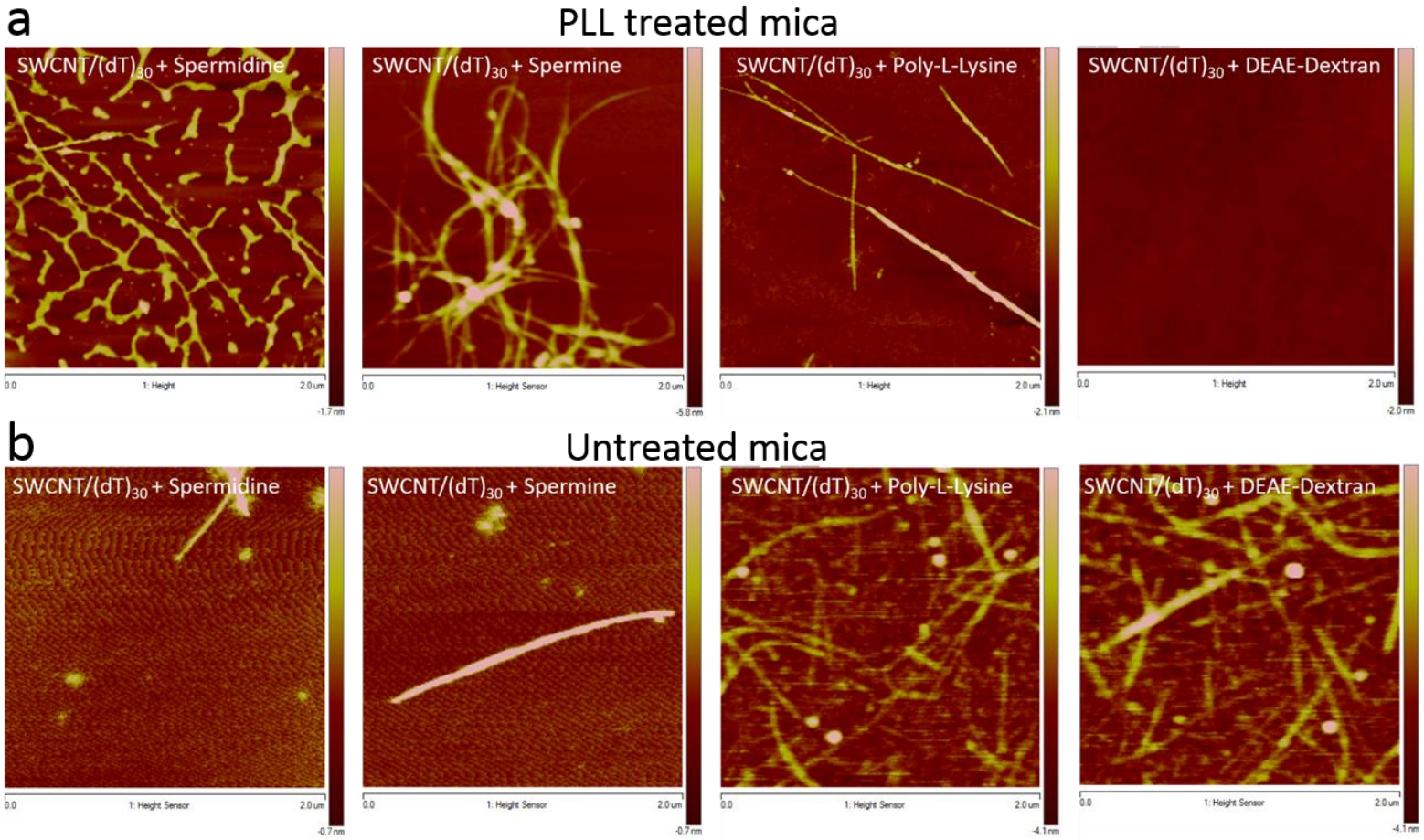

Supplementary figure 6-5. AFM images of SWCNT/$(dT)_{30}$ with spermidine, spermine, PLL and DEAE-Dextran on (a) positively charged PLL treated (b) negatively charged untreated mica.

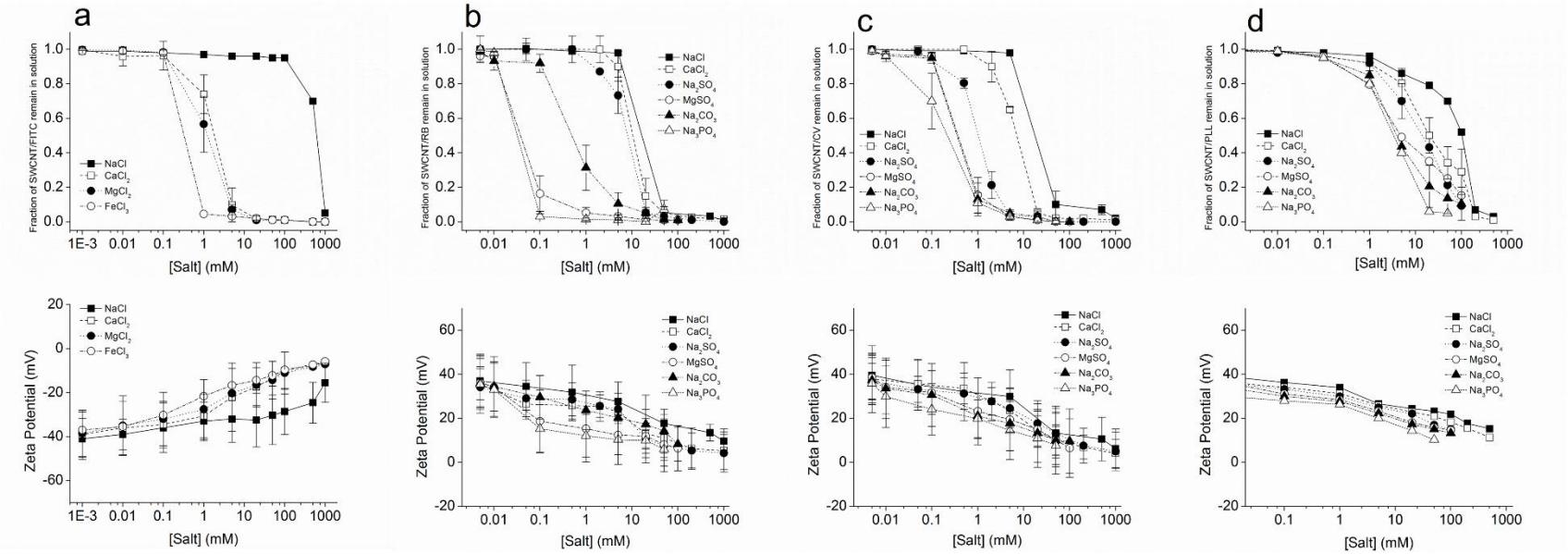

Supplementary figure 6-6. Aggregation of (a) SWCNT/FITC (b) SWCNT/RB (c) SWCNT/CV and (d) SWCNT/PLL with addition of salts and its zeta potential changes.

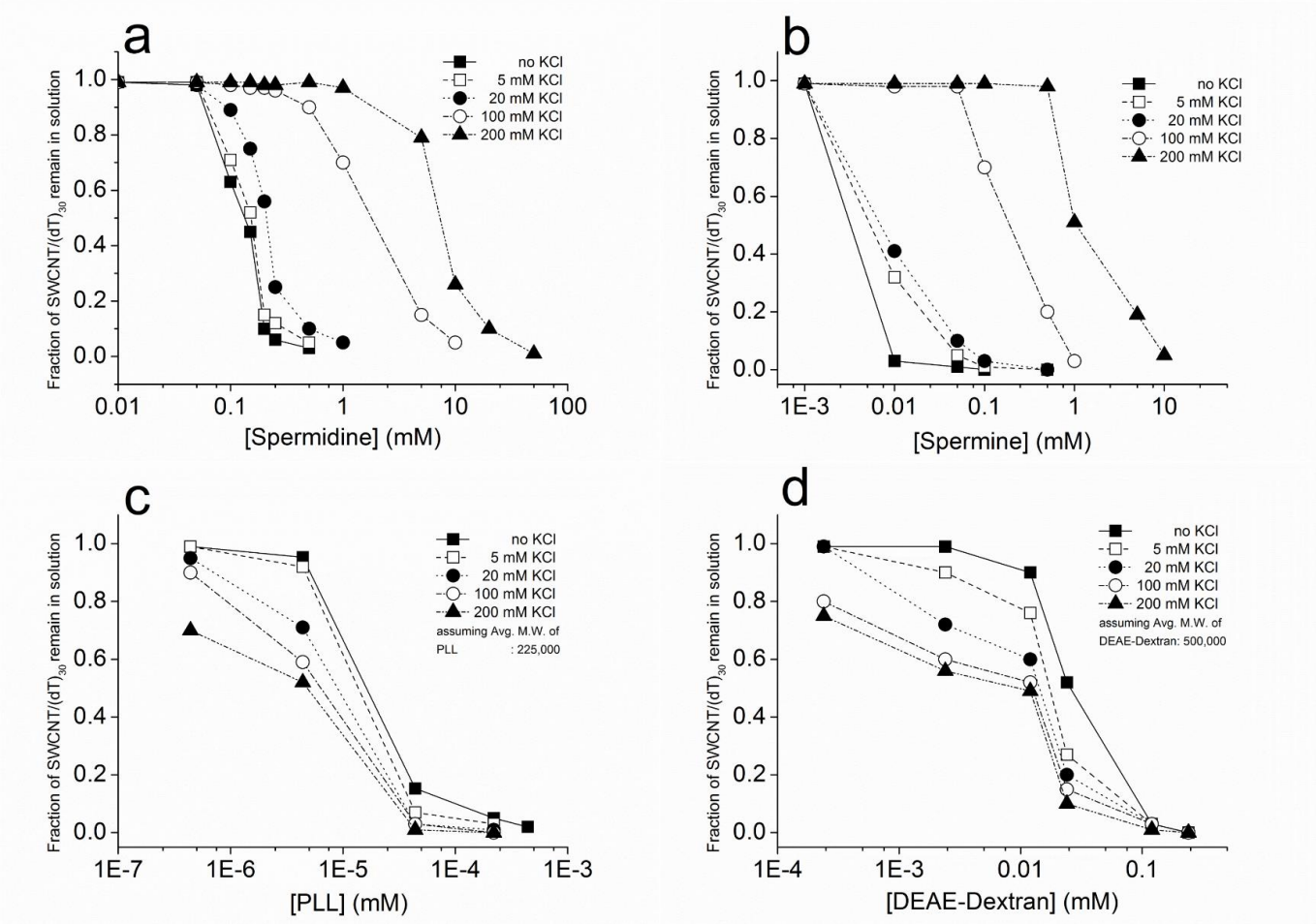

Supplementary figure 6-7. KCl concentration dependence of SWCNT/$(dT)_{30}$ aggregation by (a) Spermine (b) Spermidine (c) PLL and (d) DEAE-Dextran.

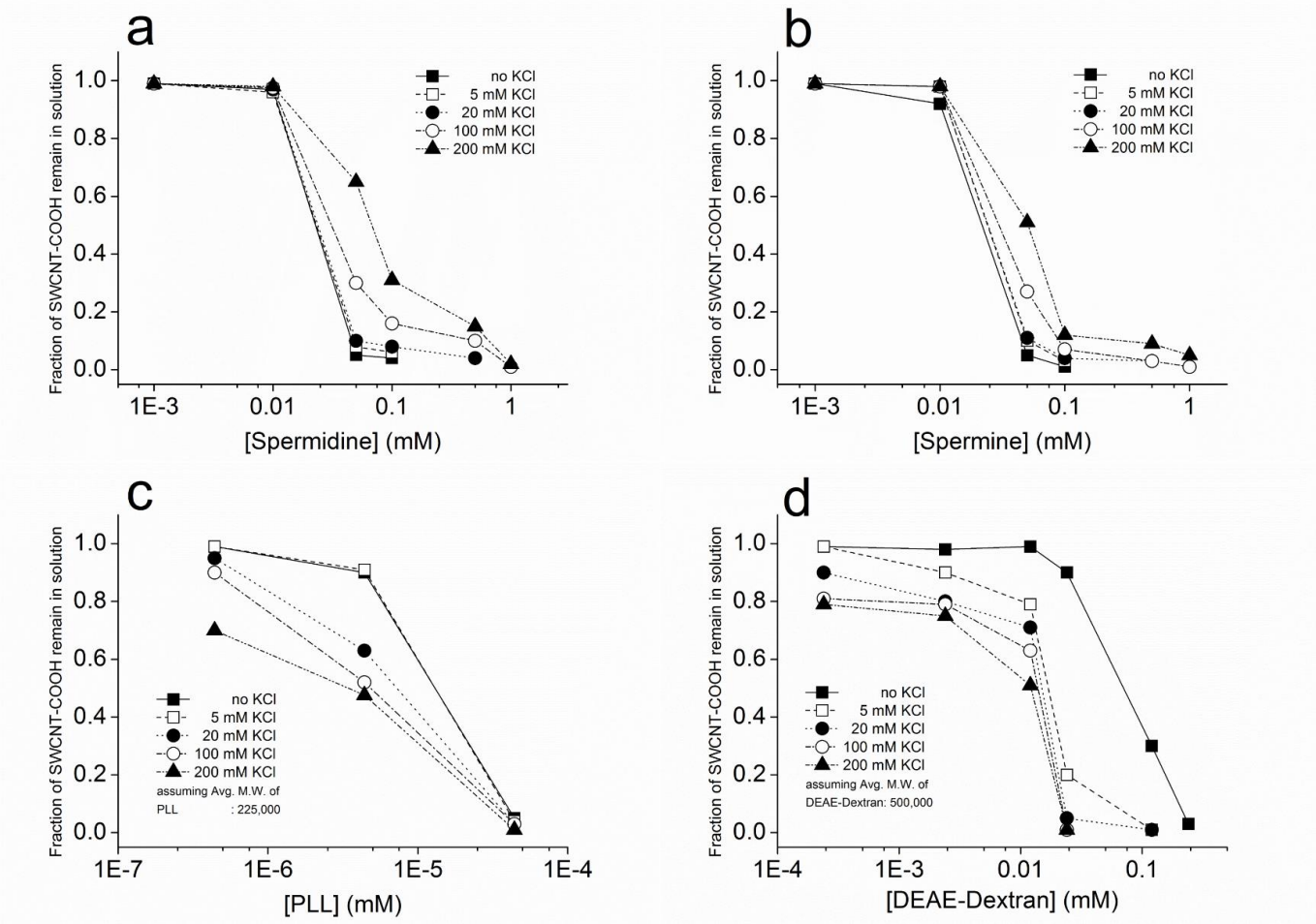

Supplementary figure 6-8. KCl concentration dependence of SWCNT-COOH aggregation by (a) Spermine (b) Spermidine (c) PLL and (d) DEAE-Dextran.

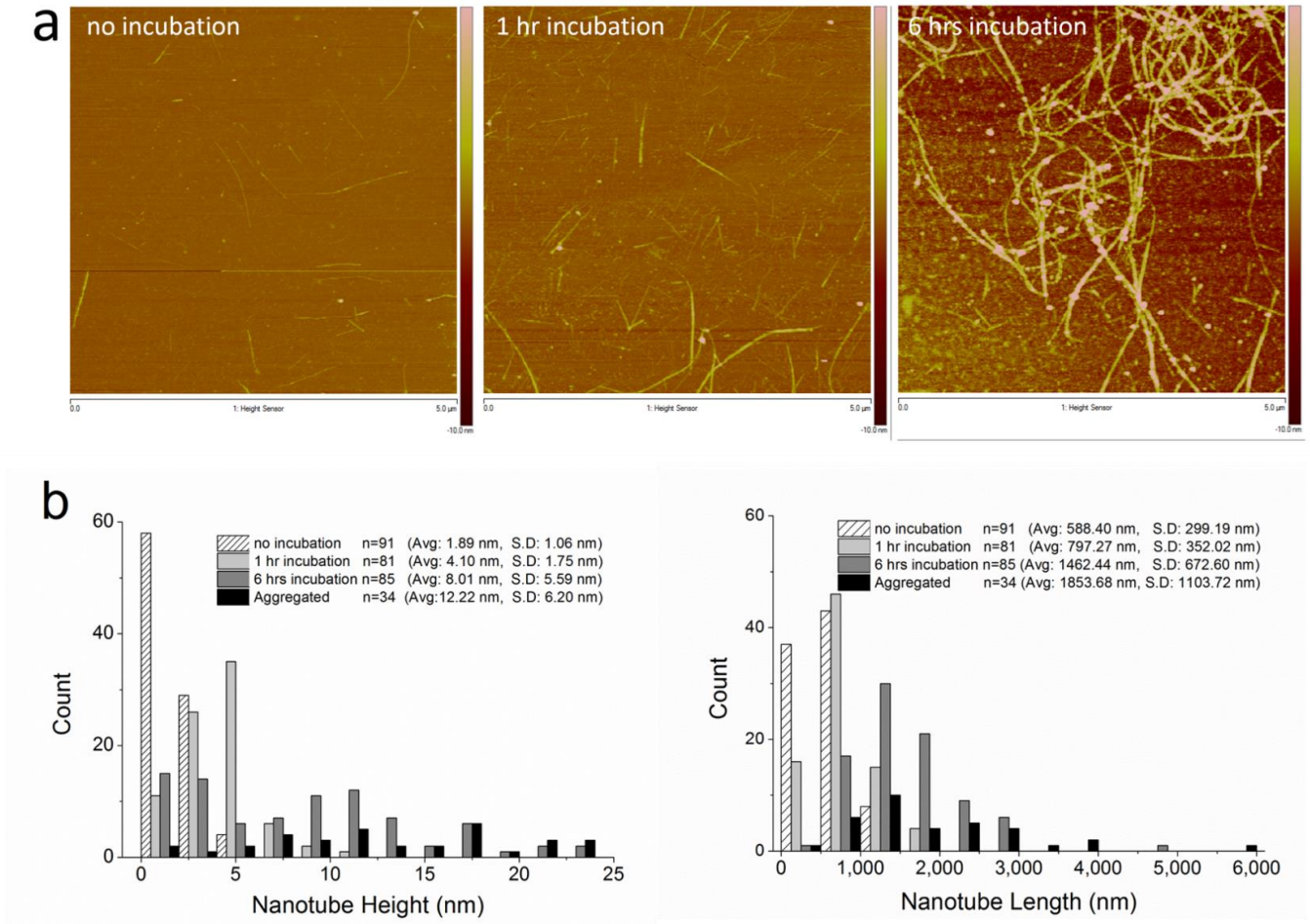

Supplementary figure 6-9. (a) AFM images of SWCNT/$(dT)_{30}$ (b) SWCNT/$(dT)_{30}$ height and length analysis upon incubation with $CaCl_2$ with designated time point.

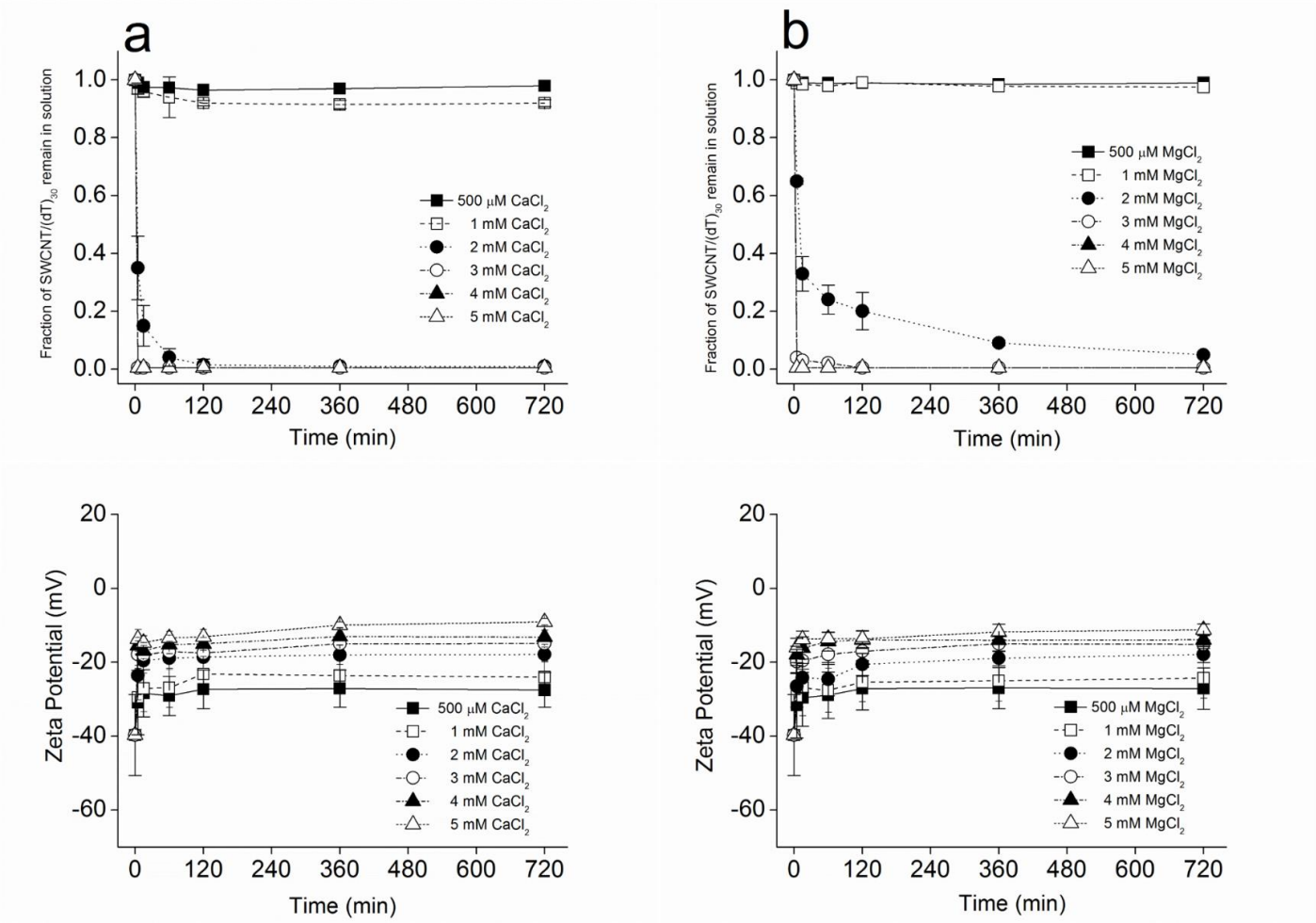

Supplementary figure 6-10. Aggregation kinetics of SWCNT/$(dT)_{30}$ upon incubation with varying concentration of (a) $CaCl_2$ and (b) $MgCl_2$.

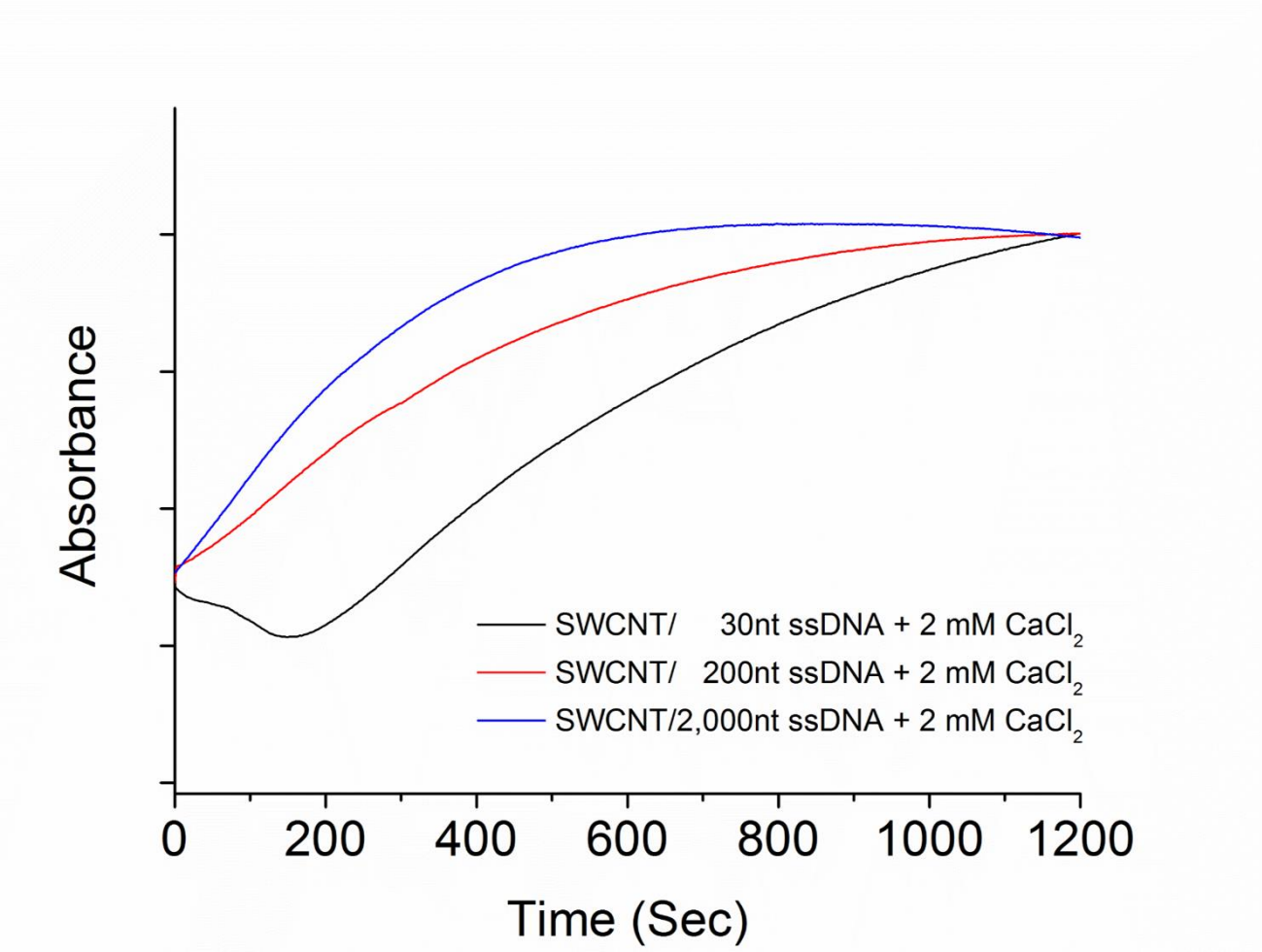

Supplementary figure 6-11. SWCNT aggregation kinetics depending on length of DNA used to disperse SWCNTs.

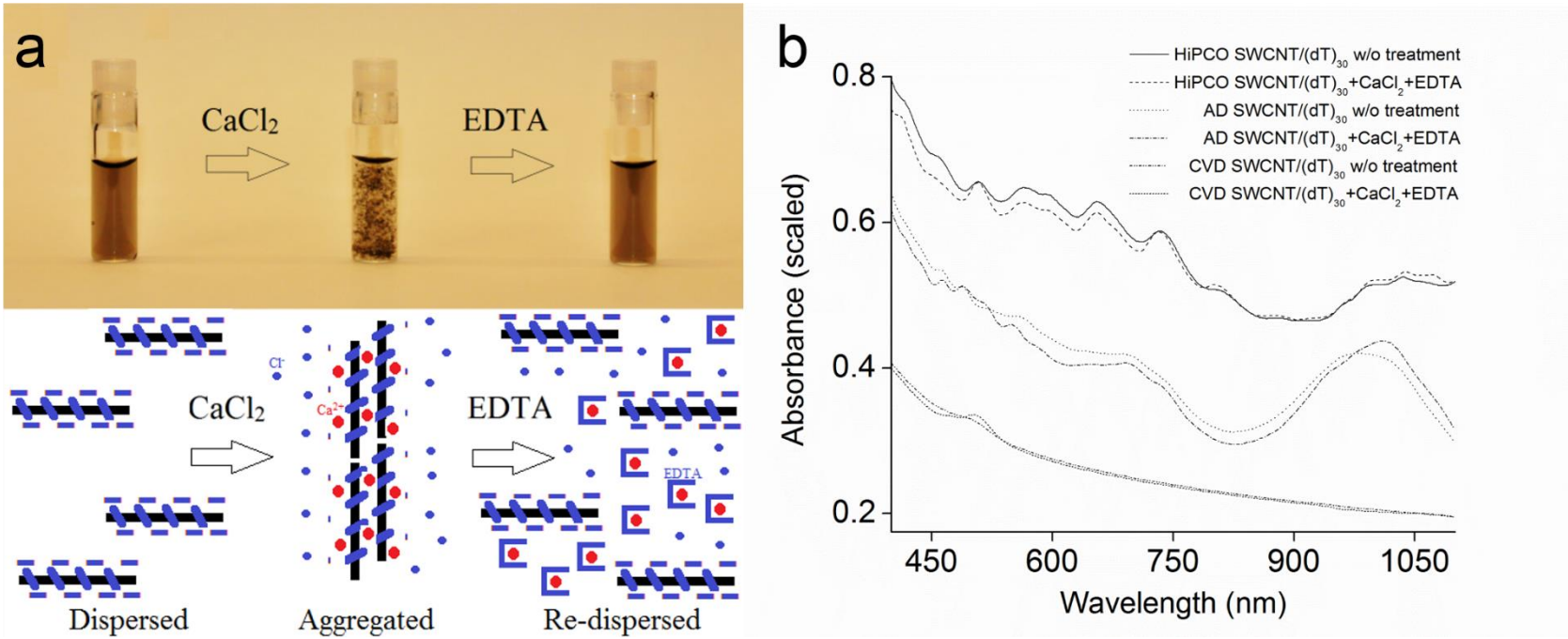

Supplementary figure 6-12. (a) Proposed mechanism of $CaCl_2$ and EDTA mediated aggregation and re-dispersion of SWCNT/$(dT)_{30}$ (b) Visible-IR absorbance changes upon aggregation and re-dispersion by $CaCl_2$ and EDTA.

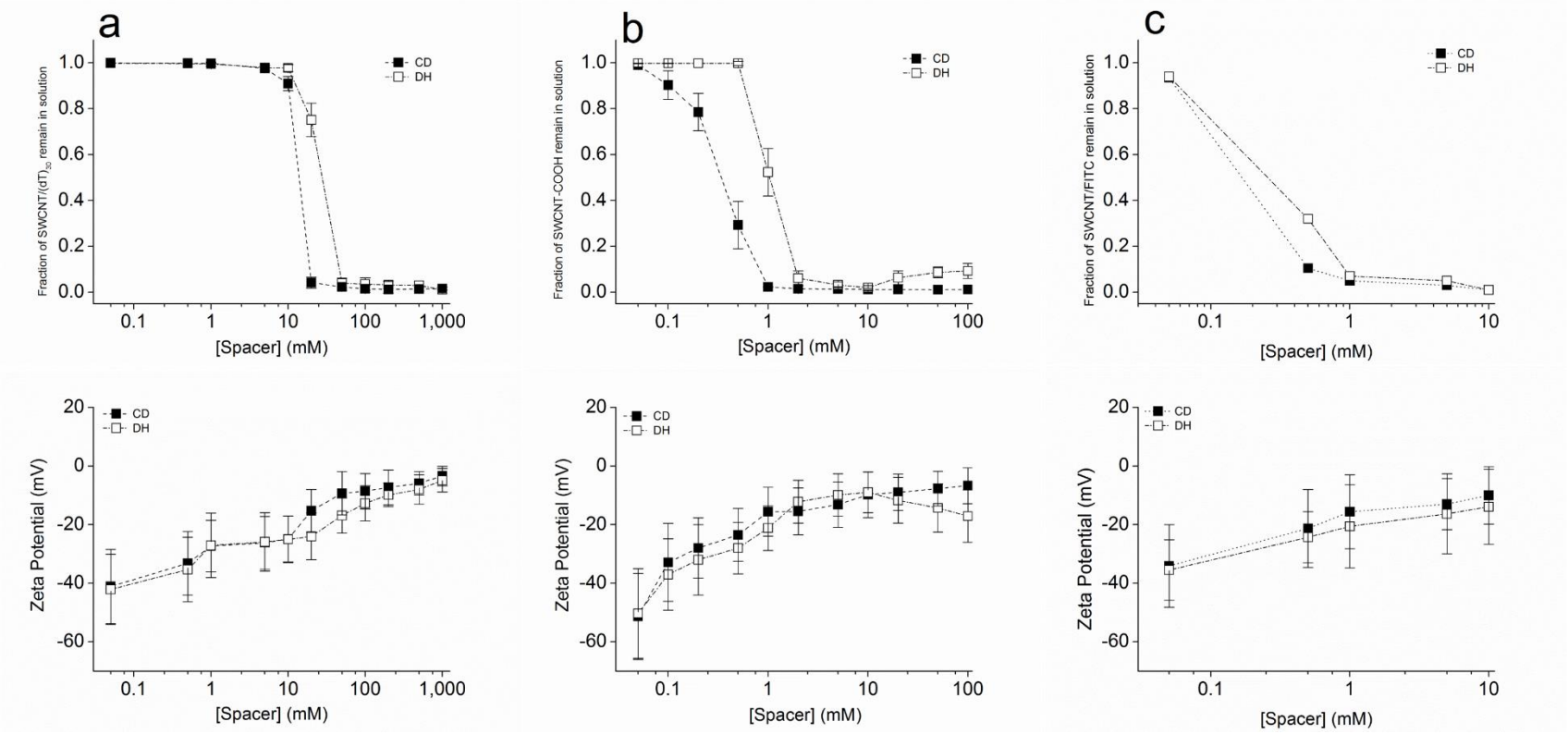

Supplementary figure 6-13. Cystamine Dihydrochloride (CD) and Diaminohexane (DH) mediated aggregation of (a) SWCNT/$(dT)_{30}$ (b) SWCNT-COOH and (c) SWCNT/FITC.

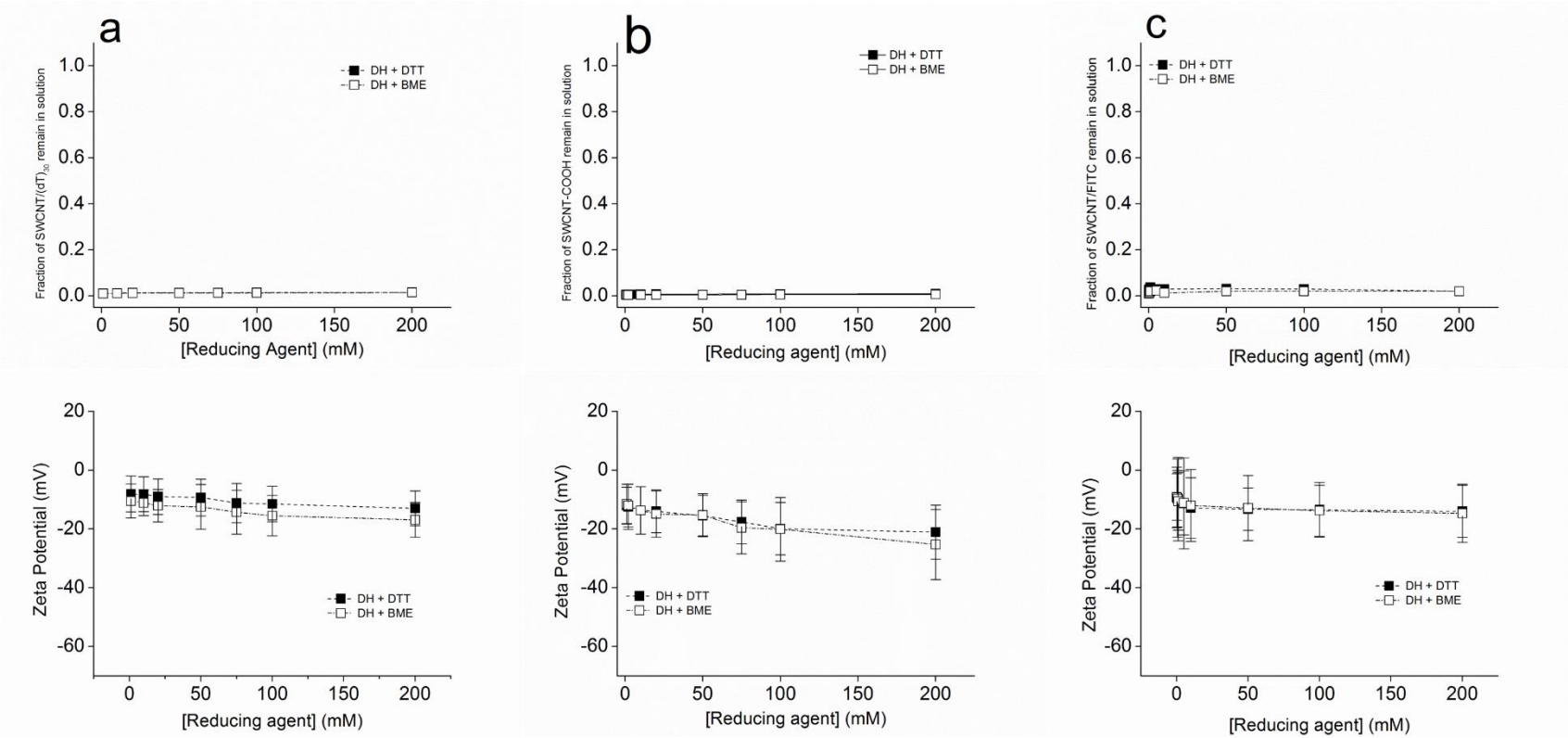

Supplementary figure 6-14. Disulfide bond reducing agents {Dithiothreitol (DTT), 2-Mercaptoethanol (BME)} mediated re-dispresion of (a) SWCNT/(d T)$_{30}$ (b) SWCNT-COOH and (c) SWCNT/FITC aggregated by diaminohexane (DH).

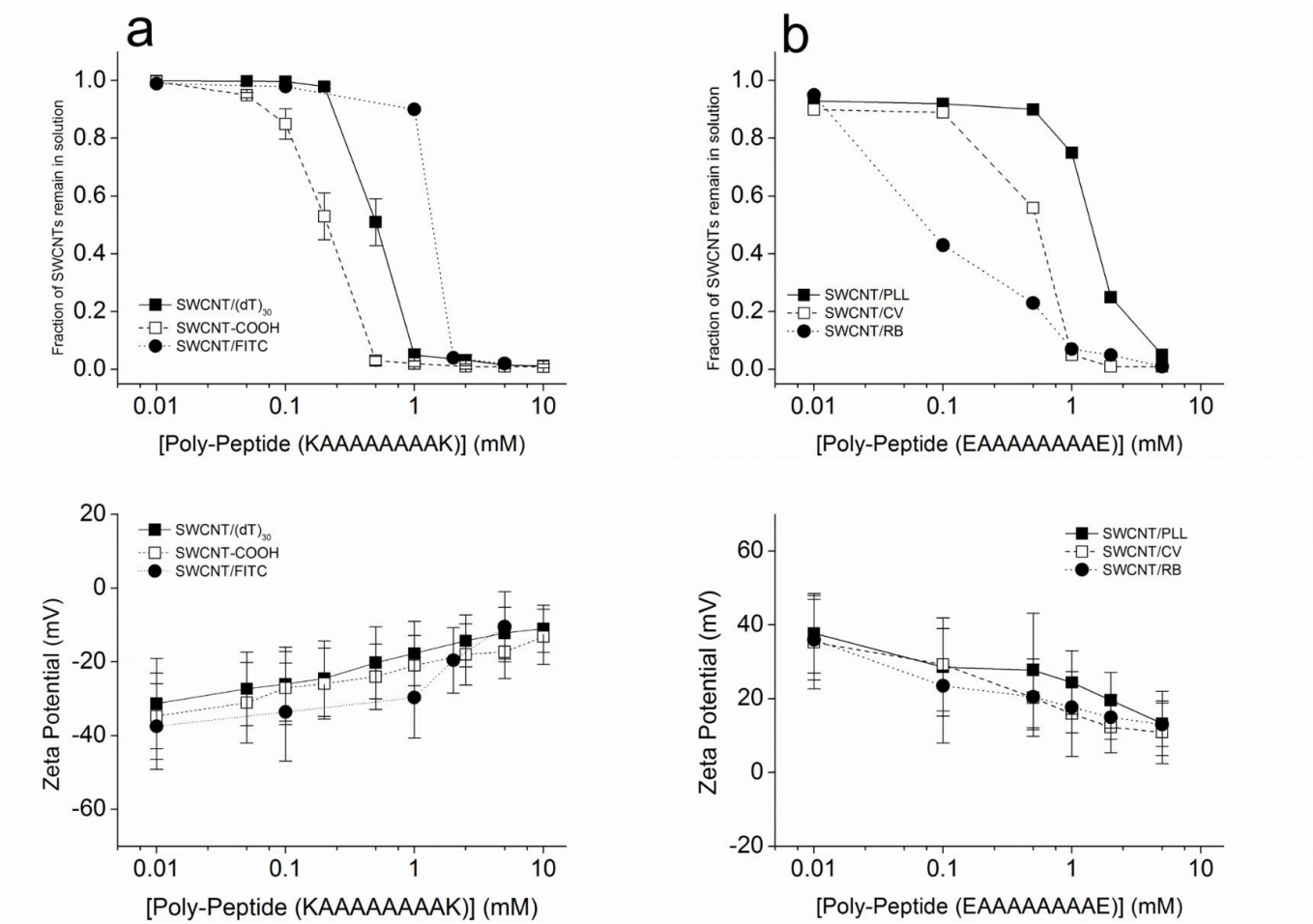

Supplementary figure 6-15. Fraction of individual SWCNTs remain in solution dispersed by (a) negatively charged dispersants with poly-peptide (KAAAAAAAAK) and (b) positively charged dispersants with poly-peptide (EAAAAAAAAE).

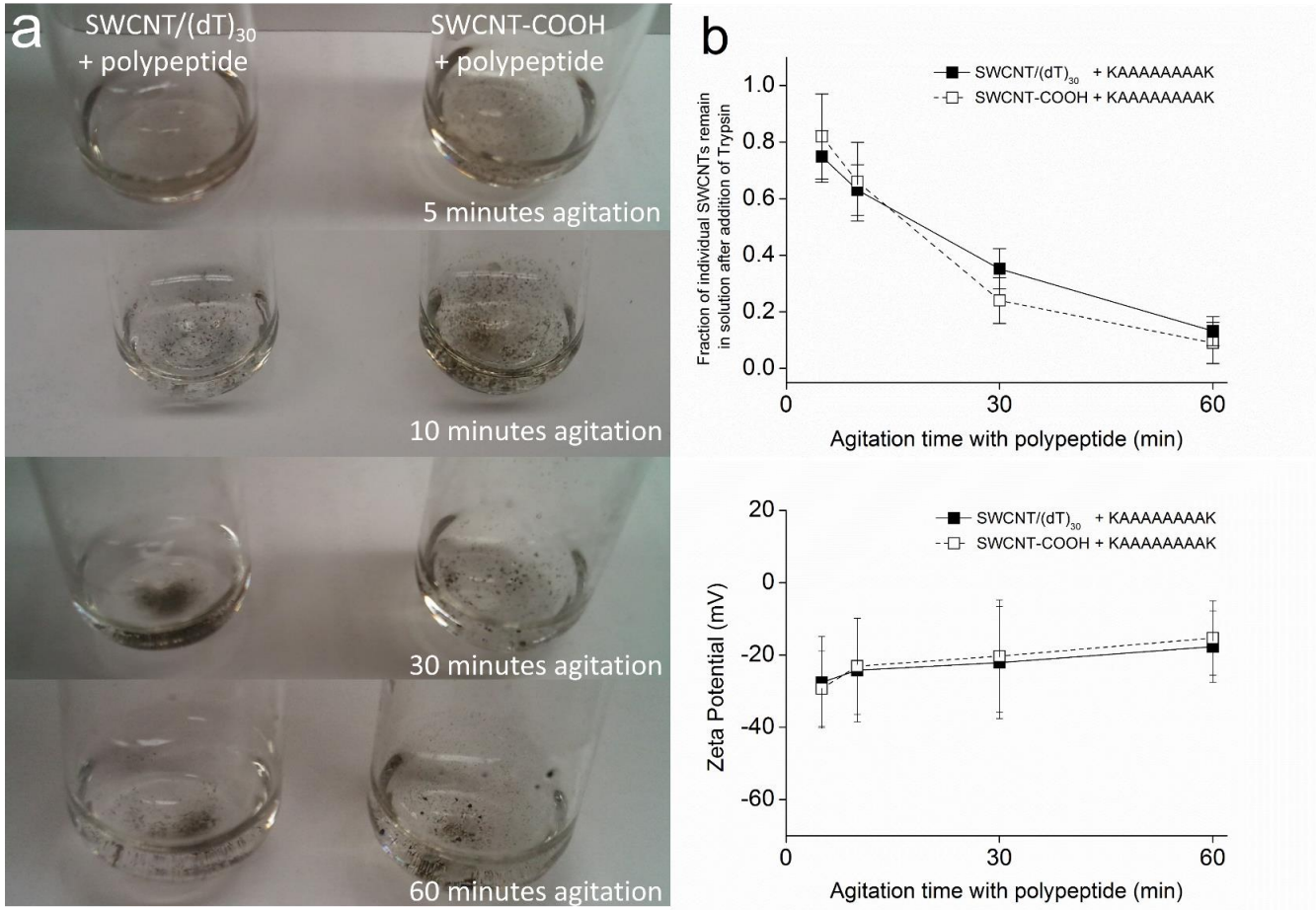

Supplementary figure 6-16. (a) Growth of SWCNT aggregates size depending on agitation time with poly-peptide (b) Fraction of SWCNTs re-dispersed with trypsin depending on agitation time with polypeptide.